Wavelet Analysis and Classification of Surface Electromyography Signals

Jeff Kilby

**Thesis submitted in partial fulfilment
of the degree of
the Master of Engineering**

**Auckland University of Technology
Auckland
New Zealand**

October 2005

Acknowledgement

I wish to express my gratitude to my supervisor, Dr Hamid Gholam Hosseini for his patience, support, guidance and advice throughout this research. I also greatly appreciate the assistance given by Professor Peter McNair and Grant Mawston from the Physical and Rehabilitation Research Centre, at Akoranga Campus of Auckland University of Technology for imparting professional knowledge and information on working with muscle signals.

I would like to thank my wife, Vera and my son, Max for their support, patience and love in the process of completing this work.

Sincere thanks are also extended to helpful friends, participants, data collectors Minetta Mendonza and Mike Jebb, and all staff of the School of Engineering and for their kindness and encouragement during my studying period at the Auckland University of Technology.

Abstract

A range of signal processing techniques have been adopted and developed as a methodology which can be used in developing an intelligent surface electromyography (SEMG) signal classifier. An intelligent SEMG signal classifier would be used for recognising and treatment of musculoskeletal pain and some neurological disorders by physiotherapists and occupational therapists. SEMG signals displays the electrical activity from a skeletal muscle which is detected by placing surface electrodes placed on the skin over the muscle.

The key factors of this research were the investigation into digital signal processing using various analysis schemes and the use of the Artificial Neural Network (ANN) for signal classification of normal muscle activity. The analysis schemes explored for the feature extraction of the signals were the Fast Fourier Transform (FFT), Short Time Fourier Transform (STFT), Continuous Wavelet Transform (CWT), Discrete Wavelet Transform (DWT) and Discrete Wavelet Packet Transform (DWPT).

Traditional analysis methods such as FFT could not be used alone, because muscle diagnosis requires time-based information. CWT, which was selected as the most suitable for this research, includes time-based information as well as scales, and can be converted into frequencies, making muscle diagnosis easier. CWT produces a scalogram plot along with its corresponding frequency-time based spectrum plot. Using both of these plots, overviewed extracted features of the dominant frequencies and the related scales can be selected for inputs to train and validate an ANN.

The purpose of this research is to classify (SEMG) signals for normal muscle activity using different extracted features in an ANN. The extracted features of the SEMG signals used in this research using CWT were the mean and median frequencies of the average power spectrum and the RMS values at scales 8, 16, 32, 64 and 128. SEMG signals were obtained for a 10 second period, sampled at 2048 Hz and digitally filtered using a Butterworth bandpass filter (5 to 500 Hz, 4^{th} order). They were collected from normal vastus lateralis and vastus medialis muscles of both legs from 45 male subjects at 25%, 50%, and 75% of their Maximum Voluntary Isometric Contraction (MVIC) force of the quadriceps.

The ANN is a computer program which acts like brain neurons, recognises, learns data and produces a model of that data. The model of that data becomes the target output of an ANN. Using the first 35 male subjects' data sets of extracted features, the ANN was trained and then validated with the last 10 male subjects' data sets of the untrained extracted features. The results showed how accurate the untrained data were classified as normal muscle activity.

This methodology of using CWT for extracting features for analysing and classifying by an ANN for SEMG signals has shown to be sound and successful for the basis implementation in developing an intelligent SEMG signal classifier.

Table of Contents

List of Figures

List of Tables

Statement of Originality

'I hereby declare that this submission is my own work and that, to the best of my knowledge and belief, it contains no material previously published or written by another person nor material which to a substantial extent has been accepted for qualification of any other degree or diploma of a university or other institution of higher learning, except where due acknowledgement is made in the acknowledgements.'

Jeff Kilby

31 October 2005

Chapter 1
Introduction

1.1 Background

Feature extraction and pattern recognition is the key in processing and analysing biomedical signals. The use of the signal analysis is apparent in the field of clinical health for diagnosing health related problems and rehabilitation using biomedical signals such as Electrocardiography (ECG or EKG) and Electromyography (EMG) signals. The EMG signals, also commonly known as myoelectric signals, are obtained by means of recording the electrical activity of striated muscle using sensors or electrodes. ECG signals from the heart record the signals from the heart activity whereas EMG signals are from the skeletal muscles and record the activity of muscle as it contracts during movement.

An accurate and computationally efficient means of classifying myoelectric signal patterns has been the subject of considerable research effort in recent years where having effective feature extraction is crucial for reliable classification [1]. Numerous research and studies concentrated on feature extraction and pattern recognition in the biomedical signal or biosignal processing have achieved tremendous contribution to the facilities developed and available for the signal analysis in the clinical field today.

With computers and software becoming more and more powerful tools which are able to process complex algorithm on numerous data at high speed, the advancement in digital signal processing applied to biomedical signals is an inevitable one and ongoing. Software such as LabVIEW and MATLAB are well known for their use in mathematical processing and virtual instrumentation for laboratory requirements. They are commercially available where both have built-in functions or tools for signal processing.

In signal processing, determining the *frequency content* of a signal by Fourier transform is one of the main aspects in feature extraction and understanding the characteristics of a signal. However, obtaining the frequency content alone is not sufficient for analysing biomedical

signals due to it being non-stationary in nature [2, 3]. Fourier transform loses the time information after transforming time-based signal to frequency-based signal.

It is an essential and in the interest of analysing biosignal to obtain 'time-based' information of when a particular frequency content occurs [3, 4]. *Wavelet transform* is a method capable of achieving this so called the *time-frequency content* or the *time-frequency based representation.*

Other aspects of a signal such as the *mean* and *median frequency* of the *power spectrum* and the *(RMS)* value of signal's electrical potential also play an important role to the whole task of features extraction for signal characterisation. The ultimate aim of this exercise is to develop a system with the ability for signal classification by features, a powerful and promising tool for diagnosing problems.

The application of wavelet transform in analysing biological signals has only become increasingly developed in the last fifteen years [3, 5]. The wavelet theory is a relatively recent mathematical development where its application is a potentially promising and exciting area of research. Its application to the analysis of EMG signals is even more recent [3].

In the field of Surface Electromyography (SEMG), wavelet analysis has not been as widely used compared with the ECG signals [3, 4]. Some of the other established research in this field did not provide and record many details on the procedure in developing and designing the software system to process SEMG signals with wavelet analysis. In addition to this scarcity of the extensive use of wavelet analysis in SEMG signals feature extraction, there is no prominent system yet developed to manage and file these signal features. Building records of a database of the signal features is of importance in creating a system to the further use in signals classification.

SEMG uses surface electrodes placed on the skin overlying the muscle observed. The other common EMG uses needle electrodes penetrated into the muscle, thus signals obtained are focused on a particular muscle motor unit. Needle EMG is an invasive method which can cause stress to the patient involved [6], hence SEMG is a preferable method of gathering

signals. Further, SEMG obtains signals sourced from a group of muscle rather than one single muscle unit.

In summary, there are practical gaps which need to be filled by this research within the use of wavelet analysis for SEMG signal processing. This research designed and developed appropriate practice-oriented methodology and descriptive procedures for SEMG signal acquisitions, feature extraction processing, classification and validation by Artificial Neural Network (ANN).

This research explored and demonstrated the ability and potential in achieving reliable means for the diagnostic equipment development of a SEMG signal analyser using comparative database by this proposed technique.

The following sections discuss the background of muscles, EMG signals and reviews recent developments in the literature relating to SEMG, wavelet analysis and the application of ANN in research. The aim, objectives and research methodology are also presented.

1.2 Muscles and Surface Electromyography Signals

The study of electromyography signals or EMG signals is the study of muscle activity obtained in the form of electrical signals. EMG is sometimes referred to as myoelectric activity. EMG is measured using similar techniques to that used for measuring ECG and other electrophysiological signals such as electroencephalography (EEG) in sleep assessment [7].

A muscle is comprised of many small fibres. In humans, the muscle systems are classified based on by their appearance and location of cells [8]. The two types of muscles are striated muscle and smooth muscle (non-striated). Striated muscle includes skeletal and cardiac muscle. Skeletal muscle is almost exclusively attached to the skeleton and constitutes the bulk of the body's muscle tissue. Skeletal muscle contraction maintains posture and produces movement. Its structure is composed of multinucleated skeletal muscle fibres shown in Figure 1.1. This is the type of muscle where EMG is applicable. Cardiac muscle allows the

heart to contract and propel blood through the circulatory system. It is regulated by the sinoatrial node or the heart's pacemaker where its signal study is known as ECG. The smooth muscle differs in structure from that of striated muscle as it is composed of elongated, thin fibre and contains a single nucleus. Its major role is in the physiologic regulation of the airways, blood vessels and gastrointestinal tract [8].

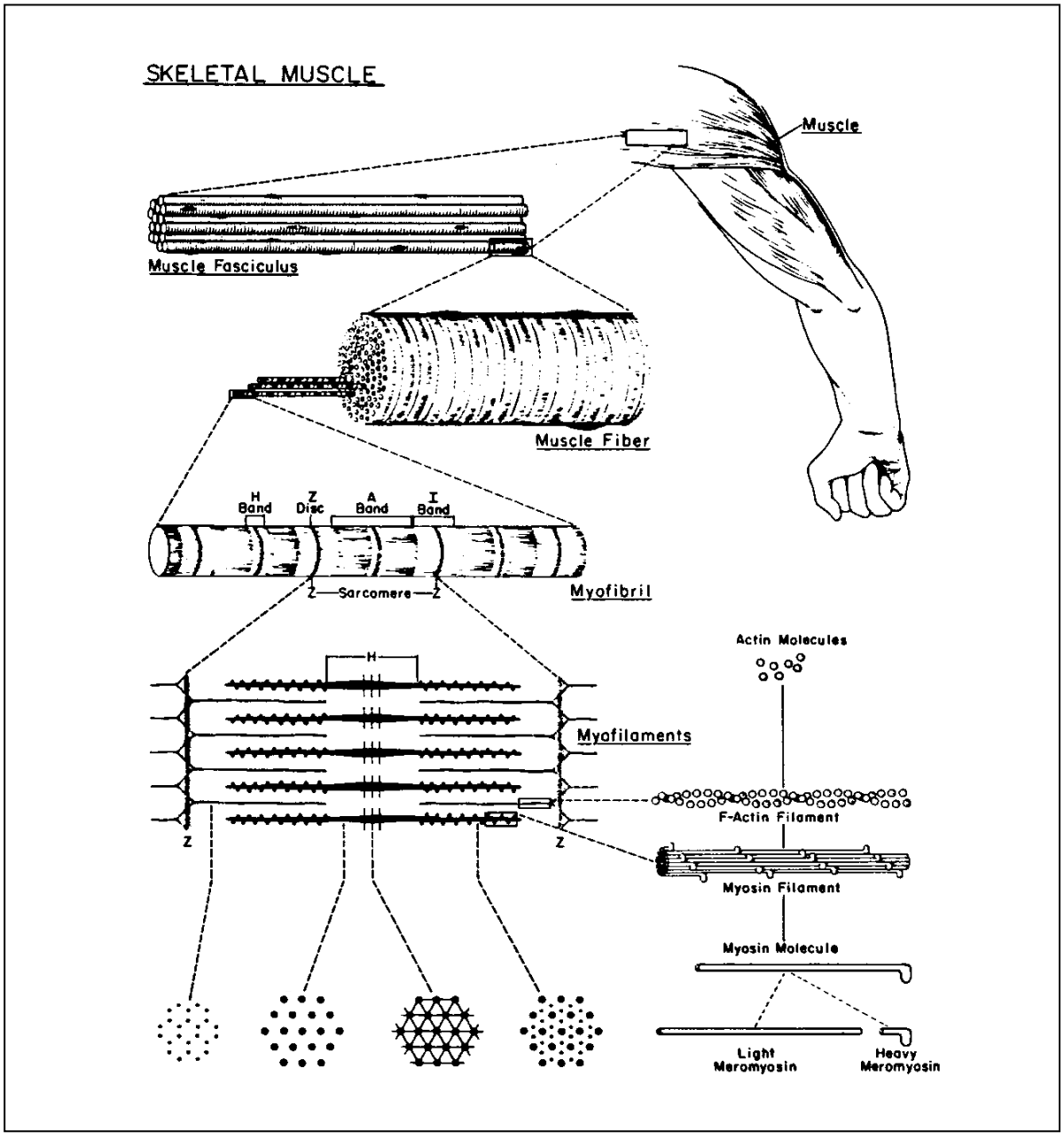

Figure 1.1 Diagram of the organisation of the skeletal muscle from the gross to the molecular level. Cross section F, G, H and I are at levels indicated. Sourced from Bullock J, Boyle, J and Wang, M B: textbook of Physiology, ed 3, Philadelphia, PA, Williams & Wilkins, 1995 [8].

Skeletal muscle consists of groups of motor units [9]. A motor unit is made up of all skeletal muscle fibres supplied by one motor neuron from the spinal cord. A muscle can have few or many motor units associated with them. A muscle with many motor units is capable of more precise movements than a muscle with fewer motor units for the same number of muscle fibres [9].

Within the study of EMG, normal striated muscle is electrically silent at rest [10], but when it is active, as during contraction or stimulation, an electrical current is generated. When a muscle contracts, microvolt level electrical signals are created within the muscle which can be measured from the surface of the body [11]. The action potentials produced by the muscle cells induce potential differences in the overlying skin that can be recorded by surface electrodes. The more fibres that are stimulated the stronger the muscle contracts and a greater force is produced. The successive action potentials or electrical impulses produced by the muscle activity can be displayed on a cathode-ray oscilloscope screen in the form of continuous wavelike tracings.

Surface electromyography or SEMG, which is the focus of this research, is the procedure that measures muscle activity from the skin. Through the application of SEMG, the combination of electrical activity or action potentials from the numerous muscle fibres that contribute to a muscle contraction can be collected and analysed [12].

The EMG signal from the muscle is sensed by electrodes placed on the skin surface overlying the muscle and then sent to a computer. The EMG signals are collected in data files where they are then processed and analysed using special mathematical procedures. Procedure such as wavelet analysis allows the frequencies within the EMG signal to be broken down into features. The features represent the electrophysiological characteristics of the muscle fibres contributing a muscular contraction [13]. These measures can also be related to force production [14], muscle fatigue [15] and deficits in the musculoskeletal system [16].

The amplitude characteristics of SEMG signals have a random or stochastic behaviour with no periodic form in the wave pattern as there is in the ECG signals [13]. The amplitudes of these signals can range from 0 to 10 mVpp or 0 to 1.5 mV_{rms} [14, 17]. The usable frequency range of the signal is between 0 to 500 Hz, with dominance being in the 50 to 150 Hz range [17]. Usable signals are those with energy above the electrical noise level. Signals above

500 Hz is considered noise and does not contain much important information and hence it needs to be filtered out by a low pass filter [14, 17].

Hence, SEMG signals are the summation of electrical activity of muscles. Since surface electrodes are placed on the skin surface, the signals contain information from all muscle activity within the 'pick-up' range of the electrodes, so not necessarily summation of activity from one motor unit. SEMG represents the average motor unit activity of most superficial muscles whereas using needle EMG, electrical activity obtained from muscle contraction is represented as the motor unit action potential (MUAP) as produced from a single anatomical motor unit [18].

The benefits of SEMG over needle EMG is that it provides unique spatial information besides the conventional MUAP variables such as amplitudes [19]. These extra spatial features are of the endplate position that determined the fibre length, the depth and direction of MUAP. SEMG is also non-invasive and patient friendly whereas patient acceptance for needle EMG is limited due to pain. However, needle EMG is versatile, quick and gives a unique opportunity to measure muscle membrane instability. Within MUAP variables it shows the recruitment pattern and spontaneous activity while SEMG does not, but only shows the muscle fibre conduction [19]. The analysis time for needle EMG only can be taken in a short period while SEMG can be taken moderately longer. By using needle EMG, many more muscles can be analysed than by SEMG where it is limited. The analysis of SEMG signals generally uses more data in quantitative form, where although possible but not usually is used in needle EMG analysis [19].

Surface Electromyography is used to control prosthetic devices and to study neurological control in human movement. It is recently used as a diagnostic tool for the clinicians [2]. The frequency spectrum of signal has been used to determine muscular fatigue, force production and muscle fibre signal conduction velocity. The analysis at low frequency power spectrum provides information about spatial and temporal recruitment of motor units [2]. Each muscle is suggested to exhibit differing high-energy frequency bands and characteristic power spectrum, therefore it is possible to analyse SEMG patterns to see which muscle is the source of activity [2].

De Luca, one of the leading professionals in the field of biomechanics, has executed thorough research into the use of SEMG which can be grouped in three applications [20]:

1. **The activation of muscles** where **s**ignals can provide the timing sequence of one or more muscles performing a task.
2. **The force/EMG signal relationship** which provides information about the force contribution of individual muscles and groups of muscles.
3. **The use of the EMG as a fatigue index** where the signal displays time-dependent changes prior to any force modification so having the potential to predict the onset of contractile fatigue.

The difficulties in interpreting SEMG signals are due to several factors involved during signal acquisition. The SEMG signals are affected by anatomical and physiological properties of the muscles. They can also be affected by the control scheme of the nervous system and/or electronic instrumentation used to detect and record signal [2]. De Luca also described the factors that affect the information contained in EMG signal and force produced by a muscle [20]. Quantitatively the signal amplitude normally indicates the amount of torque or force measured about a joint. It is impossible to get the accurate relationship due to the complexity and interaction of the many physiological factors such as the fibre membrane properties, anatomical such as length of fibres and technical factors such as size and shape of electrode related to measurement of the force and/or accompanying muscle activity. Proper detection helps manage and minimise these effects of complexity. De Luca [20] had discussed, identified and classified these factors which gave rise to the complexity of SEMG signal measurement much in depth and details in his work which can be viewed in Appendix A.

In summary, the factors that influence the surface EMG are classified into two categories, the non-physiological and the physiological [21]. The non-physiological factors include aspects from:

- The anatomic such as due to the shape of the volume conductor, thickness of the subcutaneous tissue layer, tissue inhomogeneities, distribution of the motor unit territories in the muscle, size of the motor unit territories, distribution and number of fibres in the motor unit territories, length of the fibres, spread of the endplates and

tendon junctions within the motor units, spread of the innervation zones and tendon regions among motor units.

- The detection system such as from the skin electrode contact that gives impedance and noise to the signal, spatial filter for signal detection, interelectrode distance, electrode size and shape, inclination of the detection system relative to muscle fibre orientation and location of the electrodes over the muscle.
- The geometrical where muscle fibre shortening occurs and shift of the muscle relative to the detection system.
- The physical such as from the conductivities of the tissue and amount of crosstalk from nearby muscles.

The physiological factors that influence the SEMG signal measurement includes [21]:

- The fibre membrane properties such as from the average muscle fibre conduction velocity, distribution of motor unit conduction velocities, distribution of conduction velocities of the fibres within the motor units and shape of the intracellular action potentials.
- The motor unit properties such as from the number of recruited motor units, distribution of motor unit discharge rates statistics and coefficient of variation for discharge rate and motor unit synchronisation.

Although all of these factors exist, it is still constructive to use EMG signal to describe the state of the muscle by placing surface EMG in the location isolated from where these factors can significantly affect the intended signal quality [20].

1.3 Literature Review on Recent Development

Research in SEMG signals range from signal acquisition techniques, surface electrodes, signal processing, electrical potential, muscle activities and algorithm design to the use of Artificial Neural Network (ANN) for signal classification. Since this research focused in the feature extraction and signal classification, this section discusses more about the recent development in signal processing for analysis or feature extraction and the application of ANN for signal classification.

Research by Anctil et al [22] discussed modelling surface electrode which recorded EMG responses. This method determined potential derived from an analytical expression instead of the standard approach of using surface electrode being presented as a series of discrete point electrodes. This method introduced and offered significant computational advantages in terms of efficiency for modelling surface electrodes potentials [22].

The field of biosignal analysis research is very wide itself. For example, Thakor and Zhu [23] focused their research more into the filtering and noise cancellation techniques of signal processing the ECG signals. Another research by Chu et al [24] used EMG activity to detect muscle activity in regards to hamstring flexibility assessment of stand-and-reach and sit-and-reach. The signal would provide a comparison of the myoelectric activities in hamstring and low back muscle during stand-and-reach and sit-and-reach and ultimately, to know which method is a potential danger in terms of high loading for muscle strain.

More recent significant advances in signal processing include research by Englehart et al [1] which was concerned with improving the accuracy of transient myoelectric signal pattern classification. This was achieved by incorporating time-frequency based representation such as the Short Time Fourier Transform (STFT), the wavelet transform (WT) and the wavelet packet transform (WPT) in the feature sets. The outcome showed an effective representation for classification in the later stage using ANN [1].

Crowe et al [4] applied wavelet transform to the Electrocardiogram (ECG) where their research preliminary results showed that wavelet transform is worthy of further investigation as a signal analysis tool for application of ECG and ECG's compression. It was discovered that wavelet transform offered an extremely efficient means of compressing raw ECG data. The wavelet transform was obtained directly by using the dilated sampled mother wavelets with the data using the discrete version of the wavelet transform.

Crowe et al research [4] showed how apparent wavelet transform was formed graphically for the ECG signals due to its periodic pattern where heart muscle contracts and beats in a rhythmical manner. It showed that by applying wavelet transform to ECG signals which is periodic in nature, you are able to extract quite easily useful information in terms of features and patterns of the original signal. However, with EMG signals which are random and non-

stationary in nature, applying wavelet analysis is much harder in terms of recognising pattern and features of the raw signal.

Sparto et al [3] used wavelet transform for their research on EMG signals of fatigued back muscles which is a risk factor for a commonly known complaint such as lower back pain. They discussed how Fourier transform was successfully being used to measure the level of muscular fatigue in terms of analysing frequency contents but with the assumption of EMG signals being stationary, which is not in nature [2, 3]. The wavelet transform is a novel technique for analysing non-stationary signals that has only recently been applied to the study of EMG. Their main objective is also to develop techniques, using the wavelet transform to analyse the EMG for quantification of the back muscle fatigue during dynamic repetitive working conditions which produce a non-stationary EMG signal.

Sparto et al [3] described and showed comparison of the frequency spectrum of the fatigue signals using both Fast Fourier transform and wavelet transform. The traditional Fourier transform could not detect temporal patterns of frequency changes as there is no information gained describing when the frequency components dominate the signal. Although a practical way to overcome this lack of temporal or time domain information is to decrease the sampling time, as it is called Short Time Fourier Transform (STFT), the common problem due to this technique is that it suffers from poor frequency resolution. Fatigue during sustained isometric contractions consistently demonstrated a shift of the frequency content of the signal from higher to lower frequencies using STFT. Hence the assumptions of stationarity of the EMG signals may be violated in most practical applications, due to variation in the tension, length and velocity of the muscle when dynamic work is performed.

Sparto et al [3] demonstrated that wavelet transform could eliminate this problem. Wavelet transform maps signals using a set of basis functions that can be designed depending on the needs of the analysis. Morlet mother wavelet was used for scaling and translating version with the original signal. The complete set of wavelet coefficients constituted the wavelet domain representation of the original signal. Thus the wavelet transform expresses a signal simultaneously in both time and frequency domains where its time-frequency transformations can be distinguished when changes in the frequency content occurred.

Sparto's experimental investigation involved subjects standing in a frame and pushing against a force sensor at 70% of their maximal voluntary contraction (MVC) strength, while extending their trunk from a forward posture of 35 degrees to upright standing, at a constant velocity of 15 degrees per second. The subject was able to control the amount of force that he was generating by obtaining feedback from a computer monitor. Ten repetitions per minute were performed and the pacing was controlled by the sound generated from the computer.

Using a bipolar surface electrode, the EMG signals were preamplified with a gain of 1000, low-pass filtered at 1000 Hz and also amplified more to obtain peak-to-peak voltage of 5 V during MVC. The signal was then digitised at 1536 Hz using 12-bit, ± 10 V range, analogue-to-digital board and stored on computer for subsequent analysis. The data from 5 exertions at the beginning (0-30 sec), middle (75-105 sec) and end (150-180 sec) of the repetitive endurance test were carried for the wavelet analysis. The wavelet decomposition of the EMG signal was performed using the Daubechies wavelet of order 4 within the Wavelet Toolbox in MATLAB. The original signal and wavelet representation of the signal was at scales 1-9. Comparison was also being made for the EMG signals analysed using STFT. The research ultimately will allow clinicians gain insight into working conditions that are likely to cause fatigue. It was proposed that if back muscle fatigue can be documented using these tools, it may be possible to make recommendations for altering potentially risky work conditions. What this paper does not present is a user friendly technique in storing and using the data for interpretating the conditions read from the signal features, which will be another further very useful procedure that can be developed.

A way of managing data of EMG signals to be used for diagnosis is through feature extraction and classification. To build a form of database for an intelligent signal classifier, a technique called the Artificial Neural Network (ANN) is increasingly well known for this type of use and capable for applications such as biosignal classification and modelling.

ANN used by Wang and Buchanan [25] was applied to the modelling of muscle activation dynamics. They developed a neural network algorithm for the muscle activation and compared it with the actual EMG signals obtained from the joint moment of arm muscles, biceps and triceps. The objective was to predict activation muscle from EMG signals and their relationship. The outcome showed that the predicted result of the ANN is similar to

actual muscle activation from the EMG signals measured in the experiment. Thus, the ANN model can be used to represent the relationship between EMG signals and joint moments well. EMG signal is correlated with muscle activity where the larger the EMG signal, the more activated the muscle is.

The introduction of ANN brought new possibilities in the development of adaptive methods of structures recognition and solving complex classification problems. Another application of ANN in classification through signal pattern recognition was used in the research of EEG artifact removal by Ksiezyk et al [26] for sleep assessment. The recognition and elimination of artifacts in EEG signal is an essential to the development of practical systems of EEG analysis. The artifacts or unwanted aspects in the raw EEG signal are such as physiological artifact of body movement and respiration and other electrical noise. The method of ANN identifying these artifacts is by certain mapping from the set of the realisation examples. However, performance of ANN depends heavily on input parameters where its outcome can be validated for different input parameter sets [26].

Birkedal et al [27] made a pattern recognition system with ANN which was able to distinguish five intentions of movement, sit down, stand up, stand quiet, walk right and walk left from subjects suffering from spinal-cord injury. This research aimed to regain voluntary control of their paralysed muscle in the lower limb by means of functional electrical stimulation using the correlation between the paralysed limb and the contraction of another non-paralysed limb from the upper body. The EMG obtained from the upper body movement was employed as a control signal to enable paralysed subjects to move again using the signal processing method. The EMG signal was processed and analysed using STFT and Continuous Wavelet Transform (CWT). ANN is used to classify a given intention of movement on the basis of the selecting features. The neural network was trained to take two approaches for the EMG data [27]. The first approach was to extract features at the moment of movement intention defined by the change of the upper limbs angles. Two thirds of the files were used to train the neural network and the last third to validate it. The second approach consisted of an extraction of several features, before, during and after the period which define the intention of movement. The system is also trained to recognise the non-intention of movement [27].

Other applications of ANN in the field of biosignal classification were shown in the works by Englehart et al [1], Ferguson and Dunlop [28] and Moshou et al [29]. Englehart et al [1] used neural networks Linear Discriminant Analysis (LDA) for statistical use and Multilayer Perceptron (MLP) for neural classifier that evaluated the performance of each form of signal representation involved, which were STFT, wavelet transform and WPT. Their emphasis of research was the signal representation that most dramatically affects the classification performance by LDA and MLP. Although this was the case, the performance of the feature extraction and the dimensionality reduction was dependent upon the capabilities of the neural network used.

1.4 Objectives and Methodology

This research is part of an ongoing research to develop an intelligent and user friendly EMG classifier. This research aims to investigate the possibility of using wavelet analysis to extract features from muscle contractions and to use ANN in training and validation as a base methodology for classifying and recognising patterns for normal muscle signals.

In this research project, wavelet analysis techniques are used to extract features from muscle fibre firing patterns and electrophysiological characteristics of muscle during varying levels of force production. By collecting data from healthy or normal subjects, a normative database is built for normal muscle signal where ultimately the ANN classifier would differentiate the abnormal from the normal muscle. It is important to develop this normative database with respect to differential diagnosis of neurological and musculoskeletal disorders. Existing research evidence clearly indicates that when any type of neurological or muscle injury occurs the recruitment and electrophysiology of the muscle is altered [30-32].

In the future, the normative database of different muscle disorders can be produced for a further research project where they can be used as a diagnostic tool for determining whether an individual may have a specific neurological and, or musculoskeletal disorder. The advantage of such technique is that it is non-invasive and relatively inexpensive. This should have implications to the wider community in terms of aiding the early diagnosis of neurological and musculoskeletal disorders. Such technique can also be used to monitor the

progression or regression and the effect of rehabilitation on musculoskeletal [33] and neurological disorders [34].

The research thus aims to construct a database of processed SEMG signals that have had their features extracted by wavelet analysis, a technique which has become more common in signal processing [16]. This allows an ANN to be developed for classifying and validating signal features where ultimately an intelligent signal classifier can be built. A commercially available database based on this type of signal processing, however, is not available at this stage. An established database will become very useful for further use and research in designing an EMG signal analyser to compare and diagnose normal or abnormal muscle.

The aims of this research are:

- To build a database by collecting SEMG signals from healthy subjects and extract features of the signals using the wavelet analysis technique.
- To train and validate data using ANN for classification of normal muscle signals.

The project comprises a number of different procedures such as program design and pre-processing; signal collection, processing and analysis or features extraction; database development, classification and validation using ANN.

To achieve these aims, the outline of the procedures are grouped into two stages which are the signal processing by wavelet analysis and signal classification by ANN.

1.4.1 Signal Processing by Wavelet Analysis

This stage of research is to conduct feature extraction of SEMG signals by building system programs to digitally process signals using the wavelet analysis technique. This system program will be developed using LabVIEW along with the MATLAB for software validation purposes. The objectives in this part of research are as follows:

1. To develop system programs using LabVIEW which is to build programs known as 'virtual instruments'. These programs are to be tested and validated using known sample signals and comparing them with results by MATLAB programs, which are built separately. Five programs are designed to analyse EMG signals using the following schemes or techniques:

    - Fast Fourier Transform (FFT) which shows the frequency spectrum and power spectrum of the EMG signals.

    - Short Time Fourier Transform (STFT) which shows the windowed frequency spectrum in terms of time. This is presented in a spectrogram.

    - Continuous Wavelet Transform (CWT) using the Morlet mother wavelet. The output is presented in a scalogram showing the scales of the wavelet in time domain. From this, suitable scales which give valuable information for determining RMS values of the signal, mean and median frequencies from the average power spectrum were selected.

    - Discrete Wavelet Transform (DWT) using the most suitable mother wavelet Daubechies (db05) [35]. This program shows the multiresolution analysis of the wavelet transform at a particular scale. Prior to the execution of discrete wavelet transform analysis, the most suitable wavelet was selected by statistical analysis of a decomposed and reconstructed EMG sample signal [35].

    - Discrete Wavelet Packet Transform (DWPT) using the mother wavelet Daubechies (db05). This program shows the signal decomposed down to level 6 on the low-pass filter tree within the time domain.

    From five of these programs, the one that gives the most satisfactory results for signal classification in ANN will be selected.

2. To collect a sufficient number of raw SEMG signals from real subjects with healthy or normal extensor knee muscles, the vastus lateralis and the vastus medialis. The participants are to undergo Maximum Voluntary Isometric Contraction (MVIC) tests.

3. To process and analyse signals by extracting their features using a program with the most suitable technique selected in step 1, which in this case is the CWT. The feature parameters obtained are the root mean square (RMS) values of the signals, the mean and median frequencies from the average power spectrum.

1.4.2 Signal Classification by Artificial Neural Network

The objectives of this stage of research are as follows:

1. To feed the extracted features of the SEMG signal data into the MATLAB's neural network toolbox in order to train the ANN to recognise the features of normal muscle signal pattern.

2. To validate the ANN signal classifier by testing it with a number of untrained normal muscle signal data.

3. Analysing and interpreting results from the tests and validations upon performance of all the developed methods involved.

Therefore apart from the general background, literature review and aim of this research as described so far in chapter 1, the following chapters are structured accordingly in line with the objectives. Chapter 2 Digital Signal Processing describes the principles of digital signal processing for biosignals which will include brief theories of Fast Fourier Transform and wavelet transform analysis. This chapter also explains the software development environment involved for the use of this research. Chapter 3 Data Acquisition and SEMG Signal Processing covers the practical procedures for data collection and the final software design for data acquisition, signal processing for analysis and feature extractions. Chapter 4 SEMG Signal Classification using Artificial Neural Network describes the development and

operation of ANN for signal training and validation. Chapter 5 Discussion and Conclusion discusses the pros and cons of the results and techniques from chapter 4 and 5 along with the conclusions and recommendations for future work in this field of research.

Chapter 2
Digital Signal Processing Techniques

2.1 Introduction

This chapter covers the principles of some digital signal processing techniques as applied to biosignals, and in particular the myoelectric EMG signals. Biosignal will be defined and its characteristics are described. The signal processing techniques as applied to EMG signal are then outlined and important aspects will be explained in more details. Moreover, this chapter presents specific brief theoretical principles underlying the feature extraction methods used, which are Fast Fourier Transform (FFT), Short Time Fourier Transform (STFT), Continuous Wavelet Transform (CWT), Discrete Wavelet Transform (DWT) and Discrete Wavelet Packet Transform (DWPT).

2.1.1 Biosignals: Definitions and Classifications

In general, biosignals can be classified as continuous or discrete [36, 37]. Continuous signals are signals that are defined at any point in time which are processed by Fourier and Laplace transforms and other analogue signal processing methods. They are refined by analogue systems such as filters, amplifiers and computers. Discrete signals are only defined at discrete points in time which can be thought of as the results of continuous signals that have been time sampled and amplitude quantised. This means that a certain time is picked and the amplitude at that time is measured. Discrete signals are processed by methods such as the Discrete Fourier Transform and treated by digital systems such as digital computers [36]. Through the use the equipment and software in this project, the process of the EMG signal utilised discrete signals since the nature of signals obtained are time sampled rather than continuous.

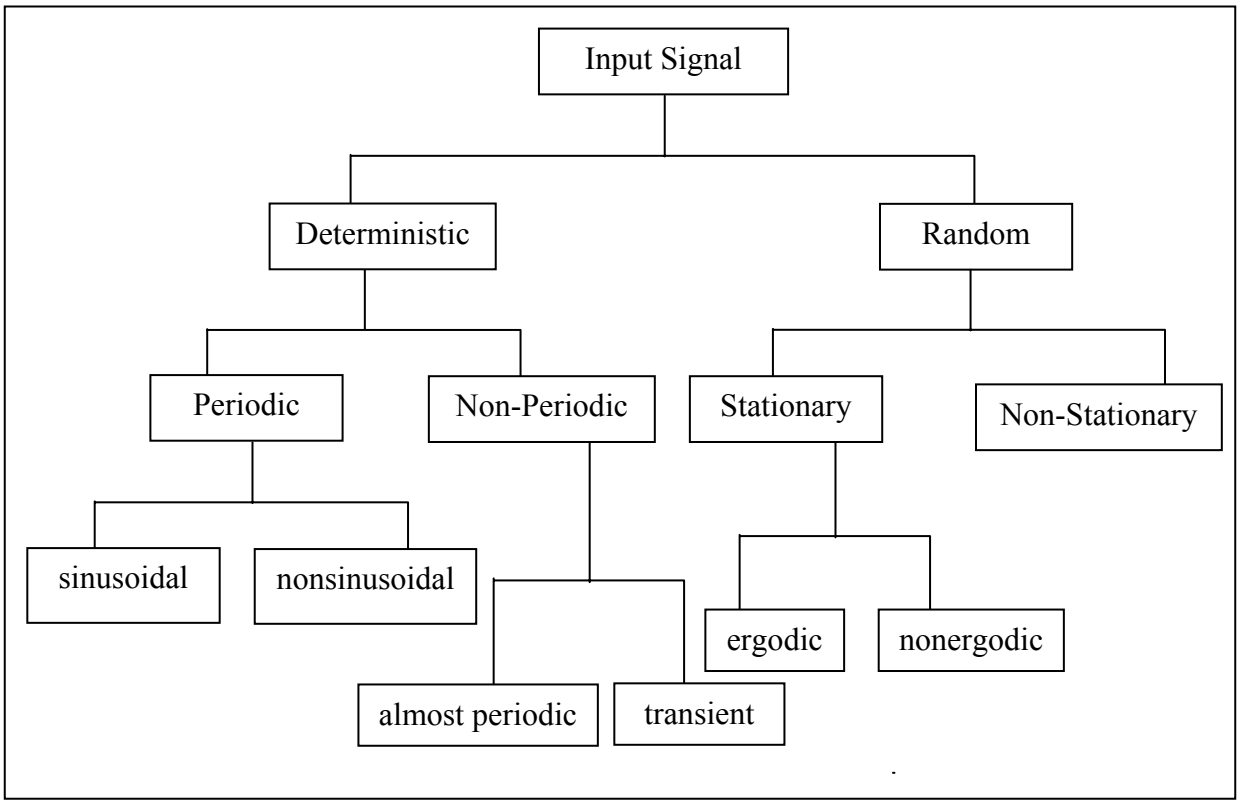

Figure 2.1 Signal classification adapted from Cohen, 1986: textbook of Biomedical signal Processing: Volume 1 Time and Frequency Domain Analysis, Boca Raton, FL, CRC Press, 1986 [36].

Biosignals can also be classified as deterministic or random. Deterministic signals can be expressed by explicit mathematical relationships whereas random signals cannot be exactly expressed. Deterministic and random signals can be further classified as drawn in Figure 2.1 which is adapted from Cohen, 1986 [36]. A signal is called to be stationary when the signal properties do not change much over time. Biosignals such as SEMG signals are random and contain numerous non-stationary or transitory characteristics: drift, trends, abrupt changes, and beginnings and ends of events [38].

2.1.2 Signal Processing: Data Acquisition

Generally, the processing of SEMG signals can be divided into three stages process [39]. The first step is data acquisition that includes amplification, analogue to digital conversion and signal conditioning. Secondly, a signal processing stage to extract desired features from the biosignal, and thirdly, a feature selection stage by retaining information that is important

for the later application such as classification of signals using an Artificial Neural Network (ANN). The schematic diagram of the stages is shown in Figure 2.2. In this research case, the signal features were selected in terms of the root mean square values (RMS) of the signals, mean and median frequencies from the average power spectrum for the purpose of training and validating ANN at the later stage.

Data acquisition involves the recording of the bioelectric activity, analogue filtering and analogue-to-digital conversion [37]. A signal is first detected at the intended biological site by using surface electrodes as sensors. The electrodes also provide interface between an electrical recording device and the biological system. After being detected by the electrode, the signal is usually amplified, filtered and converted to a digital signal. One important step is the analogue to digital conversion step or A/D step. An A/D converter measures an input analogue signal, then converts and expresses it as numerical depiction of the original signal. A/D converters essentially convert a continuous analogue signal into discrete or digital signal [37].

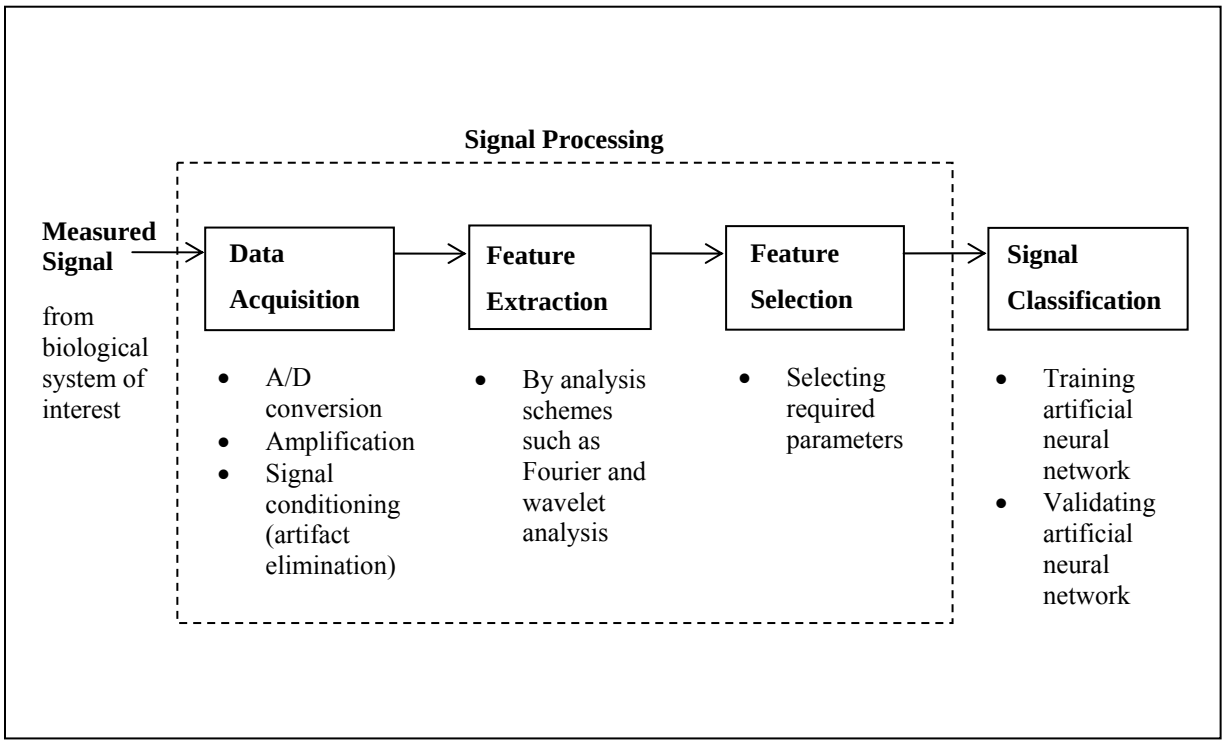

Figure 2.2 Schematic of signal processing stages.

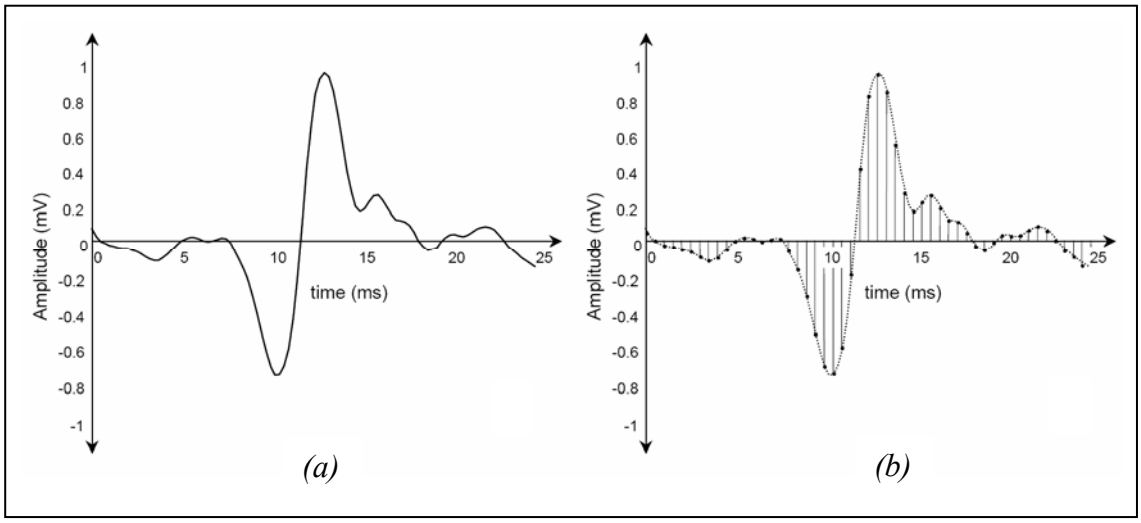

Figure 2.3 (a) A typical analogue EMG signal detected by the DE-2.1 electrode. (b) The digital sequence resulting from sampling the signal in (a) at 2 kHz (every 0.5 ms). Sourced from De Luca, G., Fundamental Concepts in EMG Signal Acquisition, Delsys Inc, 2003, Figure 2, p2 [17].

In A/D conversion, a process called *digital sampling* is executed where an example of this is depicted in Figure 2.3a where a typical analogue EMG signal or a sample Motor Unit Action Potential (MUAP) was obtained with Delsys Inc. DE-2.1 surface electrode [17]. During A/D conversion, a sequence of numbers is generated to represent the amplitude of the analogue signal at a specific point in time. The analogue signal is called to be *sampled* and the result of this number of sequence is called a *digital signal* as shown in Figure 2.3b [17].

An essential parameter involved in digital sampling is the *sampling frequency* which influences the accuracy in reconstructing the sampled signal. Figure 2.3b used a sampling frequency of 2 kHz, which means signals are sampled at every 0.5 ms.

Knowing the minimum acceptable sampling frequency is of critical importance in order to correctly reproduce the original analogue information. The rule for this is known as *Nyquist Theorem* where sampling frequency has to be ***at no less than twice the frequency of the original sampled signal*** [17]. When sampling frequency is too low, the Nyquist Theorem is violated. This leads to an incorrect reconstruction of the signal, typically referred to as *aliasing*. Aliasing occurs when the original signal is *undersampled* as not enough points have been gathered to capture all the information correctly. An example is shown in Figure 2.4

where its original signal is 1 Hz and sampling frequency is 1.67 Hz, reproducing a signal of only 0.33 Hz, a result of undersampling the original 1 Hz signal.

Comparing with Figure 2.3, the sampling frequency of 2 kHz used is more than twice the typical usable frequency range of SEMG signals between 0 to 500 Hz [17]. The recreated signal in Figure 2.3(b) is sufficiently reproduced. Figure 2.4 uses the sampling frequency of 1.67 Hz which is less than twice its original signal of 1 Hz and hence does not reproduce a correct signal.

Another important part in data acquisition is the amplification and signal conditioning which includes artifact elimination of the signals. Amplification is needed because muscle signal is generally weak and only generates in the microvolt range, which is typically 10,000 times smaller than the voltage from a flashlight battery [39]. Since the SEMG signals are small, their measurement is also susceptible to interference from electrical equipment, such as lights or movement of cable that carry signals from the body to the measuring instrument. Where signal gathering requires the subjects to perform a full range of movement exercises, interference from movement of lead wires and electrodes can be a problem. To eliminate these artifacts or 'the unwanted' interfered signal, typically a differential amplifier is used as first stage pre-amplification at the electrode site which effectively cancels the ambient electrical noise while amplifying the small physiological signal.

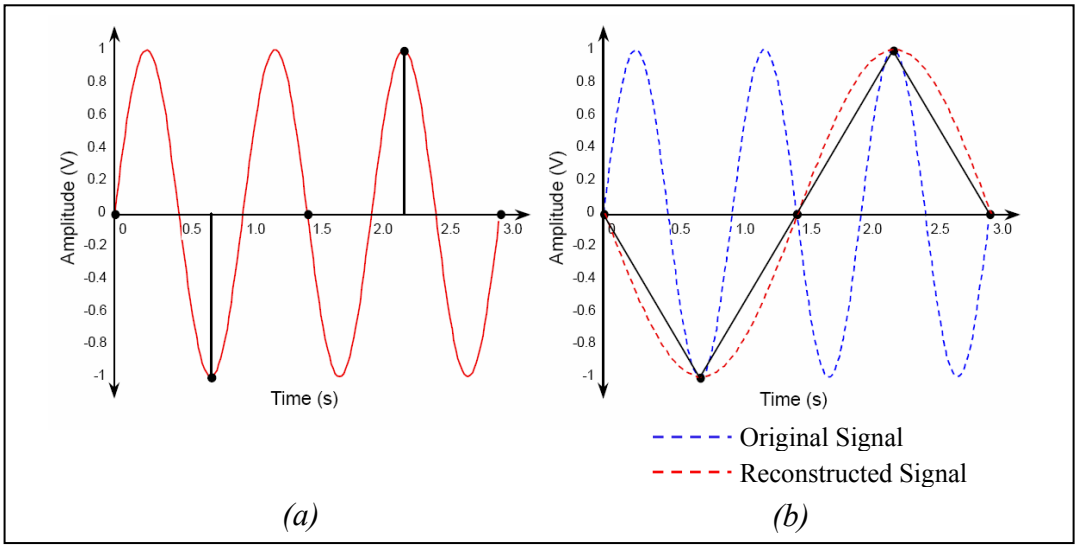

Figure 2.4 (a) Sampling a 1 V, 1 Hz sinusoidal signal at 1.67 Hz. (b) Reconstructing the sinusoid sampled at 1.67 Hz yields a signal at 0.33 Hz (interpolated). The original 1Hz signal is undersampled. Sourced from De Luca, G., Fundamental Concepts in EMG Signal Acquisition, Delsys Inc, 2003, Figure 4, p5 [17].

In the amplification process, only the signal generated by the muscle must be amplified and not other electrical noise such as ambient 50/60 Hz emissions from other AC equipment [39, 40]. In the past, it was common to remove this electrical noise by using a sharp notch filter [40], but there are problems with notch filtering because EMG has large signal components at 50/60 Hz and neighbouring frequencies. The result of notch filtering is the loss of essential EMG signal information making reliable SEMG measurement a challenge, so notch filtering should be avoided as a general rule [40]. Hence, to reduce electrical noise and gain a quality EMG signal, preamplifier is placed as near as possible to the electrode site at the pre-amplification or the first stage of amplification process [40]. Additional amplification stages may follow to refine and condition signals.

After the signal is digitised, conditioned and amplified, a digital signal processor (DSP) is used to extract the feature of the EMG that is proportional to overall muscle tension [39]. This is the second step of the signal processing which is described in the following section.

2.1.3 Signal Processing: Feature Extraction (Analysis Schemes)

The second step is the actual processing, or signal manipulation and evaluation. In this step, processing takes place to extract relevant information from the biosignal and present it to the user. The extracted feature is basically the energy envelope of the raw EMG waveform [39]. The energy envelope is the average over time of the magnitude of the EMG voltage. During feature extraction, the signal is modified and changed until the desired output is reached [36].

The EMG signal is typically analysed using a variable related to the size or amplitude of the signal [7]. When the user is interested in the amplitude of the signal, the signal is frequently rectified and averaged in some format or variable to indicate EMG amplitude. Rectified, averaged EMG, integrated EMG, and linear envelope displays can all be used to display the amplitude of the EMG signal. The second category of analysis for the EMG signal is frequency analysis, including analysis of zero crossings, spectral analysis, numerous time-frequency algorithms and many other techniques [7].

There are a range of EMG analysis schemes available for feature extraction. In the literature, a number of digital signal processing methods for analysis schemes have been applied to the SEMG signals but the most popular methods include Fast Fourier Transform (FFT), Discrete Wavelet Transform (DWT) and Discrete Wavelet Packet Transform (DWPT) [1-4, 29, 41]. The analysis techniques in which the signal is modified or processed for feature extraction are the ones which become of importance in this research. Brief theories of specific techniques selected for this research are presented in the sections 2.2 and 2.3 which include FFT, Short Time Fourier Transform (STFT), and wavelet transform analysis including DWT, DWPT and Continuous Wavelet Transform (CWT).

2.1.4 Signal Processing: Feature Selection

The third stage of signal processing is the feature selection. In general, the role of this stage is to retain information that is important for application at the later stage and discarding that which is irrelevant. Depending on what types of application, the aim of feature selection stage is to provide more efficiency by having certain variables or parameters for meeting the end purpose of signal processing. Englehart et al [1] referred to it as the dimensionality reduction where they included feature selection and projection to feed into a signal classifier. Their work on feature selection involved methods attempting to determine the best subset of the original feature set, and feature projection to determine the best combination of the original features. Their overall aim for dimensionality reduction is to have classifier a with fewer inputs and fewer adaptive parameters which should lead to a classifier with better generalisation properties [1].

In this research, the signal features were selected in terms of the root mean square (RMS) value of its electrical potential and mean and median frequencies of the power spectrum. These parameters will be discussed theoretically in the last section of this chapter. The database of the selected features were developed and recorded with Microsoft Access program.

2.2 Fourier Transform Analysis

Fourier transform is one of the most widely used signal analysis tools applicable to a variety of fields such as spectral analysis, digital filtering, applied mechanics, acoustics, medical imaging, modal analysis, numerical analysis, seismography, instrumentation and communications [42]. Fourier analysis is a mathematical technique for transforming a signal from time domain to frequency domain by breaking down a signal into constituent sinusoids of different frequencies. Fourier transform is a generalisation of the Fourier series where function is represented by the sum of sines and cosines. Instead, Fourier transform uses exponentials and complex numbers.

The Fourier transform of input signal $x(t)$ is defined as the following notation in equation (2.1) where ω is the angular frequency where $\omega = 2\pi f$ with f is the input frequency, $x(t)$ is the time domain signal and $F(\omega)$ is its Fourier transform represented in frequency domain.

$$F(\omega) = \int_{-\infty}^{\infty} x(t) e^{-j\omega t} dt \tag{2.1}$$

which is the sum over all time of the signal $x(t)$ multiplied by complex exponential [38].

Equation (2.1) that expresses Fourier transform calculates the frequency, amplitude and phase of each sine wave needed to make up any given signal. It is a linear transform from time to frequency domains and can be used to analyse the spectral component of a signal.

2.2.1 Fast Fourier Transform (FFT)

The most common method for determining the frequency spectrum of the SEMG signal is the Fast Fourier Transform (FFT) [43]. Since a digital computer only works with discrete data, a technique called *Discrete Fourier Transform* (DFT) is used. FFT is a practical application name employed for the DFT that maps discrete-time sequences into discrete-frequency representation given by equation (2.2) [42].

$$F(k) = \sum_{n=0}^{N-1} x[n] e^{-j 2\pi k t / N} \qquad \text{for } k = 0, 1, 2, \ldots N\text{-}1 \qquad (2.2)$$

where $x[n]$ is the input sequence, $F(k)$ is the DFT, $2\pi k$ is the angular frequency of input sequence frequency k and N is the number of samples in both discrete-time and the discrete-frequency domains.

Using the FFT, the EMG signal can be mapped from the time domain to the frequency domain. To illustrate this point, a sample SEMG signal obtained from 50% Maximum Voluntary Isometric Contraction (MVIC) of vastus lateralis, an extensor knee muscle sampled at 2048 Hz is depicted in Figure 2.5a. The frequency spectrum resulted from FFT is demonstrated in Figure 2.5b. It can be seen that the signal is random in characteristics with dominant components between 50-75 Hz. However, there is no information describing when each of the frequency components dominates the signal.

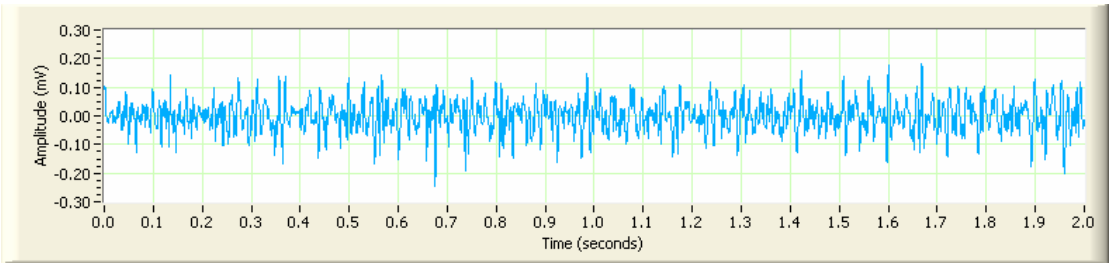

(a)

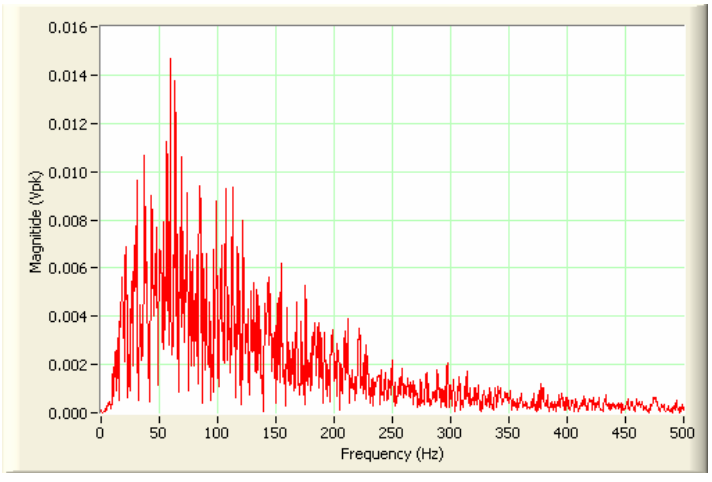

(b)

Figure 2.5 (a) A SEMG signal obtained from the vastus lateralis muscle at 50% Maximum Voluntary Isometric Contraction (MVIC). (b) Fourier transform of signal in (a) showing the frequency spectrum of signal over magnitudes in peak-to-peak voltage.

The Fourier transform of a pulse creates a unique representation of a periodic signal; the narrower the pulse, the higher the frequency, the broader its spectrum. Any periodic waveform can be synthesized by summation of sinusoids with suitable phase and amplitude relationships and any pulse can be expressed as continuous, double-sided distribution of spectral components. Each component of a complex wave is an integer multiple of the original wave.

For many signals, Fourier analysis is extremely useful because the signal's frequency content is of great importance. By using FFT, the frequency spectrum of any signals, including SEMG, are clarified and recognised by breaking down the signal into its corresponding sinusoidal of different frequencies. However, FFT has a serious drawback. In transforming to the frequency domain, signal is assumed to be stationary, hence time information is lost. When looking at a Fourier transform of a signal, it is impossible to tell when a particular frequency content of the signal took place in time [3, 4, 38]. For signal properties which do not change much over time such as a stationary signal, this drawback is not significant. However, many biomedical signals contain numerous non-stationary or transitory characteristics: drift, trends, abrupt changes, and beginnings and ends of events. These characteristics are often the most important part of the signal, and Fourier analysis is not suited to detecting them. Wavelet analysis is becoming more common in the digital signal processing method for analysing SEMG signals since it preserves the time domain of the signal [38].

An example of work by Sparto [2, 3] showed Fourier transform was successfully being used to measure the level of muscular fatigue in terms of analysing frequency contents but with the limitation of having required or assume the EMG signals to be stationary, which is not in nature.

2.2.2 Short Time Fourier Transform (STFT)

In an effort to correct this deficiency, Dennis Gabor (1946) adapted the Fourier transform to analyse only a small section of the signal at a time using a technique called windowing the signal [38]. Gabor's adaptation, called the Short-Time Fourier Transform (STFT), maps a

signal into a two-dimensional function of time and frequency. The STFT represents a useful compromise between the time- and frequency-based views of a signal. It provides some information relating to 'when' and 'at' what frequencies a signal event occurs [38].

However, this information is obtained with limited precision, and that precision is determined by the size of the window. While the STFT compromise between time-frequency based can be useful, the drawback is that once a particular size for the time window is selected, that window is the same for all frequencies. Many signals require a more flexible approach in which the window size can be varied to more accurately determine either time or frequency. This limitation can also be addressed by wavelet transform analysis. Table 2.1 shows the quality of resolutions that depend on the window size [44]. In general, a narrow window gives good time resolution but poor frequency resolution and a wide window results in poor time resolution but good frequency resolution.

Table 2.1 Time and frequency resolution by window width.

Narrow Window	Good time resolution	Poor frequency resolution
Wide Window	Poor time resolution	Good frequency resolution

The cause of this condition is due to the time and frequency which are dependent according to the Heisenberg uncertainty principle [45], which states that the product of the standard deviation in time and frequency is limited by:

$$\Delta\omega\Delta t \geq \frac{1}{2} \tag{2.3}$$

This means that decreasing the deviation in frequency or increasing the resolution must result in an increase in the deviation in time or decrease in resolution and vice versa. This is the fundamental weakness of the STFT. The boundary of the Heisenberg Uncertainty Principle is reached if a Gaussian window is used. Another serious drawback of STFT is that it also assumes signal stationarity within the window size, hence not suitable for processing biomedical signals which normally are non-stationary in nature [2].

The concept of STFT is simply by multiplying the time domain signal $x(t)$ which is to be analysed, with an analysis window $\gamma*(t-\tau)$ where τ is the time delay and then compute the Fourier transform of the windowed signal. This is expressed as in the equation (2.4) [46].

$$F_x^{\gamma}(\tau,\omega) = \int_{-\infty}^{\infty} x(t)\gamma*(t-\tau)e^{-j\omega t}dt \tag{2.4}$$

where $F_x^{\gamma}(\tau,\omega)$ is the STFT of time domain signal $x(t)$, ω is the angular frequency where $\omega = 2\pi f$ with f is the input frequency, $\gamma*$ is the window and τ is the time delay. The STFT of a discrete-time signal $x[n]$ is obtained by replacing the integration in equation (2.4) by summation defined in equation (2.5) [46].

$$F_x^{\gamma}(m,e^{j\omega}) = \sum_n x[n]\gamma*(n-mN)e^{-j\omega n} \tag{2.5}$$

Frequency ω is normalised to the sampling frequency where the sampling rate is higher than the rate used for calculating the spectrum. The short-time spectrum is a function of the discrete parameter m and the continuous parameter ω where in practice the discrete frequencies used are

$$\omega_k = 2\pi k/M, \quad k=0,\ldots,M\text{-}1 \tag{2.6}$$

thus

$$F_x^{\gamma}(m,e^{j\omega}) = \sum_n x[n]\gamma*(n-mN)e^{-j2\pi k/M} \tag{2.7}$$

The squared magnitude of the STFT, $\left|F_x^{\gamma}(\tau,\omega)\right|^2$ is called *spectrogram* illustrating the energy distribution along the frequency direction at a given time [46, 47]. An example of a signal processed by STFT is illustrated in Figure 2.6. Similarly, Figure 2.6a, like in Figure 2.5a, is a sample SEMG signal obtained from 50% MVIC of vastus lateralis, an extensor knee muscle sampled at 2048 Hz. Figure 2.6b is the spectrogram that demonstrates the results of STFT of the signal in Figure 2.6a. The window length selected is 0.5 seconds with an overlapping of 0.25 seconds and the brighter lines in the spectrogram represent the amplitude of the frequencies that dominate within the window length appointed. With the windowing, it clearly shows the time of when the frequency occurs. Between the duration of 0.25-0.50 seconds from the initial contraction, the dominant frequency is 75 Hz. Also between the duration of 1.0-1.25 seconds and 1.25-1.50 seconds, the dominant frequencies are between 50-75 Hz.

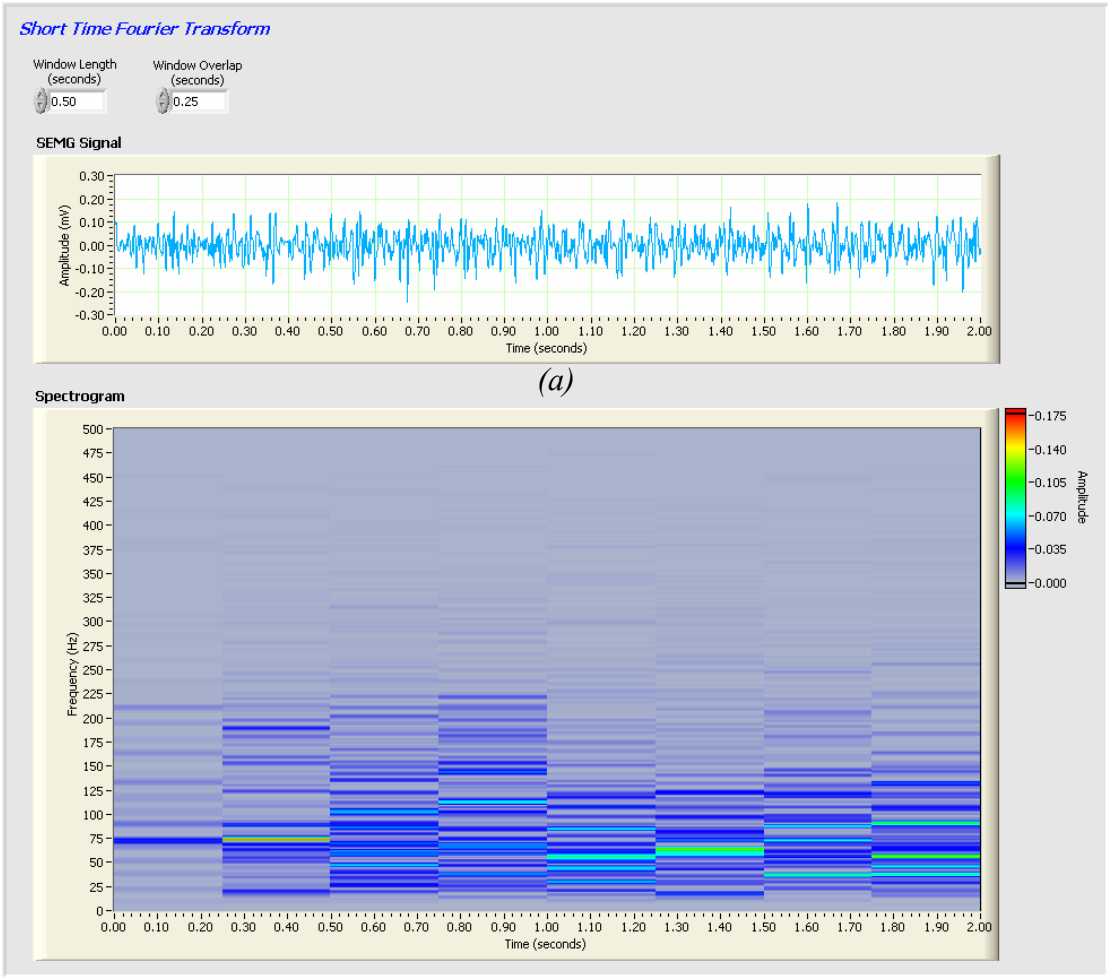

(a)

(b)

Figure 2.6 (a) A SEMG signal obtained from the vastus lateralis muscle at 50% MVIC. (b) Results of STFT showing spectrogram of the frequency spectrum of signal with time of occurrence.

2.3 Wavelet Transform Analysis

The extra feature obtained from the wavelet analysis is the presence of a time frame or frequency-time domain of when precisely the signals are acquired. Therefore, instantaneous property information of the signals is available for the analysing purposes. Considering the STFT, the time-frequency resolution depends on only the size of the window. A short window leads to a high resolution in time but a low-frequency resolution. This resolution problem suggests that there are needs to use variable lengths in analysing windows with short ones for high frequencies and long ones for low frequencies [45]. Wavelet transform is the

method which is able to accommodate this with the use of related time-scale analysis, thus providing a flexible time-frequency resolution. The wavelet analysis does not use a time-frequency region, but rather a time-scale region [38].

The basic idea underlying wavelet analysis is expressing any general signal as an infinite series or linear combination set of wavelet functions. Each element in the wavelet set is constructed from one prototype of original window, called the *mother wavelet* [45, 48]. This set of function can also be called a wavelet family obtained by manipulating the mother wavelet in two ways. One way is to move the mother wavelet to various locations on the signal called translating or shifting. Another way is to dilate or compress the mother wavelet, called scaling. Translation and scaling are used to convert the frequency of the mother wavelet into *daughter* wavelets.

Dilating the mother wavelet produces a low frequency daughter wavelet that maps onto a lower frequency region of the signal [38, 49]. The dilated or wider wavelets represent high scale numbers in wavelet analysis. On the other hand, compressing or squeezing the mother wavelet produces a high frequency daughter wavelet that maps onto a higher frequency region of the signal. The narrow or squeezed wavelets represent lower scale numbers in wavelet analysis. These daughters are also time-varying signals superimposed on each other in synchronisation. Thus, wavelet analysis allows the use of long time intervals for more precise low-frequency information, and shorter regions for high-frequency information [38, 49].

Figure 2.7 showed samples of Daubechies 05 (db05) mother wavelet with (a) as the original wavelets, (b) as the dilated or stretched wavelet at high scale number mapping onto lower frequency signal range and (c) as the compressed wavelets at low scale number mapping onto higher frequency signal range.

Wavelet transform uses basis function or mother wavelet that have time width adapted to each frequency band [38]. The wavelet is a smooth, oscillating function showing a bandpass character with localisation both in time and in frequency. Wavelets are used to transform the signal under investigation into *time-scale* representation which presents the signal information in a more useful form. The idea of relative time-frequency resolution allows the time-scale component to be considered as related by a time translation and a time stretch.

This is unlike the STFT that adopts the fixed time-frequency resolution, a time translation and a frequency shift [38].

Wavelet transform can also be used to perform multiresolution signal decomposition. This process is considered sub-band coding technique which offers data compression and can be implemented using efficient pyramidal algorithms. Results of a particular research in compression and reconstruction of ECG data indicated that wavelet transform is well suited and capable of this task [4].

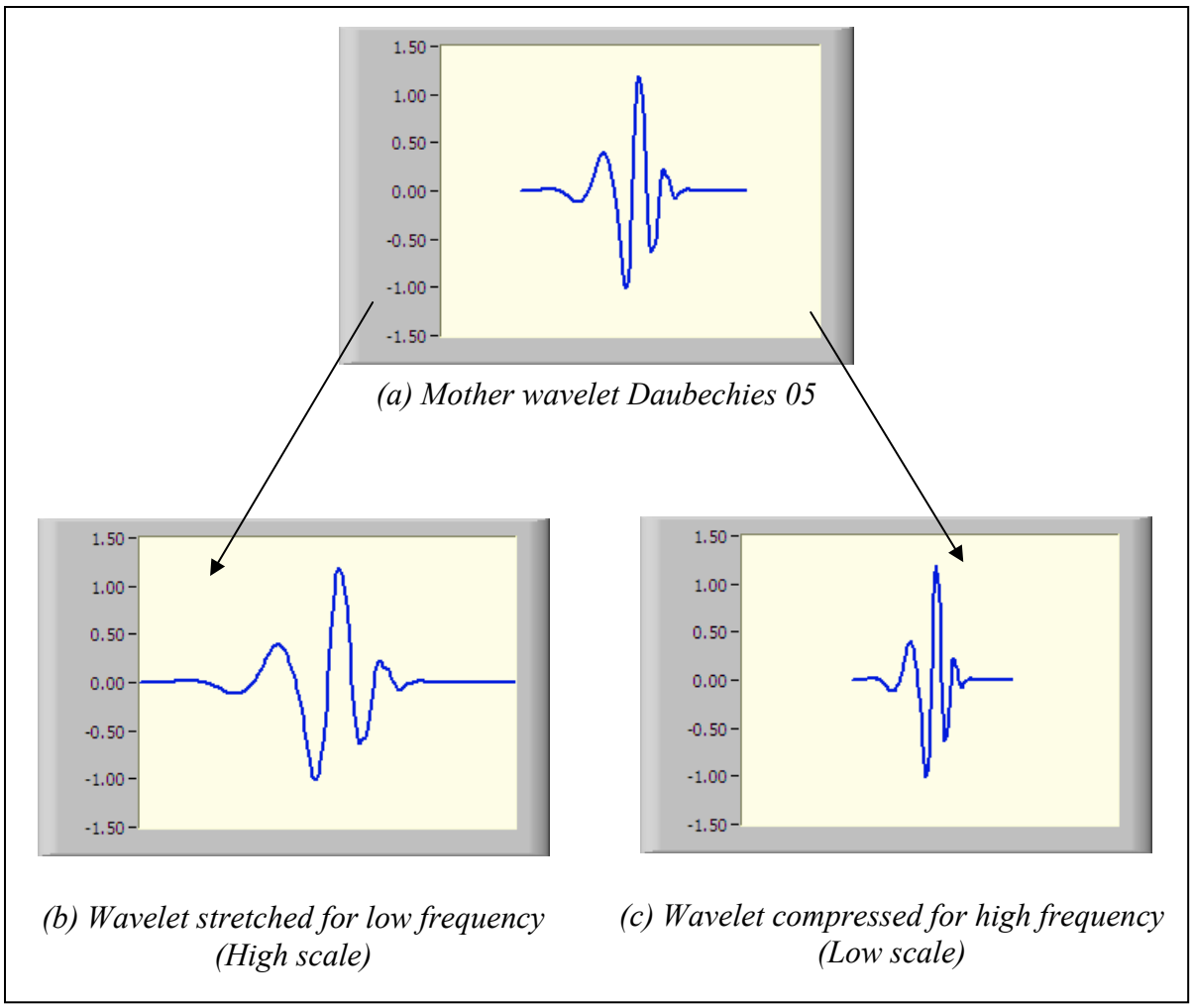

Figure 2.7 (a) Original mother wavelet of Daubechies 05 (db05). (b) Dilated mother wavelet. (c) Compressed mother wavelet.

Wavelet analysis has the advantages of having the ability to localise singularities more accurately in time domain [2-4, 38, 41, 48-50]. It produces near perfect reconstruction from the transform coefficients without the requirement of over sampling. This fact means wavelet transform has better time resolution at varied and higher scales than STFT which has identical resolution throughout. It also gives efficient implementation by pyramidal algorithms and that the scaling operation by dilation makes it a suitable method for the investigation of fractals [2-4, 38, 41, 48-50].

The mathematical expression of a wavelet family which consists of members or daughter wavelets, $\psi_{a,\tau}$ is obtained by scaling and time shifting of the mother wavelet $\psi(t)$ defined in equation (2.8) [45].

$$\psi_{a,\tau}(t) = \frac{1}{\sqrt{a}}\psi\left(\frac{t-\tau}{a}\right) \tag{2.8}$$

where $a \in \Re^+$ represent scale parameter, $\tau \in \Re$ represent the translation parameter. When a becomes large, the basis function $\psi_{a,\tau}$ becomes a stretched version of the prototype, which emphasises the low-frequency components. A small a contracts the basis function $\psi_{a,\tau}$ and stresses the high-frequency components. However, the shape of the basis function will always remain unchanged [45].

Since $\psi(t)$ can be implemented as a bandpass filter whose centre frequency can change, at a given scale, the filter yields wider or narrower frequency-response changes depending on the centre's frequency. This time-scale expression has an equivalent time-frequency expression. Since wavelets are well localised around a non-zero frequency f_0, at a scale a=1 (i.e. the mother wavelet), there is an inversely proportional relationship between scale and frequency, given by $a = f_0 / f$. Note that the factor $1/\sqrt{a}$ in equation (2.8) is introduced to guarantee energy preservation, that is to normalise the wavelet so that it has unit energy [45].

Basis wavelet chosen can be tailored to suit the application as along as it meets certain mathematical criteria. Crowe et al [4] used the types of function that have been found to be suitable for certain applications. Certain wavelets have the approximations to the ideal, while others are exact as when derived from the solutions of the dilation equation, which give the

perfect reconstruction without over sampling. A commonly used wavelet is the *Morlet* wavelet, a complex modulated Gaussian written in equation (2.9) [49].

$$\psi(t) = \frac{1}{\pi^{1/4}} e^{j2\pi f_0 t} e^{-t^2/2} \tag{2.9}$$

$\frac{1}{\pi^{1/4}}$ is the normalisation factor which ensures that the wavelet has unit energy. $e^{j2\pi f_0 t}$ is the complex sinusoidal waveform where f_0 is the central frequency. $e^{-t^2/2}$ indicates the Gaussian bell curve and has a unit standard deviation and 'confines' the complex sinusoidal waveform. The nature of $\psi(t)$ illustrates that wavelets are oscillatory about a zero mean. It is also time-limited due to the exponential component and as wavelet transforms localise events in time, the shifted versions of the Morlet mother wavelet are produced to reconstruct the original signal.

There is several other different basis or mother wavelets. Some of the common wavelets used in practice are Gaussian wave (first derivative of a Gaussian), Mexican hat (second derivative of a Gaussian), Haar and Daubechies. Some of these wavelets such as Daubechies and Haar have several families of wavelets. These families make different trade-offs between how compactly the basis functions are localised in space and how smooth or sharp they are. Within each family of wavelets, they are divided into wavelet subclasses distinguished by the number of coefficients and level of iteration [51].

The decomposition of the signal leads to a set of coefficients called wavelet coefficients. Wavelet transform decomposes a signal into multiple frequency bands which are the time and frequency coefficients. From these, edges, noise and low frequency content can be identified. At high frequency, the wavelet transform is sharper in time. At low frequency, it is sharper in frequency. The signal can consequently be reconstructed as a linear combination of the wavelet functions weighted by the wavelet coefficients. In order to obtain an accurate reconstruction of the signal, a sufficient number of coefficients have to be computed.

Two types of wavelet transform can be defined, the continuous (CWT) and the discrete wavelet transform (DWT). These are described in the following sections.

2.3.1 Continuous Wavelet Transform (CWT)

Due to the computational condition, real-world data signals have been processed at discrete time to perform in discrete signals form. Hence, unlike the DWT, the 'continuous' character in CWT is marked by its ability to operate at any scale and positions from that of the original signal up to some maximum scale determined by the application needed for detailed analysis with available computational power. The translation of CWT is also 'continuous' during computation as the analysing wavelet is shifted smoothly over the full domain of the analysed function [38].

Similarly, the CWT is defined as the sum over all time of the signal multiplied by scaled, shifted versions of the wavelet function. Given the input signal $x(t)$, the CWT is defined in equation (2.10) [45, 52].

$$CWT_x(a,\tau) = \int_{-\infty}^{\infty} x(t)\psi^*_{a,\tau}(t)dt \tag{2.10}$$

where a represents the scale parameter, τ represents the translation diameter of time shifting and the basis function $\psi^*_{a,\tau}$ is obtained by scaling the mother wavelet $\psi(t)$ at time τ and scale a. The asterisk indicates that the complex conjugate of the wavelet function is used in the transform. It is not needed when using Mexican hat wavelet as it is a real function.

Since $\psi^*_{a,\tau}$ is defined in (2.8) hence (2.10) also can be written in equation (2.11) [46].

$$CWT_x(a,\tau) = \frac{1}{\sqrt{a}} \int_{-\infty}^{\infty} x(t)\psi^*\left(\frac{t-\tau}{a}\right)dt \tag{2.11}$$

The CWT coefficient plots are precisely the time-scale view of the signal as referred to earlier. It is a different view of signal data from the time-frequency Fourier view, but it is not unrelated. An example of signal analysed by CWT is depicted in Figure 2.8. Figure 2.8a, like in Figure 2.5a, is a sample SEMG signal obtained from a similar source sampled at 2048 Hz. Figure 2.8b is the wavelet transform plot that demonstrates the results of CWT of the signal in Figure 2.8a. The darker and brighter regions indicate larger amplitudes and stronger transforms for the corresponding scales and time of occurrence.

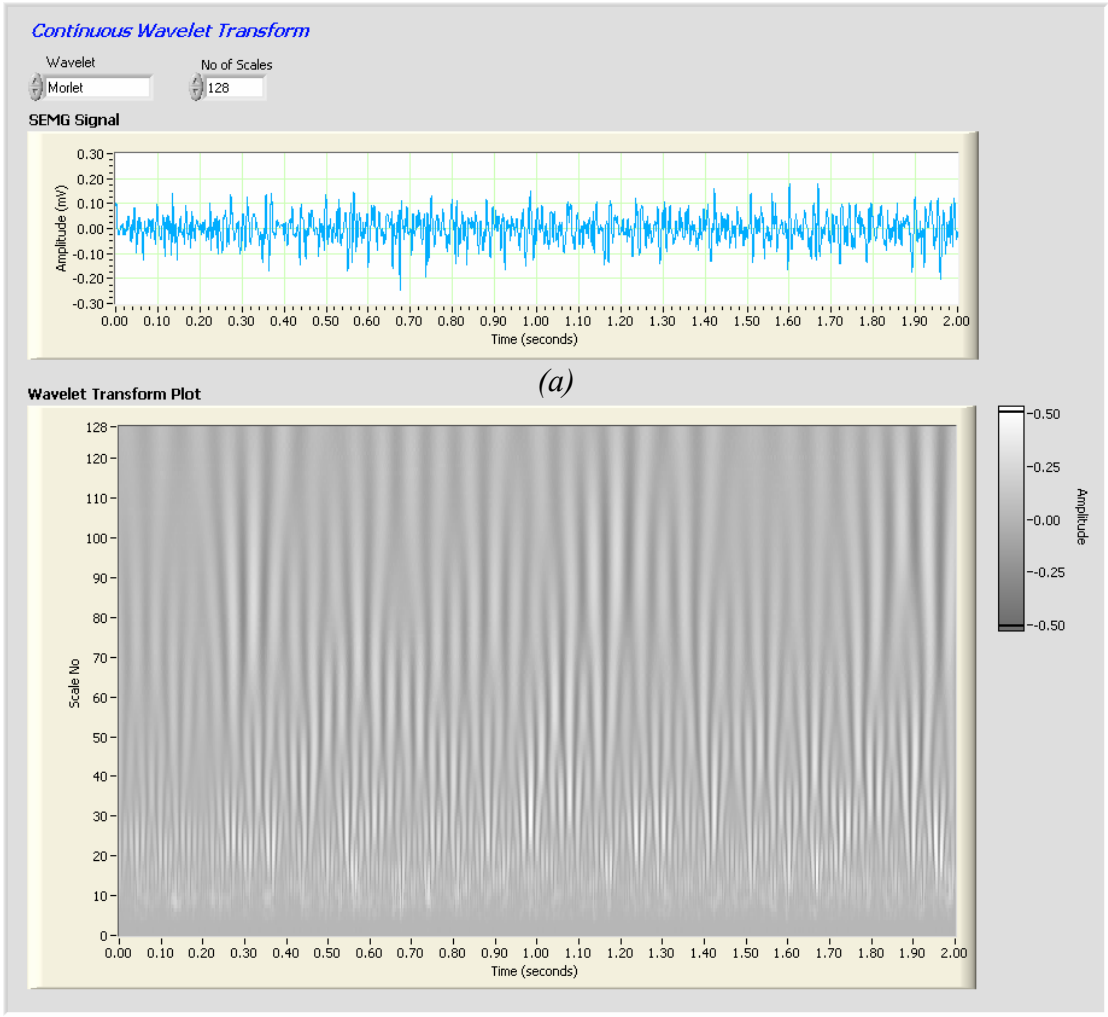

Figure 2.8 (a) A SEMG signal obtained from the vastus lateralis muscle at 50% MVIC. (b) Wavelet transform plot of results by CWT.

Another type of displaying results of CWT is the *scalogram* which is the squared magnitude or power of the wavelet transform. Equation 2.12 defines the calculation formula for the scalogram [46, 52].

$$\left|CWT_x(a,\tau)\right|^2 = \left\|\frac{1}{\sqrt{a}}\int_{-\infty}^{\infty} x(t)\psi^*\left(\frac{t-\tau}{a}\right)dt\right|^2 \tag{2.12}$$

Scalogram, like spectrogram, can be represented as images in which intensity is expressed by different shades of grey. Figure 2.9(b) depicts scalogram for $x(t)$ of signal in Figure 2.9(a) sourced from the same subject as in Figure 2.5(a).

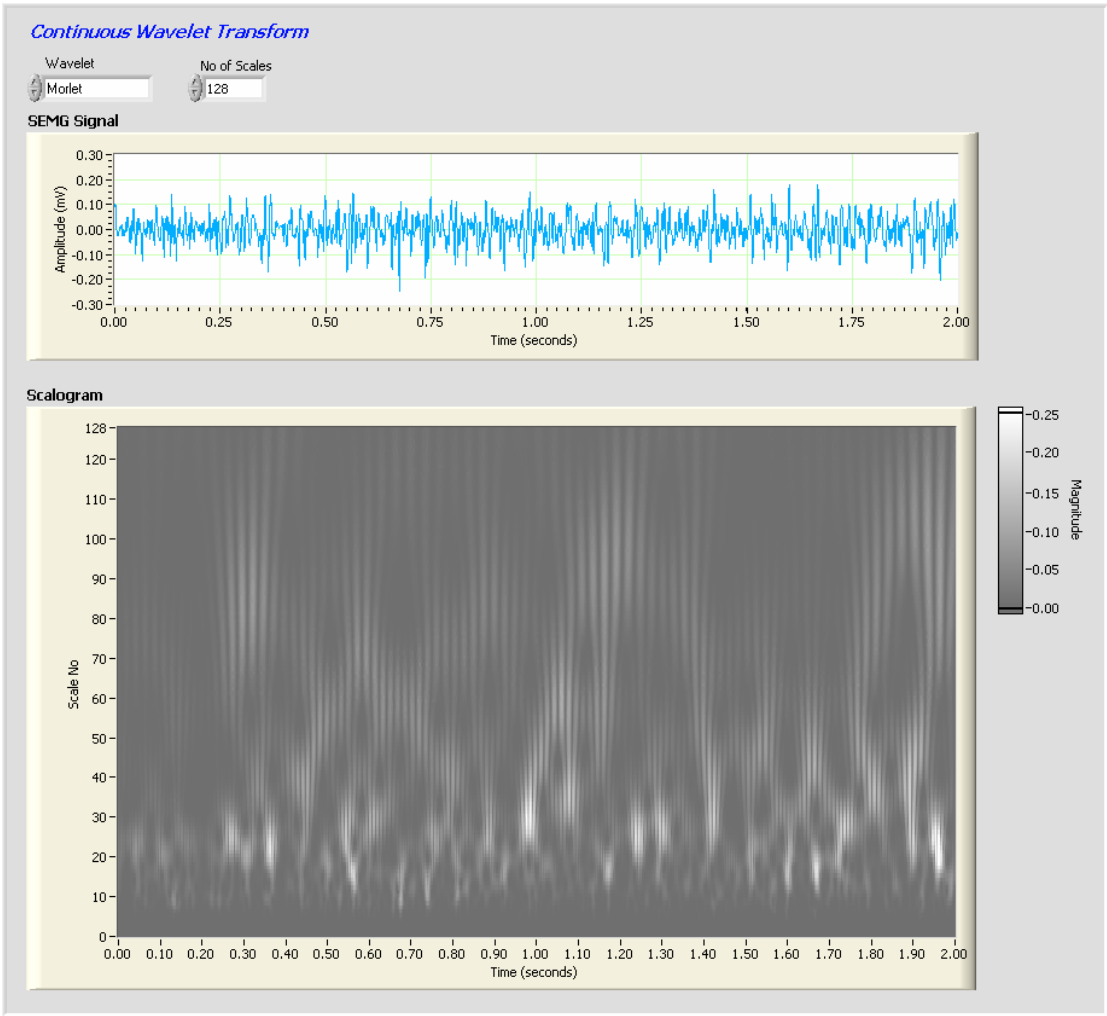

(b)

Figure 2.9 (a) An SEMG signal obtained from the vastus lateralis muscle at 50% MVIC. (b) Scalogram of results by CWT showing stronger transform at the brighter region.

The scalogram, which is the power factor of a wavelet transform plot, gives better definitions on the dominant scale components and time localisation. The scalogram contains the energy distribution along time and scale [45].

2.3.2 Discrete Wavelet Transform (DWT)

Discrete Wavelet Transform (DWT) uses the *multiresolution analysis* (MRA) based on multirate filter banks. The multiresolution theory was developed by Mallat, Daubechies and Meyer [38, 45, 46]. While the translation of CWT is carried out in a smooth continuous fashion, DWT is in discrete steps. DWT applies to discrete sequences $\{x[n], n \in Z\}$ where time is also in discrete form.

The wavelets used in DWT are discrete versions of the continuous wavelets used in CWT. Transforming wavelets to discrete signals partially depends on the chosen algorithm. However, it does not explicitly calculate a digitised version of mother wavelet $\psi(t)$. Rather, DWT acts as a bank of low-pass and high-pass filters that decompose a signal into multiple signal bands. The decomposition process can be iterated, with successive approximations being decomposed in turn, so that one signal is broken down into many lower resolution components. This is called the wavelet decomposition tree as seen in Figure 2.10.

The level of decomposition or analysis to show the frequency content of a signal by DWT is referred to as *scale index*. Since the analysis process is iterative, in theory it can be continued indefinitely. In reality, the decomposition can proceed only until the individual details consist of a single sample or pixel.

The output from the low-pass filter $G_0(k)$ is a smoothed version of the input signal $x[n]$ where the high-frequency components of the signal are removed. The high-pass filter $G_1(k)$ removes the low frequency components and the result is a signal containing high-frequency component details of the input signal.

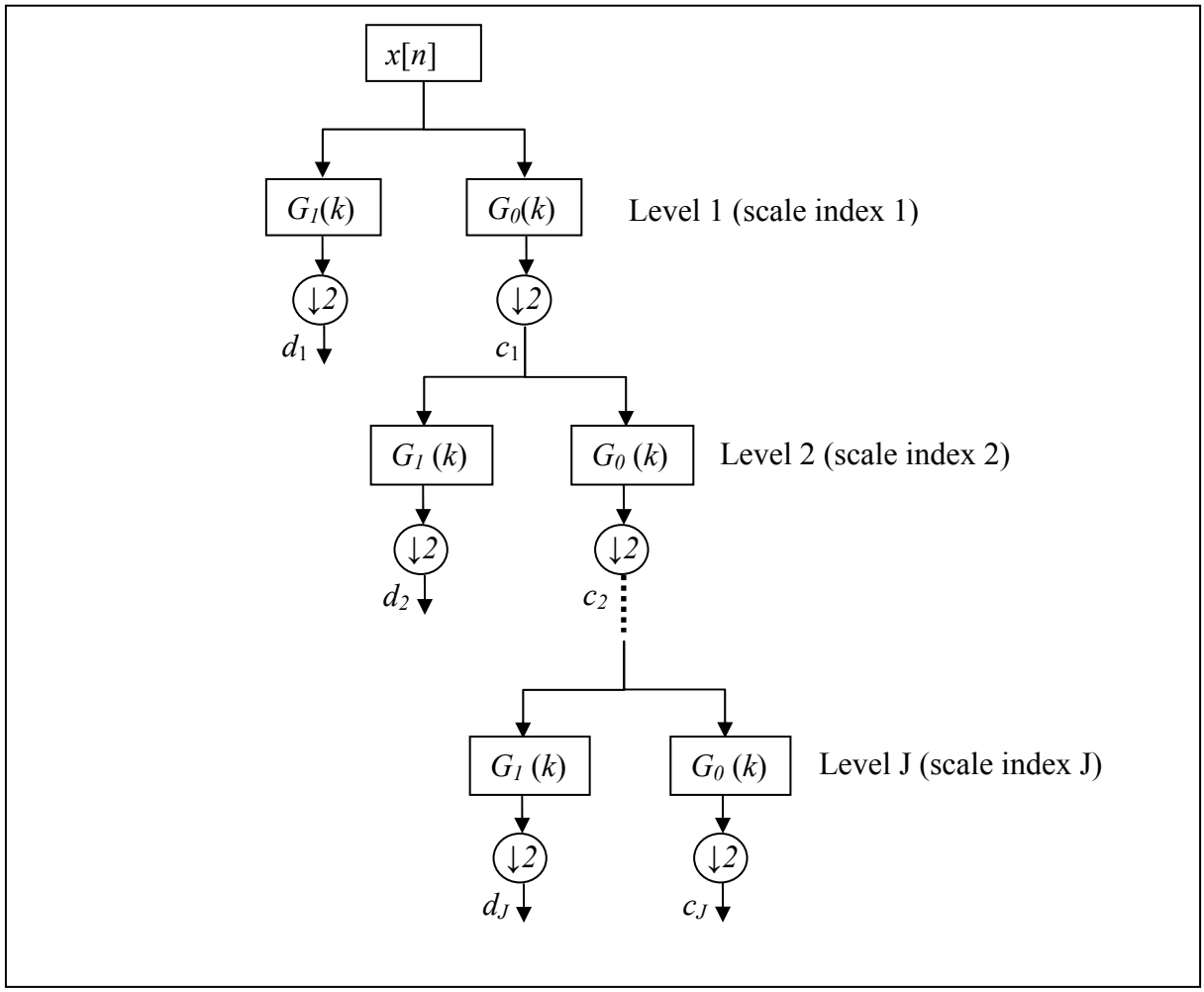

Figure 2.10 Wavelet decomposition tree or analysis filter bank using the DWT pyramid algorithm, where input signal is filtered recursively with pairs of low-pass $G_0(k)$ and high-pass $G_1(k)$ filters. The output from each filter is subjected to down-sampling by a factor of 2, denoted by '2↓'.

In a digital operation, when the original signal $x[n]$ passes through the two filters, the output emerges as two signals with the same number of data. Thus the number of output data obtained will be twice as many as the number from the start. In order to avoid this, *down-sampling* the filtered sequences by a factor of two or on a dyadic grid 2^j is performed. An example to illustrate comparison of results with and without down-sampling is depicted in Figure 2.11.

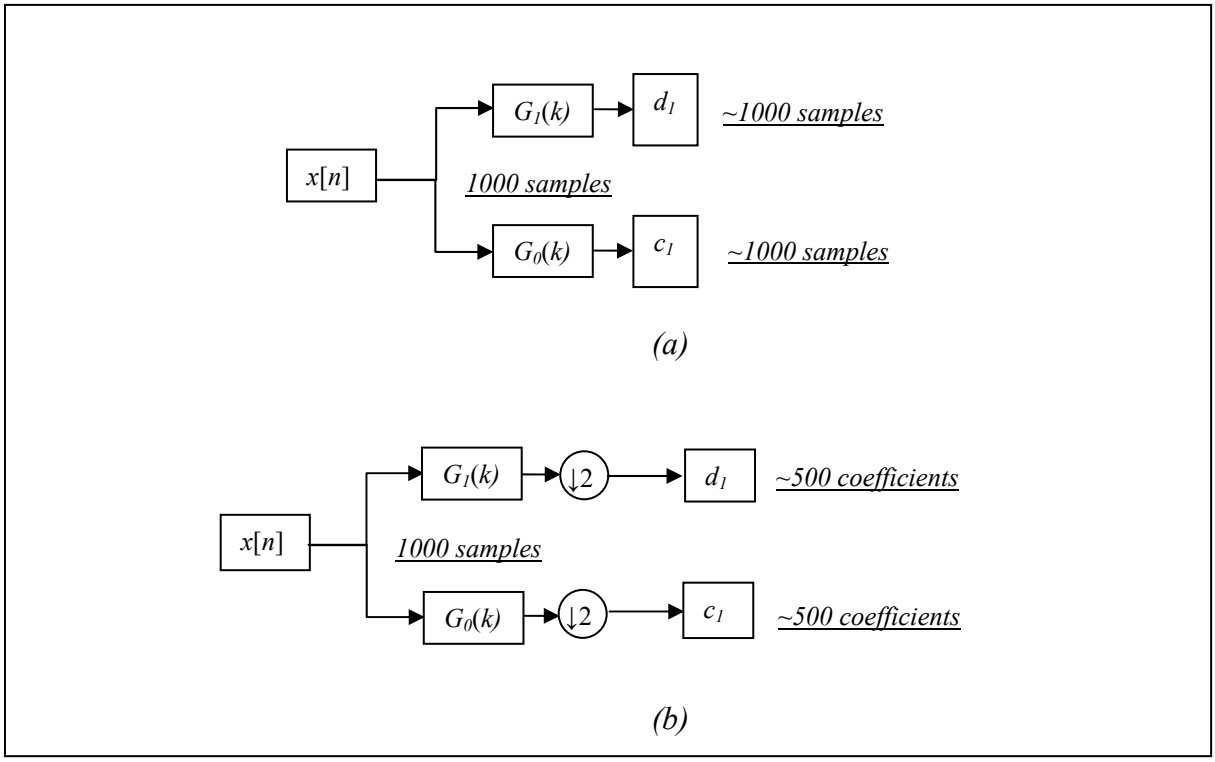

Figure 2.11 (a) Analysis filter bank without down-sampling. (b) Analysis filter bank with down-sampling by the factor of two.

Multiresolution theory uses the ideas similar to sub-band decomposition and coding. A signal is divided into a set of frequency bands, which are here introduced by sampling of dyadic grid. This, however, means that the frequency domain is divided into octave subbands. Such multiresolution analysis (MRA) derivation becomes clearer if a second function, called *scaling function* is put along side the wavelet functions.

The mathematical derivation of scaling function for DWT is defined by having given a discrete signal $x[n]; n = 1,..., N$ with its DWT up to level or scale index J. This discrete signal $x[n]$ maps the vector ($x[1],\ldots x[N]$) to a set of N wavelet coefficients containing output sequence $c_{J,k}$ and $d_{j,k}$ where j=1,2,..J, of the wavelet series approximation [45].

A scaling function $\varphi(t)$ gives a set of approximation of the signal as a set of resolution levels j, by projecting it on a set of subspaces V_j. The subspaces V_j are generated by dilation using low-pass filter $G_0(k)$ and translated versions of $\varphi(t)$. For a given level j, the subset V_j is spanned by the base of scaling functions defined in equation (2.13) [45].

$$\varphi_{jk}(t) = \frac{1}{\sqrt{2^j}}\varphi\left(\frac{t-k2^j}{2^j}\right) \qquad k \in Z \tag{2.13}$$

The approximation coefficients yield as $c_{j,k}$ which is the inner product of x and φ_{jk} [45].

$$c_{jk} = \langle x, \varphi_{jk} \rangle = \frac{1}{\sqrt{2^j}} \int x(t)\varphi^*\left(\frac{t-k2^j}{2^j}\right)dt \tag{2.14}$$

Hence, by setting stretching factor equal to 2 or dyadic grid, scaling function $\varphi(t)$ is corresponding to

$$\varphi(t) = \sqrt{2}\sum_k G_0[k]\varphi(2t-k) \tag{2.15}$$

where

$$G_0[n] = \left\langle \frac{1}{\sqrt{2}}\varphi(t), \varphi(2t-n) \right\rangle = \frac{1}{\sqrt{2}} \int \varphi(t)\varphi^*(2t-n)dt \tag{2.16}$$

The decomposition of a signal on the subspaces V_j or MRA is completely defined by the function $\varphi(t)$ or equivalently by the sequence $G_0[n]$ from the low-pass filter function G_0 from equation (2.16). The signal is decomposed or band-filtered to the frequency subband, where the scale function always defines the low-frequency signal components.

The complementary high-frequency band is, however, obtainable by the wavelet function. The wavelet function of DWT is defined by equation (2.17) [45]

$$\psi_{jk}(t) = \frac{1}{\sqrt{2^j}}\psi\left(\frac{t-k2^j}{2^j}\right), \quad k \in Z \tag{2.17}$$

where $\psi(t)$ is the mother wavelet defined in equation (2.18)

$$\psi(t) = \sqrt{2}\sum_k G_1[k]\varphi(2t-k) \tag{2.18}$$

involving scale function $\varphi(t)$ that include sequence $G_0[k]$ from the low-pass filter function and sequence $G_1[k]$ from the high-pass filter function. Equivalently, sequence G_1[n] is defined by equation (2.19).

$$G_1[n] = \left\langle \frac{1}{\sqrt{2}}\psi(t), \varphi(2t-n) \right\rangle = \frac{1}{\sqrt{2}} \int \psi(t)\varphi^*(2t-n)dt \tag{2.19}$$

The detail of output coefficients $d_{j,k}$ is computed as inner product of $x(t)$ and wavelet function $\psi_{j,k}$ defined in equation (2.20).

$$d_{j,k} = \langle x, \psi_{jk} \rangle = \frac{1}{\sqrt{2^j}} \int x(t) \psi^* \left(t - \frac{k2^j}{2^j} \right) dt \tag{2.20}$$

and they correspond to the discrete wavelet transform as generated by the MRA:

$$d_{j,k} = DWT_{\psi x}(j,k) = \langle x, \psi_{jk} \rangle = \frac{1}{\sqrt{2^j}} \int x(t) \psi^* \left(t - \frac{k2^j}{2^j} \right) dt \tag{2.21}$$

The original signal, therefore, can be reconstructed by summing all the output detail coefficients $d_{j,k}$ and $c_{J,k}$ or from the approximation of level J by the equation defined in (2.22).

$$x(t) = \sum_k c_{J,k} \tilde{\varphi}_{Jk}(t) + \sum_{j \le J} \sum_k d_{j,k} \tilde{\psi}_{jk}(t) \tag{2.22}$$

where $\tilde{\psi}_{jk}$ are the *synthesis* or dual frame wavelets and $\tilde{\varphi}_{Jk}$ are the synthesis scale function [45]. In the case of the family of *orthogonal* wavelets, the same prototype is used to perform decomposition analysis and synthesis or reconstruction. Other bases of wavelet families which are the *biorthogonal wavelet bases* have the synthesis wavelets different from the analysis wavelet [45].

An example of signal analysed by DWT with mother wavelet Daubechies 05 (db05) is illustrated in Figure 2.12. Based on the signal decomposition and reconstruction, Daubechies 05 was found to be the most suitable mother wavelet to process this particular type of signal [35]. Figure 2.12a, like in Figure 2.5a, is a sample SEMG signal obtained from a similar source sampled at rate 2048 Hz resulting 4096 number of samples for two seconds duration. Figure 2.12b is the signal output results of signal in Figure 2.5a filtered by filter banks using MRA. Figure 2.12c shows the wavelet decomposition tree that makes up the signal in Figure 2.12b. The red dotted lines pointed from the region where the signal originated from in Figure 2.12(b).

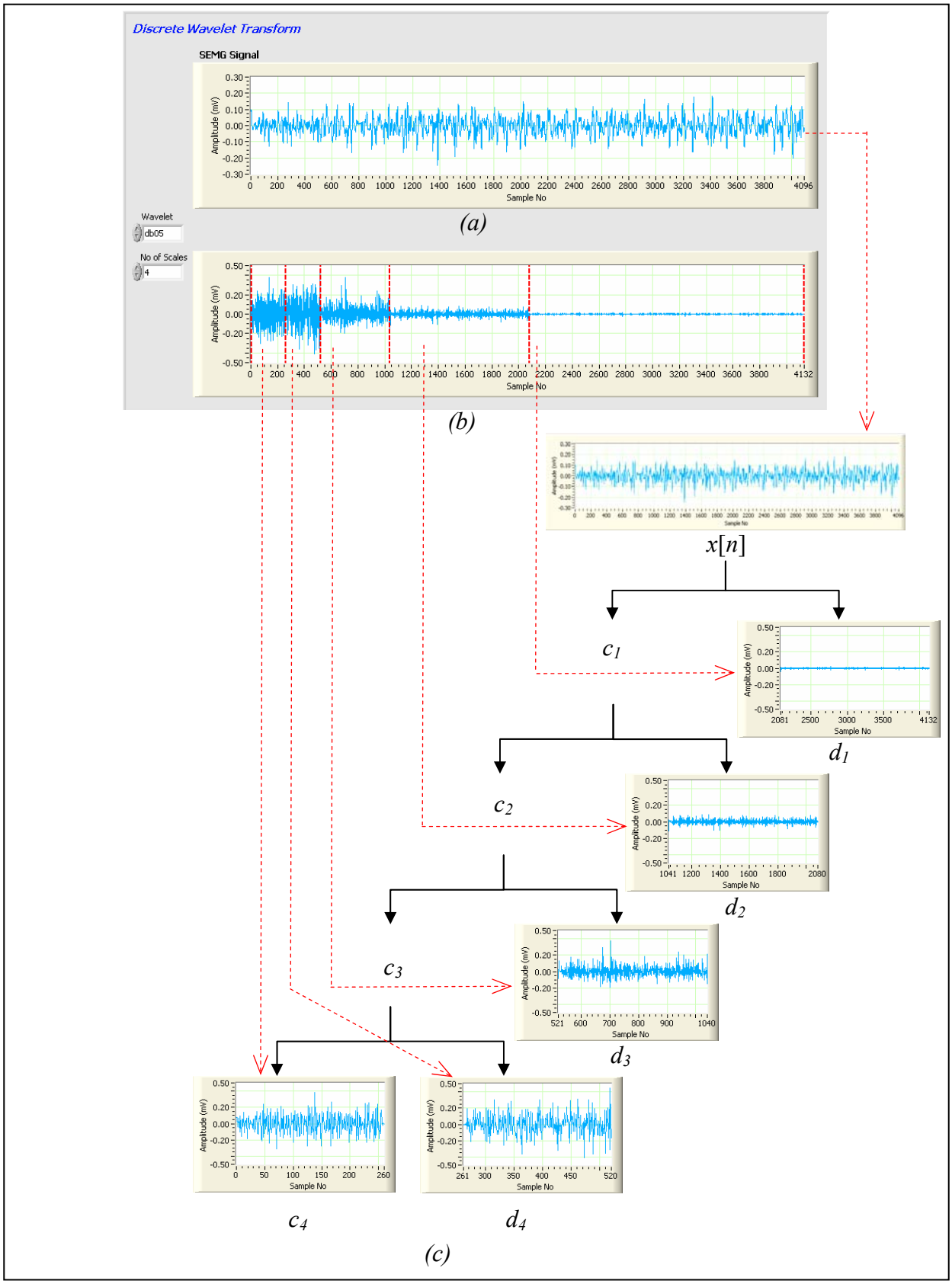

Figure 2.12 (a) A SEMG signal obtained from the vastus lateralis muscle at 50% MVIC. (b) Output signal results of (a) filtered by filter banks using multiresolution analysis. (c) Wavelet decomposition tree that makes up the output signal in (b). The red dotted lines pointed from the region where the signal originated from in (b).

DWT separates and retains the signal features in one or a few sub-bands as shown in Figure 2.12. The level of decomposition shown in Figure 2.12 is to scale index 4 and shows the sub-banding obtained from a discrete signal that has 4096 samples. This sub-banding of the DWT is variable, which means the feature of band varies such that the frequency resolution is proportional to the centre frequency. This subbanding has been shown to be more appropriate for many physical signals, but the partition is still fixed.

Since the DWT signal is being down-sampled at each successive frequency scale, it becomes a sparse transform at lower frequency scales [2]. Somehow it is believed that 'Continuous' Wavelet Transform can overcome this problem and gives an additional method of SEMG frequency analysis [2].

In DWT, for many signals the low-frequency content is the most important part as it gives the signal its identity. The high-frequency content, on the other hand, adds the characteristics or details of the signal. Hence, in MRA, the low-pass filters are used to extract the dominant component of low-frequency content. Also in DWT, the terms 'approximations' and 'details' are referred to as the components that can be used to reconstruct the signal. The approximations are the higher scale index J which is the low-frequency components of the signal. The details are the low scale which is the high-frequency components.

2.3.2a Discrete Wavelet Packet Transform (DWPT)

The DWT uses MRA that splits input spectrum into approximation and a detail or in other words, the lower and higher bands, respectively [38, 45]. However, only the lower bands are then split into a second-level approximation and detail. The process is repeated at each stage leaving the higher band or detail as one of the transform outputs. This scheme is rather restricted. The Discrete Wavelet Packet Transform (DWPT) method is a generalisation of wavelet decomposition that offers a richer range of possibilities for signal analysis. DWPT includes both output of lower and higher band to be split into several bands at a time. Unlike DWT, this yields more than 2^2 different ways to encode the signal. DWPT can apply arbitrary band splitting and hence are not bound to octave frequency resolution. [45]. The wavelet packet decomposition tree is illustrated in Figure 2.13.

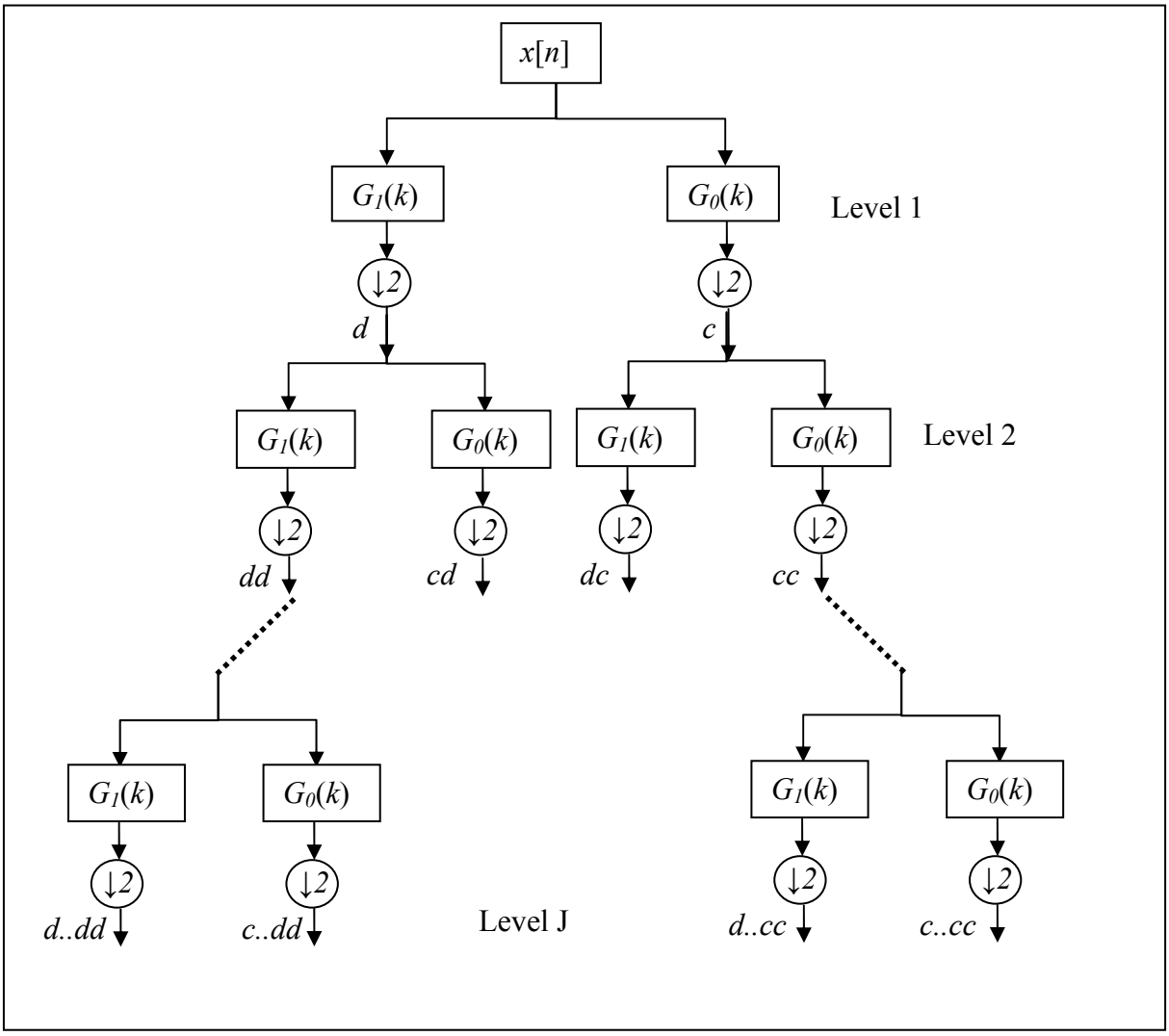

Figure 2.13 Wavelet packet decomposition tree, where input signal is filtered recursively with pairs of low-pass $G_0(k)$ and high-pass $G_1(k)$ filters. The output from both filter are subjected to down-sampling by a factor of 2, denoted by '2↓' and further band-splitting.

Similarly, like DWT, DWPT can also be approximated by digital filter banks. As illustrated in Figure 2.13, approximation is achieved by filtering the signal repeatedly from the high-pass filters to gain wavelet coefficients. Each node has a set of coefficients that can be selected to further split or not. There are many different methods used to decide the best subset of the bases family, and that can be adapted to suit a particular application. For instance, wavelet packet analysis allows the signal $x[n]$ to be represented as $x[n] = c + ccd + dcd + dd$ where it is not possible with ordinary wavelet analysis of DWT.

The general DWPT are the functions expressed in equation (2.23) [45].

$$W_{j,b,k}(t) = 2^{-j/2} W_b(2^{-j}t - k) \qquad b \in N, \quad j,k \in Z \tag{2.23}$$

Each function is determined by a scaling parameter j, a localisation parameter k and an oscillation parameter b. The function $W_b(2^{-j}t-k)$ is roughly centered at $2^j k$, has support of size $\approx 2^j$, and oscillates $\approx b$ times. The most suitable resolutions may be chosen for a particular signal, giving the option of an adaptive system.

An example of signal analysed by DWPT is illustrated in Figure 2.14 showing a wavelet decomposition tree of input signal $x[n]$ filtered by low and high pass filters with Daubechies 05 (db05) as mother wavelet. The output signals shown are *c* and *d* at level 1, and *cc*, *cd*, *dc* and *dd* at level 2. Input signal $x[n]$ is an SEMG signal obtained from the vastus lateralis muscle at 50% MVIC similarly as in Figure 2.5a sampled at rate 2048 Hz resulting in 4096 number of samples for two second duration.

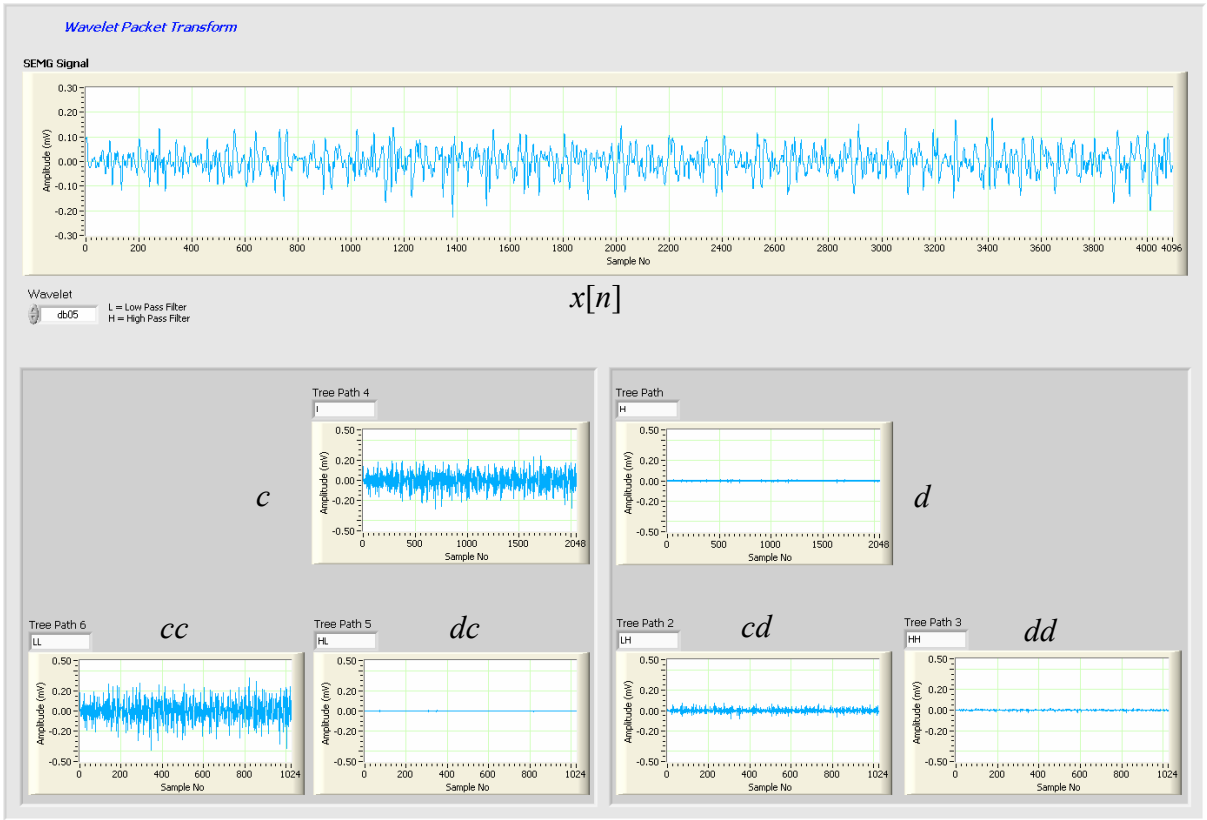

Figure 2.14 Wavelet packet decomposition tree showing top signal diagram as input x[n] and below it are the output signals of level 1 and 2 filtered by low and high filters using DWPT. Input signal x[n] an SEMG signal obtained from the vastus lateralis muscle at 50% MVIC.

In summary, the DWPT is a generalised multiresolution method that represents the entire family of subband coded decompositions. From this family of bases, the best basis can be chosen to match the non-stationarity of the signal. DWPT offers a more flexible method to arbitrary and adaptive select frequency resolution depending on the EMG application.

2.4 Quantitative Measures in Feature Selection

As described in section 2.1.2, the next stage after data acquisition and analysis is the feature selection. In this research, the signal features were selected in terms of the root mean square (RMS) value of their electrical potential, mean and median frequencies from the average power spectrum. These features are selected as they are commonly used in most EMG research using the conventional Fourier analysis method [15, 20, 53, 54]. The mean and median frequencies provided some basic information about the spectrum of the signal and its changes versus time [45].

The power spectrum may be presented in linear, logarithmic linear, or double logarithmic scales [54]. The power spectrum with linear scales is measured in volts square per hertz (V^2/Hz). The decibel (db) unit is used if the scale for power, energy, or amplitude is logarithmic.

The power spectrum of the total signal reveals the component of the individual motor unit properties [54]. The area under the power spectral curve equals the signal power. The frequency power spectral shows only smaller upward shifts in the frequency spectrum as the force of the contraction increases. This increase occurs at low levels of tension, but after about 50% of the maximum voluntary contraction, the frequency values no longer increase. *Hanning* window is used in processing the power spectrum to obtain smoothness of the output spectrum avoiding spectral leakages and outliers.

The two reliable measures of the power spectrum are the mean frequency and the median frequency. The mean frequency is the average of all frequencies from the power spectrum [54]. The median frequency is that frequency having 50% of the frequency distribution on

each side. The median frequency appears to be less sensitive to noise than the mean frequency. The mean and median frequencies also provide some basic information about the spectrum of the signal and its changes versus time [45]. They coincide if the spectrum is symmetric with respect to its centre line, while their difference reflects spectral skewness.

Equation (2.24) shows the formula of median frequency (MDF) [15].

$$\int_{0}^{MDF} P(\omega)d\omega = \int_{MDF}^{\infty} P(\omega)d\omega \tag{2.24}$$

where MDF is the median frequency in radian per second and $P(\omega)$ is power spectrum of the signal. Equation (2.25) shows the mean frequency (MNF) formula [15, 45].

$$MNF = \frac{\int_{0}^{\infty} \omega P(\omega)d\omega}{\int_{0}^{\infty} P(\omega)d\omega} \tag{2.25}$$

The RMS value of signal $x(t)$ over the time interval 0-T is determined by computing equation (2.26) [55].

$$RMS = \sqrt{\frac{1}{T}\int_{0}^{T} x^2(t)dt} \tag{2.26}$$

An example of power spectrum plot of signal in Figure 2.15a is illustrated in Figure 2.15b. The blue dotted lines show the mean frequency of 92.22 Hz and median frequency of 73.35 Hz. Figure 2.15a is also obtained from a similar source as in Figure 2.5a. Its RMS value is computed to be 0.0514 mV.

In summary, this chapter has covered the information on the different stages of processing biosignals. Starting from data acquisition, feature extraction analysis and selection, details on theoretical principles of each analysis schemes of FFT, STFT, CWT, DWT and DWPT were also discussed. Sample signal analysed by each of these schemes were illustrated accordingly. Lastly, the theoretical principles of the selected parameters or features were presented. The next chapter covers the practical application of the principles described in this chapter. Descriptive procedures of all of the methods used will be presented.

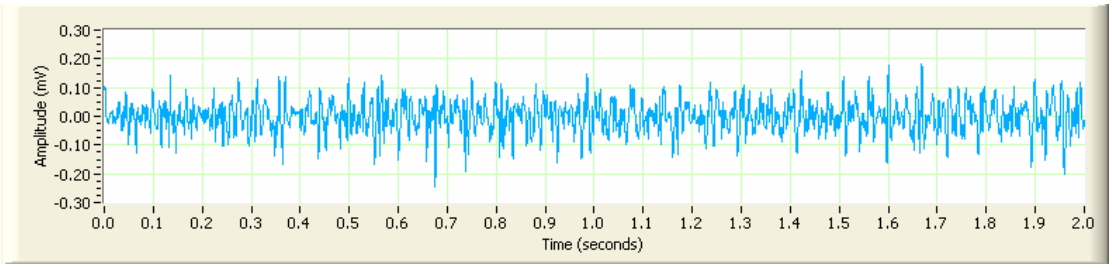

(a)

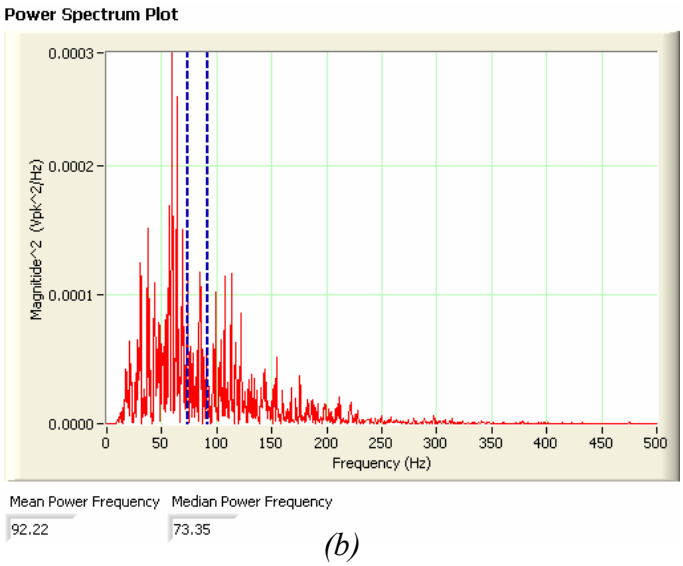

(b)

Figure 2.15 (a) A SEMG signal obtained from the vastus lateralis muscle at 50% MVIC. (b) Power spectrum plot of signal in (a) showing the blue dotted lines of mean frequency of 92.22 Hz and median frequency of 73.35 Hz.

Chapter 3
Data Acquisition and SEMG Signal Processing

3.1 Introduction

This chapter covers the experimental investigation of the principles described in the previous chapter. Descriptive procedures of all of the methods used will be presented. Starting from data acquisition, feature extraction analysis and selection, details on how theoretical principles were applied for each analysis schemes of FFT, STFT, CWT, DWT and DWPT are also discussed.

This chapter covers all aspects of the data processing involved in this research to select the features all of the data acquired. This includes the pre-processing stage, an essential part to select which analysis scheme is the most suitable for processing SEMG signals. The development concept of LabVIEW virtual instruments (VIs) for the data pre-processing and analysis are displayed with the details of the VI designs and MATLAB code programs in Appendix B1 to B10. The final or the most suitable VI design selected with further processing function is displayed in Appendix D. The descriptions of the procedures of physical preparation and setup for data collection and acquisition are also covered in this chapter. Finally, the processing results of one typical signal are presented and discussed in terms of the selected feature parameters, which are the root mean square (RMS) value of the signals, mean and median frequencies from the average power spectrums of the signal using CWT analysis.

By the end this chapter, the first objective stated in chapter 1.4 was achieved, which was to build a database by collecting SEMG signals from healthy subjects and extract features of the signals using the wavelet analysis technique. These extracted features were processed in order to train and validate Artificial Neural Network (ANN) for classifying and recognising patterns for normal muscle signals, which is to fulfil the second objective covered in chapter 4.

This is done by carrying out research into computer-aided diagnosis of SEMG signals analysis by building a program to digitally process the signals using the wavelet analysis technique. To develop this program, pilot signals are required for this pre-processing stage. Other general sampling rate settings and modes are also to be selected.

To fulfil the first aim and objectives stated in chapters 1.4 and 1.4.1, the stages were laid out as follows.

1. Software Development stage

   System programs known as 'virtual instruments' (VIs) were developed using LabVIEW. These programs were tested and validated using a sample set of pilot signals and compared with results by MATLAB program, which was built separately. Five programs were designed to analyse EMG signal using the following techniques:

   - Fast Fourier Transform (FFT) which showed the frequency spectrum and power spectrum of the EMG signals.

   - Short Time Fourier Transform (STFT) which showed the windowed frequency spectrum in terms of time. This is presented in a spectrogram.

   - Continuous Wavelet Transform (CWT) using the Morlet mother wavelet. The output was presented in a scalogram showing the scales of the wavelet in time domain. From this, suitable scales which gave valuable information for determining RMS values of the signals, mean and median frequencies from the average power spectrum were selected.

   - Discrete Wavelet Transform (DWT) using the most suitable mother wavelet Daubechies (db05) [35]. This program showed the multiresolution analysis of the wavelet transform at a particular scale. Prior to the execution of discrete wavelet transform analysis, the most suitable wavelet was selected by statistical analysis of a decomposed and reconstructed EMG sample signal.

- Discrete Wavelet Packet Transform (DWPT) using the mother wavelet Daubechies (db05). This program showed the signal decomposed down to level 6 on the low-pass filter tree within the time domain.

2. Data collection and acquisition

   Raw SEMG signals from 45 real subjects with healthy or normal extensor knee muscles, the vastus lateralis and the vastus medialis, were collected. The participants underwent Maximum Voluntary Isometric Contraction (MVIC) tests. The ethical approval, equipment, setup and protocol involved are described in a later section of this chapter.

3. Pre-processing stage

   A sample signal was processed using the five LabVIEW programs built in stage 1. The program with the analysis scheme that gave the most satisfactory results for signal classification in ANN in stage 5 was selected.

4. Feature extraction and selection

   Signals from the vastus lateralis were processed and analysed by extracting their features using the program with the most suitable technique selected in stage 3, which in this case was the CWT. The feature parameters selected were the RMS values of the signals, the mean and median frequencies from the average power spectrum. For the purpose of being concise in this study, only the signals from the vastus lateralis were processed and trained in the ANN in the next stage. Signals from the vastus medialis are saved and archived for further study.

The schematic diagram of stages 1, 2, 3 and 4 are highlighted in yellow, blue, orange and green regions respectively in Figure 3.1, an extension of Figure 2.2 depicted previously in chapter 2. Stage 5, depicted in the pink region is the next stage of objectives needed to be fulfilled for the second objective of this research, training and validating ANN for classification of normal muscle signals.

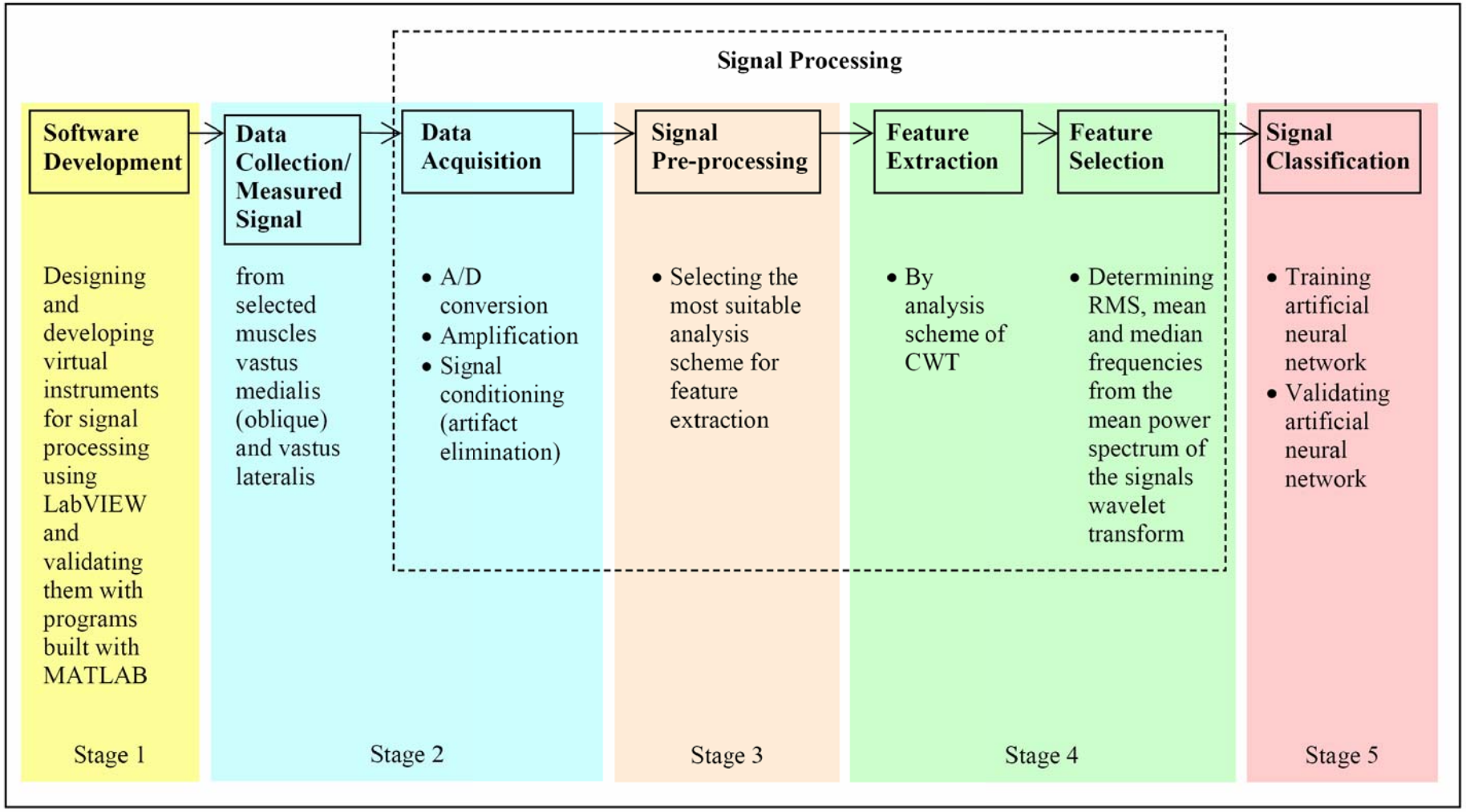

Figure 3.1 Schematic diagram of the various stages undertaken in this research.

3.2 Software Development

This stage 1 process involved the design and development of programs using LabVIEW where results were validated by programs built with MATLAB for similar purposes. It was felt required to carry out this validation in order to confirm that the software used is acceptable for the purpose of this research. All the programs built using LabVIEW and MATLAB for FFT, STFT, CWT, DWT and DWPT are depicted in Appendix B1 to B10. The main objective of this part is to select the most suitable method for analysing SEMG signals.

Another essential aspect when comparing the various methods is that all parameters have to be similar. Since the wavelet transform methods of CWT, DWT and DWPT were represented by time-scales and not apparent in the form of time-frequency spectrum, there is a need of conversion of these scales to frequencies.

It is also important to understand that the nature of scales and the fact that wavelet analysis does not produce a time-frequency view of a signal is not a weakness, but a strength of the technique [38]. Not only is time-scale a different way to view data, it is a very natural way to view data deriving from a great number of natural phenomena. However, in this case there is an essential need to convert or connect scales to frequencies where information can be of relevance. The relationship between scale and frequency can only be given in a broad sense. This frequency is called the *pseudo-frequency* corresponding to a scale. To convert from scales to frequencies is to compute the centre frequency F_c of the wavelet and to use the following relationship expressed in equation (3.1).

$$F_a = \frac{\Delta . F_c}{a} \tag{3.1}$$

where a is the scale number, Δ is the sampling number which is the number of samples taken per second, F_c is the centre frequency of a wavelet in Hz, and F_a is the pseudo-frequency in Hz corresponding to the scale a.

The centre frequency F_c is originated from the frequency maximising the FFT of the wavelet modulus [38]. By processing the mother wavelet using FFT, the centre frequency F_c is obtained from the dominant frequency appearing in the frequency spectrum.

A sinusoidal wave is generated at this centre frequency which maps onto the mother wavelet oscillations [38]. Figure 3.2 shows a generated sinusoidal at centre frequency in red mapping and translating along the mother wavelet function in blue. The mother wavelet detects the dominant frequency of the sinusoidal signal by a wavelet decomposition followed by conversion of scale to frequency as in equation (3.1). Thus the centre frequency is a convenient and simple characterisation of the leading dominant frequency of the wavelet at a given scale [38].

In this research, Daubechies (db05) mother wavelet was used in DWT and DWPT analysis, and Morlet mother wavelet in CWT analysis. The centre frequency resulted from db05 mother wavelet was 0.6667 Hz and from Morlet mother wavelet was 0.8125 Hz.

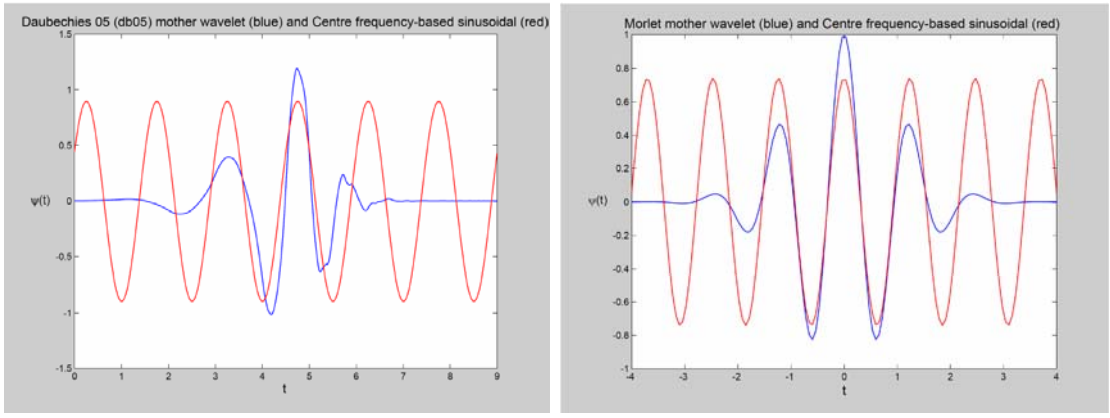

(a) *(b)*

Figure 3.2 (a) Generated centre frequency-based sinusoidal at 0.6667 Hz mapped and translated along mother wavelet Daubechies 05. (b) Generated centre frequency-based sinusoidal at 0.8125 Hz mapped and translated along mother wavelet Morlet.

One set of the sample signals was obtained for testing and running the programs of LabVIEW and validating them with programs built with MATLAB. The sample signal was 2 seconds duration of vastus lateralis muscle at 50% MVIC. The results in terms of parameters obtained and comparative aspects for each analysis techniques are drawn up in Table 3.1. From the Table 3.1, the results from both programs are comparatively close to each other. Hence, LabVIEW programs are valid to be used in the later stages of signal processing.

Table 3.1 Comparative table of results and aspects from five analysis methods using LabVIEW and MATLAB. A set of sample signals processed were obtained from 2 seconds duration of vastus lateralis muscle at 50% MVIC.

Parameters /Aspects	FFT		STFT		CWT		DWT		DWPT	
Program used L=LabVIEW M=MATLAB	L	M	L	M	L	M	L	M	L	M
Mother wavelet	N/A	N/A	N/A	N/A	Morlet	Morlet	db05	db05	db05	db05
Window size	N/A	N/A	0.5 second with 50% overlap	0.5 second with 50% overlap	N/A	N/A	N/A	N/A	N/A	N/A
Scale Index for analysis	N/A	N/A	N/A	N/A	1-256	1-256	4	4	1-6 Low Frequency Path	1-6 Low Frequency Path
Display Form	Power Spectrum of filtered signal		Spectogram of frequency-amplitude-time of filtered signal		Scalogram of scale-amplitude- time of filtered signal		Amplitude-time representation of filtered signal		Amplitude-time representation of filtered signal	
Median frequency	57.86 Hz	57.31 Hz	N/A	N/A	53.33 Hz at scale 32	53.29 Hz at scale 32	N/A	N/A	57.35 Hz at scale 32	57.28 Hz at scale 32
Mean frequency	64.43 Hz	64.21 Hz	N/A	N/A	52.86 Hz at scale 32	52.53 Hz at scale 32	N/A	N/A	55.59 Hz at scale 32	55.2 Hz at scale 32
RMS value	0.0417	0.0417	N/A	N/A	0.1774 at scale 32	0.1774 at scale 32	N/A	N/A	0.1131 at scale 32	0.1133 at scale 32

3.2.1 Software Development Concept

The concepts of the software design and development are illustrated in the flowcharts of Figures 3.3 to 3.7. The actual designs of VIs and MATLAB code for every analysis scheme are displayed in the Appendix B1 to B10 along with their results. The red words in Figures 3.3 to 3.7 are sub-programs within the VIs themselves or called sub-VIs.

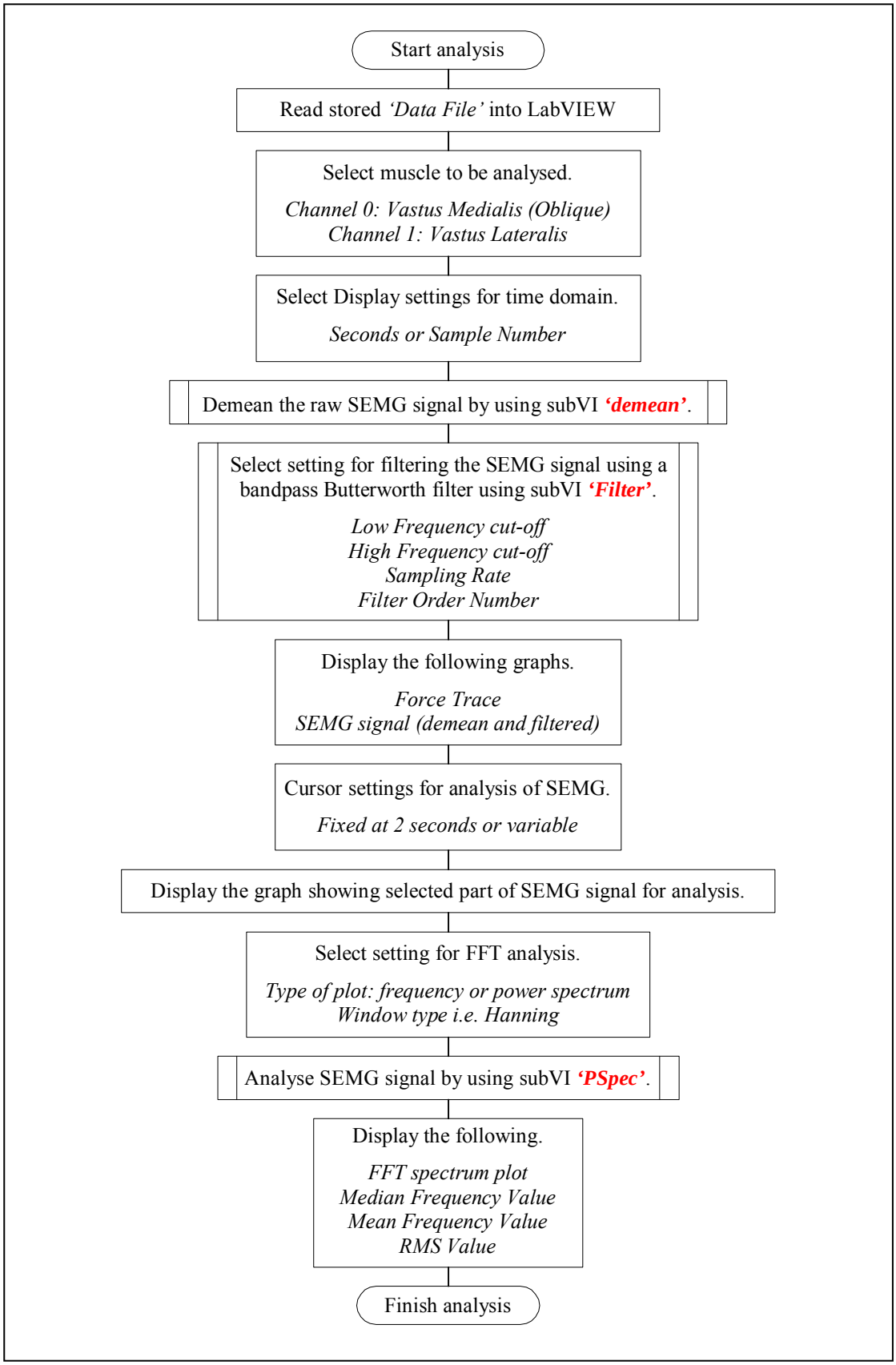

Figure 3.3 LabVIEW development flowchart for analysing and displaying the results of a SEMG signal using Fast Fourier Transform (FFT).

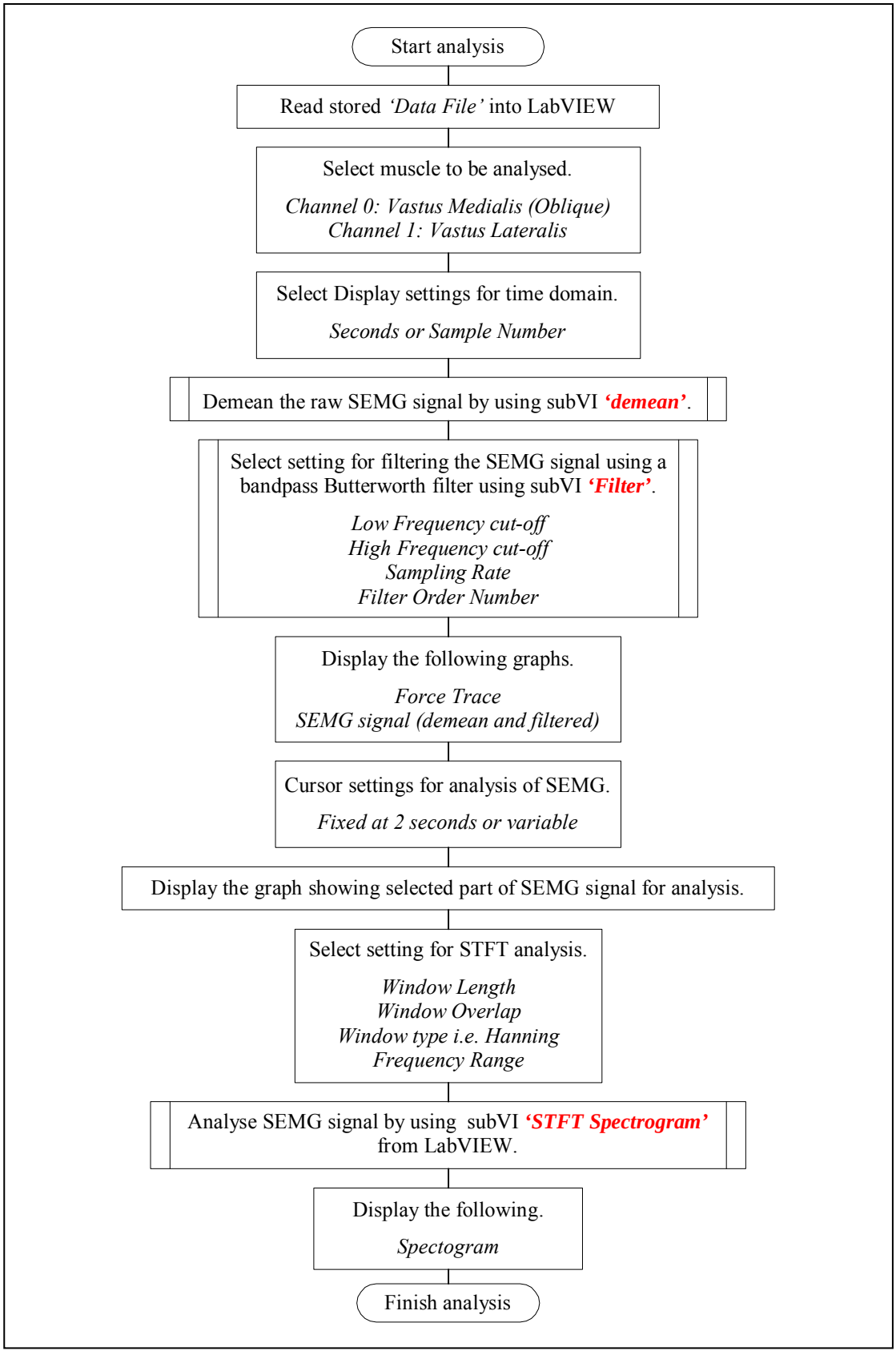

Figure 3.4 LabVIEW development flowchart for analysis and displaying the results of a SEMG signal using Short Time Fourier Transform (STFT).

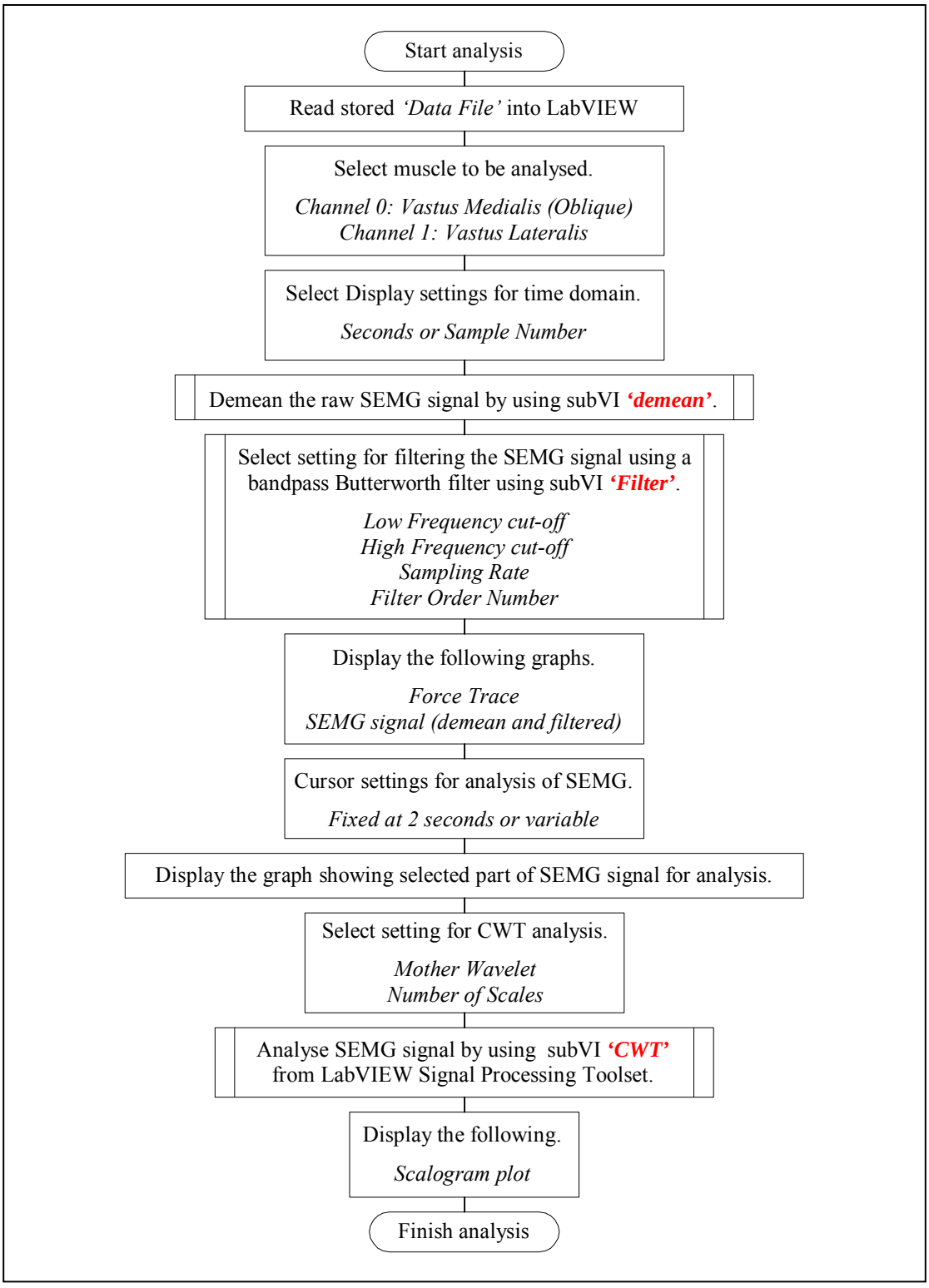

Figure 3.5 LabVIEW development flowchart for analysis and displaying the results of SEMG signal using Continuous Wavelet Transform (CWT).

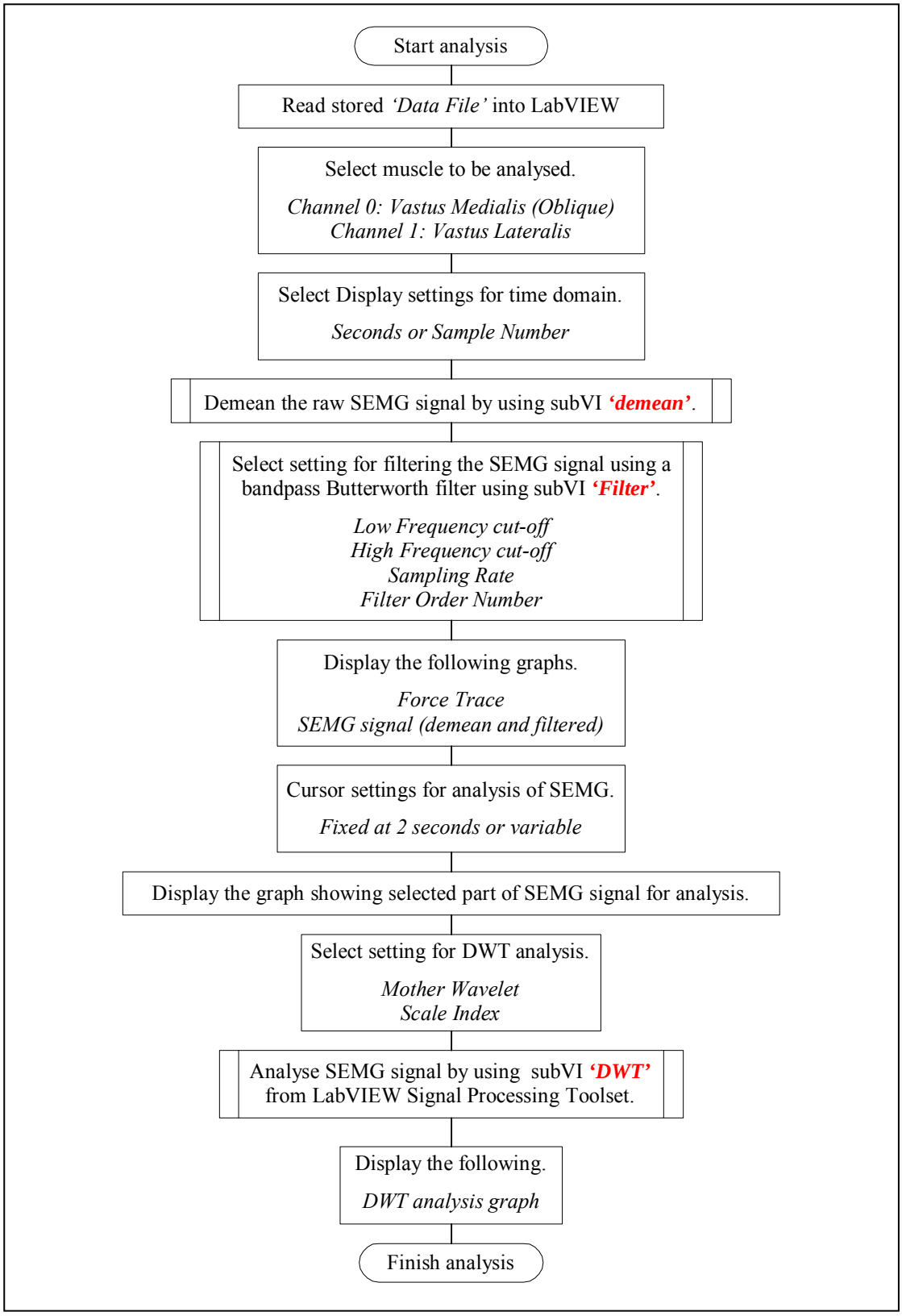

Figure 3.6 LabVIEW development flowchart for analysis and displaying the results of a SEMG signal using Discrete Wavelet Transform (DWT).

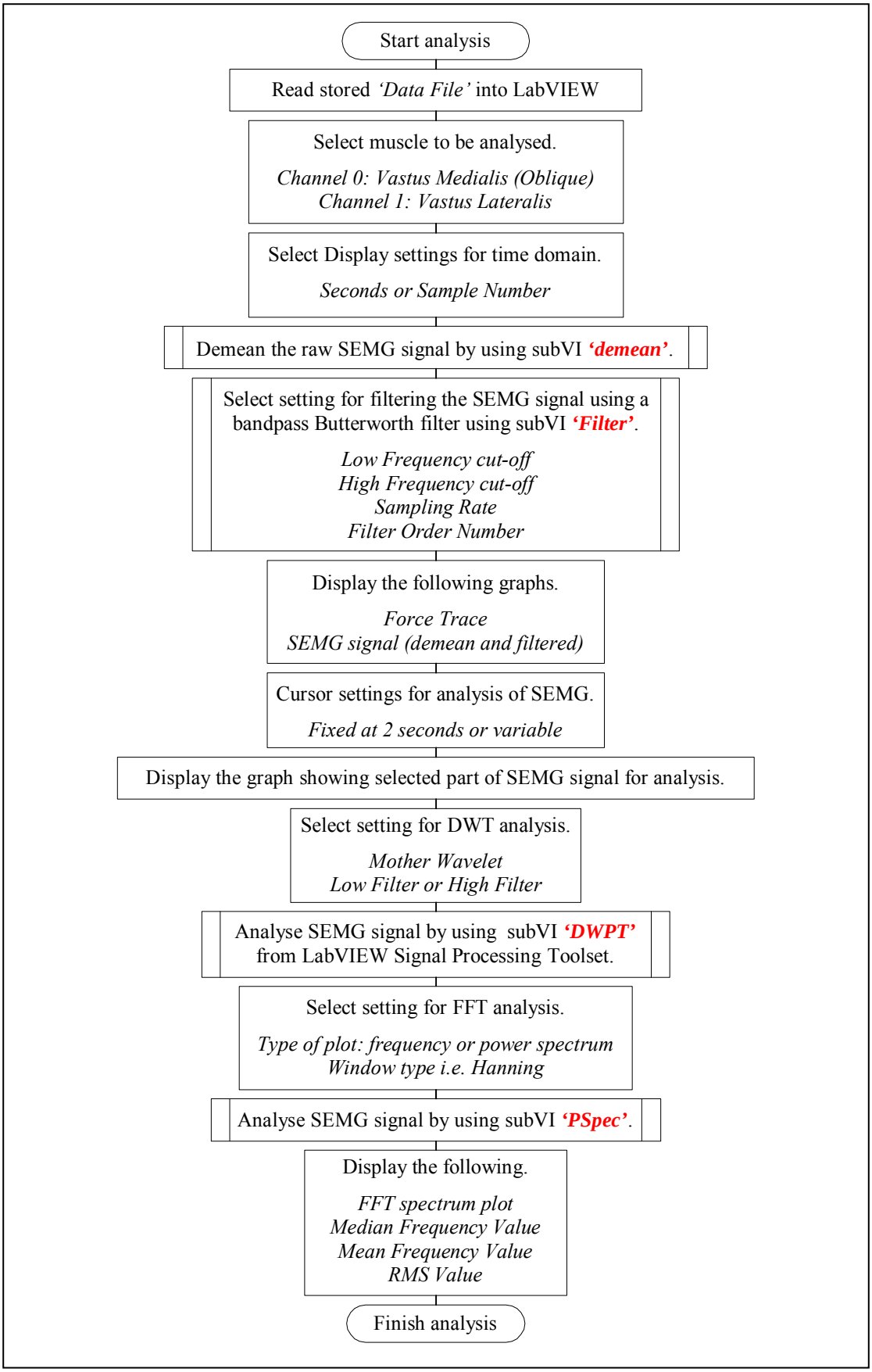

Figure 3.7 LabVIEW development flowchart for analysis and displaying the results of a SEMG signal using Discrete Wavelet Packet Transform (DWPT).

The common subVIs that were used for all analysis are *demean* and *Filter*. SubVI *demean* was to remove the DC offset or bias components that may exist in the acquired signals [45]. SubVI *Filter* was designed for filtering signal between the usable operating frequency of 5 to 500 Hz [17] using a Butterworth bandpass filter. The detailed designs of these subVIs are presented in Appendix B11. Another subVI, *PSpec* was a part of VIs for FFT and DWPT analysis for producing power spectrum.

Other subVIs such as *STFT Spectogram* was a part of VIs for STFT analysis for producing spectogram, *CWT* for CWT analysis, *DWT* for DWT analysis and *DWPT* for DWPT analysis. They are already existed as built-in programs within the LabVIEW signal processing toolset which process and analyse signals according to the analysis schemes appointed of STFT, CWT, DWT and DWPT.

3.3 Data Collection and Signal Acquisition

This section is the stage 2 of the research as illustrated in Figure 3.1 and covers the procedures taken in collecting the data. The details include description of equipment, setups and protocol which is the movement or exercise procedure to obtain Maximum Voluntary Isometric Contraction (MVIC) using maximal strength test and sustained isometric contraction.

Ethics approval was required in the experimental part of this research as it involved human subjects executing the exercise to obtain MVIC on their extensor knee muscle. Application for ethics approval was submitted and approved by the Auckland University of Technology (AUT) Ethics Committee.

Forty five subjects with no previous history of knee or severe musculoskeletal injury participated in this study. Subjects were students recruited from the Akoranga campus of AUT. Request notices were posted on notice boards throughout the AUT. Subjects were males between the ages of 18 and 35 with no history of knee injury within the twelve months.

Individuals were excluded if they had a knee injury within the last year, had any previous knee surgery, and had any current cardiovascular, neurological, cognitive or musculoskeletal ailments. People with injury to their knee or leg muscles or any form of medication may seem to give an unsatisfactory result related to this research.

Potential participants were screened for inclusion and exclusion criteria to determine if they were appropriate to participate in the study. They received verbal explanations of what was involved. Prior to assessment, procedures were explained to the participant and time was given for the participant to have any remaining questions answered before written consent was obtained.

The schematic setup of the equipment is illustrated in Figure 3.8. The apparatus used to carry out MVIC were listed in Table 3.2 along with their purpose. Figure 3.9 to Figure 3.12 show the equipment involved in this investigation.

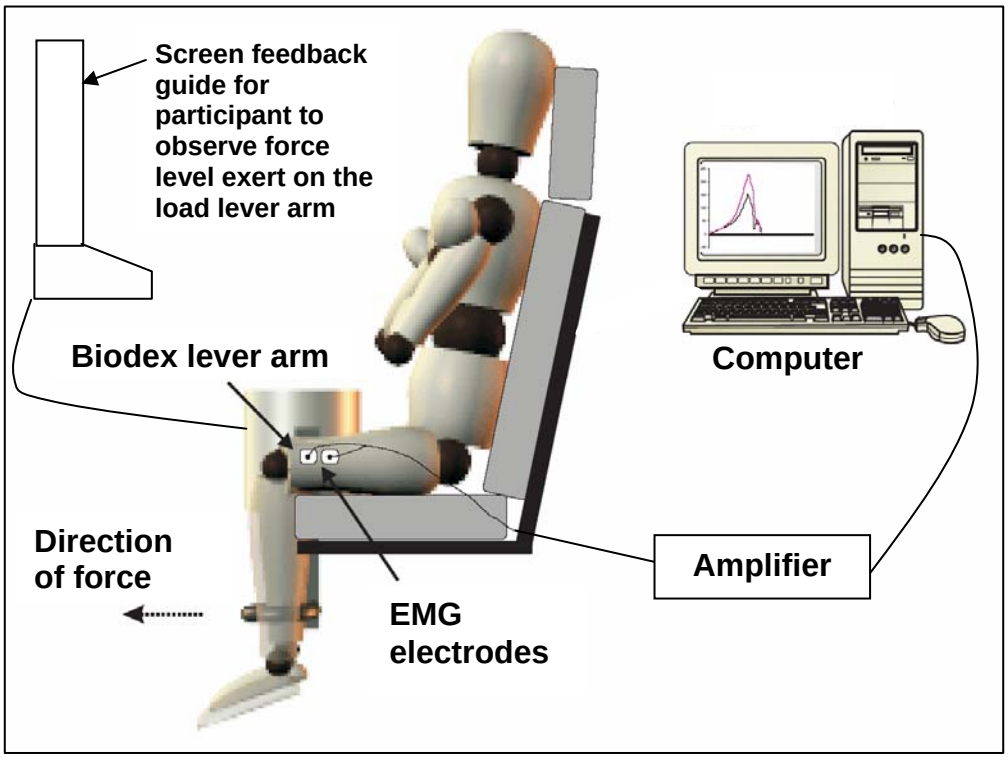

Figure 3.8 Schematic diagram of equipment setup for signal acquisition.

Table 3.2 List of equipment used for data collection of signal of vastus lateralis and vastus medialis muscles.

Equipment	Type	Source	Purpose
Data acquisition card	NI PCI-6024E multifunction data acquisition board	National Instruments	Analogue to digital interface which is to convert signal from the surface electrodes to the digital form connected and stored in the computer.
Cable connectors	BNC-210 shielded connector blocks and SH6868 shielded cable	National Instruments	To connect the amplifier/conditioner to the data acquisition card.
Amplifier /Conditioner	Grass model P511 amplifier	Grass Instruments Co. MA, USA	To condition, filter out high frequency components and amplify the raw signal.
Upright chair equipped with the attached resistance load suspension for knee-leg movement and monitor.	Biodex	Courtesy from the Faculty of Health and Science, Akoranga Campus of AUT	Special chair for participant to execute MVIC and monitor screen to display force data for feedback to the participant
Bipolar surface electrodes EMG	Norotrode 20™ Bipolar Silver/Silver Chloride EMG Electrodes	Myotronics-Noromed, Inc.	Sensors to detect bioelectric signal from muscle contractions at the vastus lateralis and vastus medialis
Surface electrodes EMG	3M Red Dot™ silver/silver chloride monitoring electrodes with foam tape and solid gel	3M Health Care	Sensors for the reference point or ground, attached on the shin below the knee
PC installed with: 1. LabVIEW 2. MATLAB 3. Microsoft XP Office Professional	1. LabVIEW v6.1 and Signal Processing Toolset v7.0 featuring wavelet analysis 2. MATLAB v7.0 3. Microsoft Excel 4. Microsoft Access 5. Microsoft Word	1. National Instruments 2. Mathworks; 3-5.Microsoft Corp.	1. To connect to the data acquisition card and to process and analyse signal. 2.To analyse signal 3. To store and manage data. 4. To store data. 5. To write report and thesis
Disposable shavers	BIC	BIC	To shave hair around the area of the detected muscle
Alcoholic swabs	Medi-Swab™ 70% v/v isopropyl alcohol	Smith+Nephew	To cleanse and prepare skin after shaving
Preparation cleanser	Green Prep Skin Prep	Mavidon ™	To lightly abrade skin and maintain good electrodes contact
Exercycle	Monark Ergomdic 828E	Courtesy from the Faculty of Health and Science, Akoranga Campus of AUT	For participants to warm up before executing MVIC

Figure 3.9 Biodex upright chair for participant to sit on.

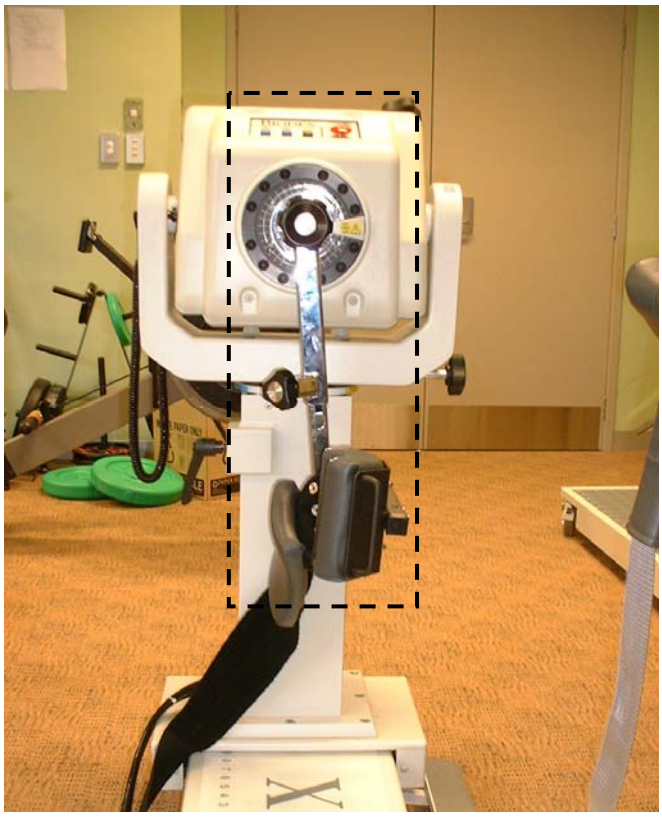

Figure 3.10 The load cell lever arm part (in black dotted box) of the Biodex upright chair.

Figure 3.11 The amplifier Grass Model P511.

Figure 3.12 The force data for each level of 25%, 50%, 75% and MVIC were displayed on the screen for feedback guide to the participant for their force exerted on the load lever arm.

To prepare participants for data collection, the subject's left and right legs were shaved at around the area of the intended muscles. This is to ensure good skin-electrode contact. It was gently abraded with skin preparation cleanser, Green Prep, then cleansed with 70% alcoholic swab and let to dry before attaching the adhesive silver/silver chloride bipolar electrodes. The surface electrodes are the main sensory contacts attached to the subject for muscle activity. They are disposable or one-off use as surfaces are self-adhesive and preferred for time efficiency and hygiene.

Figure 3.13 (a) and (b) shows the location of the bipolar electrode placements for the vastus lateralis and vastus medialis site on the quadriceps of the leg. Placement of the electrodes was done according to the set of recommendations published by Surface Electromyography for Noninvasive Assessment of Muscle (SENIAM) [56], European project for the clinical use of SEMG in the main striated muscles of the trunk and limbs. Surface electrodes were also attached at the reference points on each leg as a common or ground to subtract noise in a differential amplifier used in the system [57]. The reference point was the area with the least or no muscle at below the knee as shown in Figure 3.14.

Participants then underwent several stages of test movement or the protocol to obtain MVIC. These tests are the maximal strength test and sustained isometric knee extension test. The participants performed these tests on first the right knee then the left.

Figure 3.14 to Figure 3.17 show a subject executing exercise to obtain MVIC.

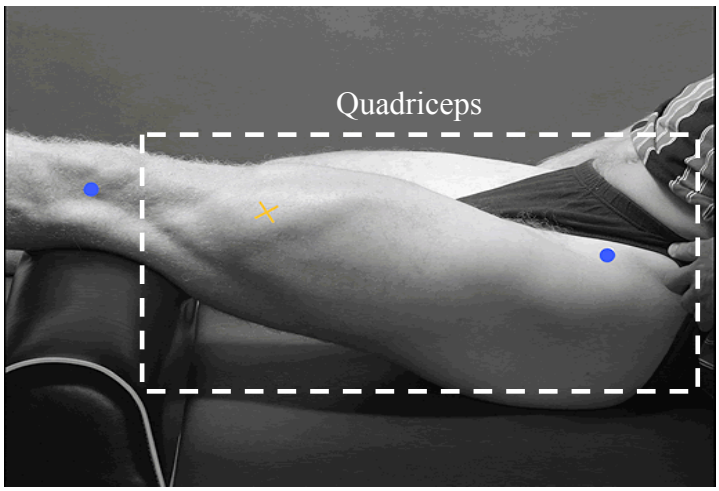

Figure 3.13 (a) Electrode placement for the vastus lateralis site marked in a yellow cross between the two reference points marked in blue dots. Further detailed information on electrode placement technique is enclosed in Appendix C1 [58].

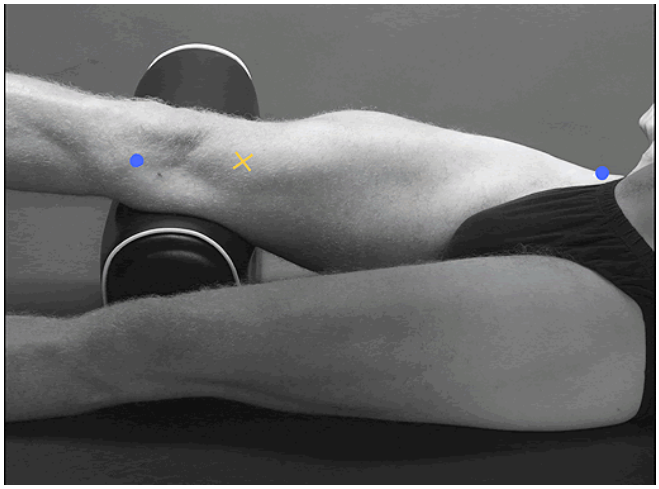

Figure 3.13 (b) Electrode placement for the vastus medialis site marked in a yellow cross between the two reference points marked in blue dots. Further detailed information on electrode placement technique is enclosed in Appendix C2 [59].

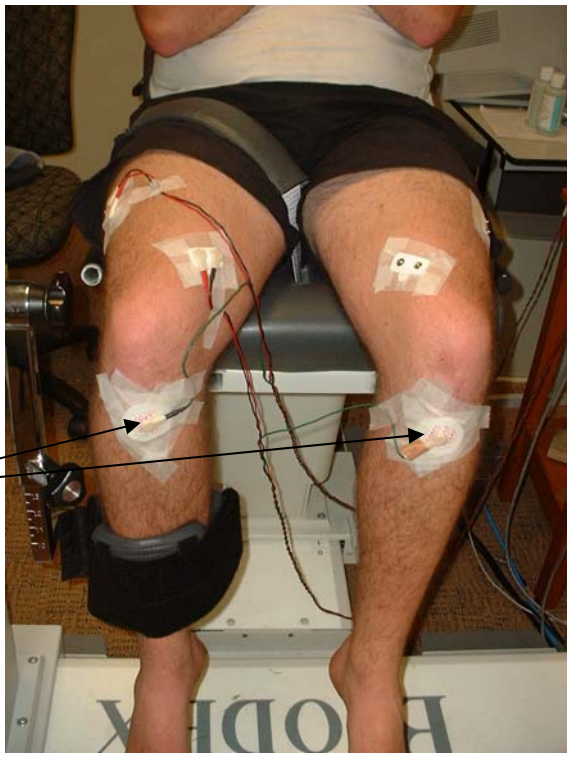

Figure 3.14 Location of surface electrodes EMG, front view.

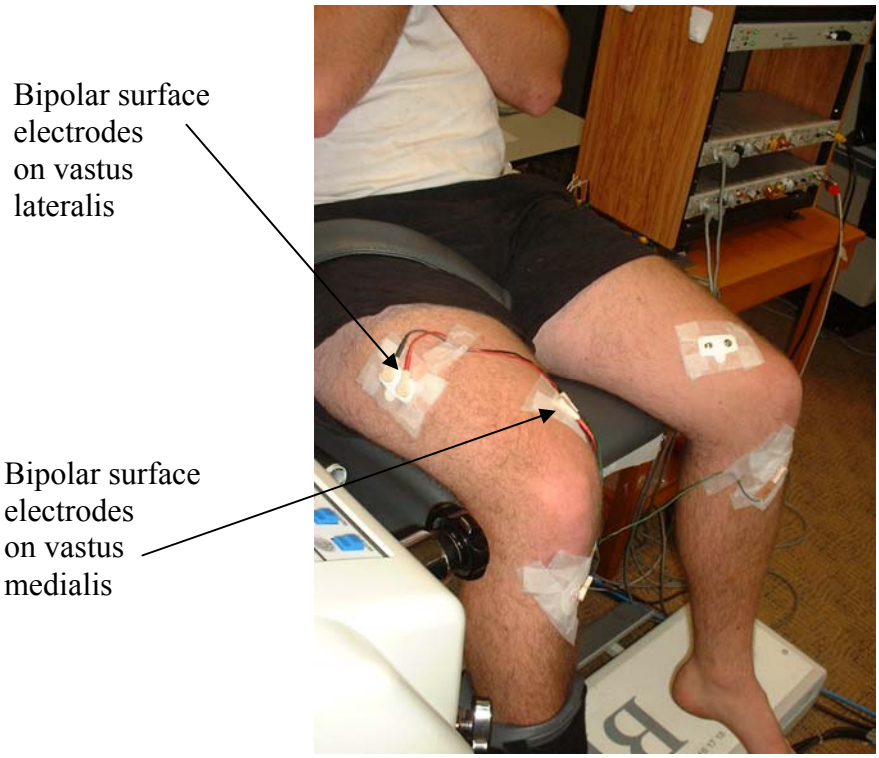

Figure 3.15 Location of surface electrodes EMG, top view.

Figure 3.16 (a) A subject executing MVIC.

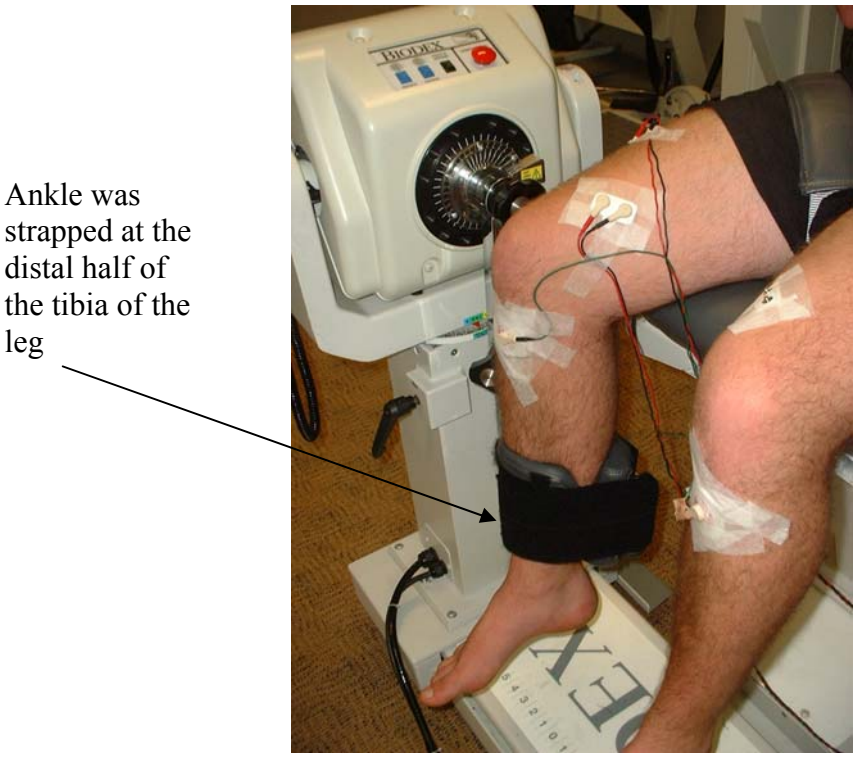

Figure 3.16 (b) A closer look at the knee and leg.

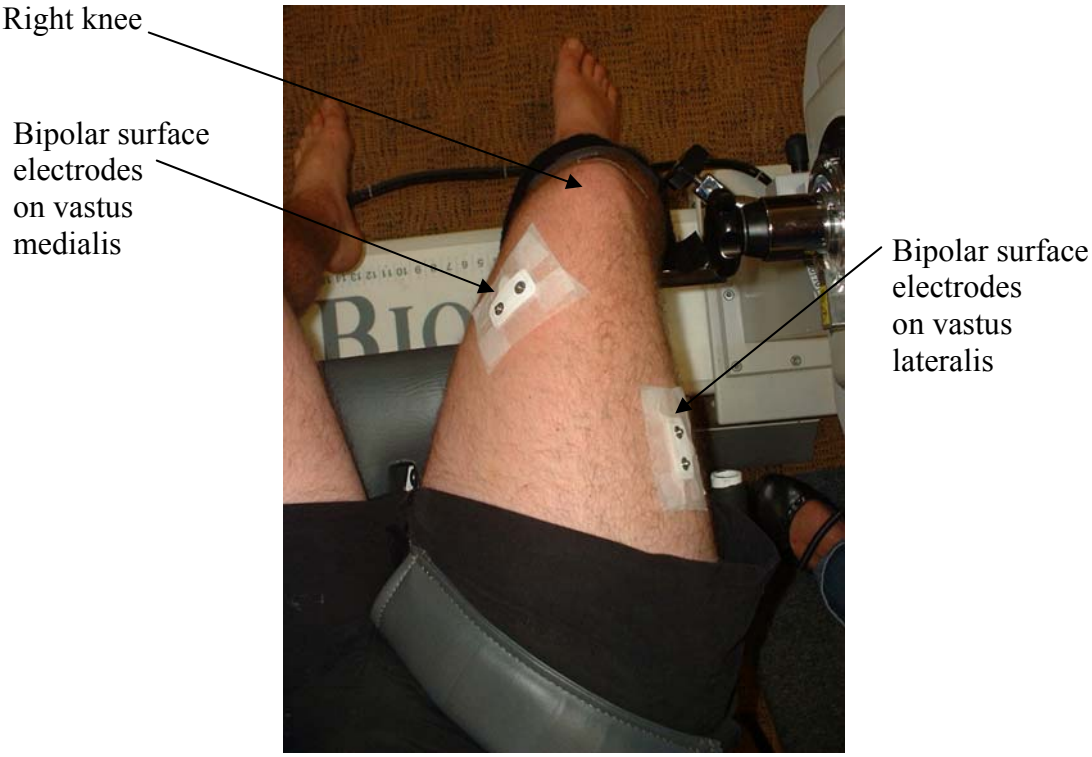

Figure 3.17 Closer look at the location of surface electrodes EMG on vastus lateralis.

3.3.1 Maximal Strength Test

The participant performed a five-minute generalised warm up that included riding on an exercycle at a self-selected pace and performing a range of motion exercises for the lower limbs. After the general warm-up was completed, the participant was seated on the Biodex upright chair set at 110 degrees with one of their knees bent to 90 degrees. The load cell lever arm was attached to the chair that measured voluntary isometric force of the quadriceps. The upper body and upper thigh of the subject were securely strapped to the chair as shown in Figure 3.16 (a) and the ankle was strapped to the load cell at the distal half of the tibia or below the calf muscle of the leg shown in Figure 3.16 (b).

The subject then performed a specific warm-up and familiarisation. This was carried out in a series of four sets of short five seconds sub-maximal isometric knee extensions by pushing the load cell lever in the force direction shown in Figure 3.8. The intensity of the contractions was gradually increased against the resistance of the load cell and within the subject's own limits. A one-minute rest followed each set of this warm-up contraction. At the end of the warm-up section, the subject was then rested for 3 minutes before the actual maximal strength test to obtain MVIC of the quadriceps.

The MVIC or 100% maximal force was executed by having the subject to push again the load cell lever, as in the force direction shown in Figure 3.8, for as long as possible and sustaining it up to 10 seconds. Three MVICs were measured and recorded for a 10 second period. There were a two-minute rest period between each MVIC test and the highest MVIC was selected for analysis. Standardised verbal encouragement was given throughout the test from the force-to-failure point.

3.3.2 Sustained Isometric Knee Extension Test

Following the maximal strength test, participants performed the sustained force production test. This test was executed by having the subject push the load cell lever for 25%, 50%, and 75% of their maximum or MVIC force. The subject was given verbal instruction and encouragement on when to start. The subject was required to perform and sustain isometric

contraction of the knee for a given force level for a period of 10 seconds. A two-minute rest period was given between each of the four force levels.

While executing this test, the force data for each level of 25%, 50%, 75% and MVIC (100%) from the previous maximal strength test were displayed on the screen for feedback to the subject. The screen was also to guide the subject to exert the right amount of force level on the load cell lever arm.

Force data from the maximal strength test were then transferred to a computer software programme that calculated individual force values for 25%, 50%, and 75% of the MVIC.

3.3.3 Signal Acquisition Settings

Muscle activities were recorded from the surface electrode EMG connected to a Grass Model P511 amplifier for signal amplification and de-noising, then onto the data acquisition card installed with its running software, LabVIEW, in the computer. The equipment was electrically isolated and all cables are specifically shielded and grounded for human use. There was no risk of electric shock to the researcher or subject. Routine maintenance ensured the safety and accuracy of the amplifier. This maintenance included regular calibration with an oscilloscope to check output signals and regular cable integrity checks made by a registered electronics technician.

The EMG signals from the surface electrodes were amplified 100 times, bandwidth filtered between 1 Hz and 3 kHz. Raw analogue signals were converted to digital data and recorded via the LabVIEW data acquisition VI program at a sampling frequency of 2048 Hz. The data acquisition program is a common program which had been previously used and available from the Physical and Rehabilitation Research Centre at the Akoranga Campus of AUT. The data was then transferred or fed into other LabVIEW VI programs that had been developed previously using the FFT, STFT, CWT, DWT and STFT analysis for the pre-processing stage.

3.4 Signal Pre-processing

At this stage one sample signal of 2 seconds duration of vastus lateralis muscle at 50% MVIC was used in five LabVIEW programs built with five different analysis schemes of FFT, STFT, CWT, DWT and DWPT.

From five programs built in stage 1, the one that gave the most satisfactory results for signal classification in the ANN was Continuous Wavelet Transform or CWT. CWT was the most satisfactory analysis tool for this research purpose as it produced a better display of the wavelet transform. It gave the most detailed information in terms of range of frequencies for each scale used. DWT and DWPT, although could be used to focus on characters at particular index level, did not give the overall outlook of the transform which was essential for the initial attempt to view what scales and when the dominant transform occurred.

For the purpose of completing the feature extraction and selection process using CWT analysis, several other functions needed to be built into the analyser program. For example; calculating the RMS values, mean and median frequencies of the average power spectrum. Based on the CWT analyser shown in the Appendix B5, the development flowchart for the VI concept of the extended version of the CWT analyser is shown in Figure 3.18. SubVI *PSpec Aver* is a sub program to form the average power spectrum. Appendix D shows the full LabVIEW design of this extended version of the CWT analyser and the subVI *PSpec Aver*. More details on calculating the RMS value, mean and median frequencies are described in the section 3.5.

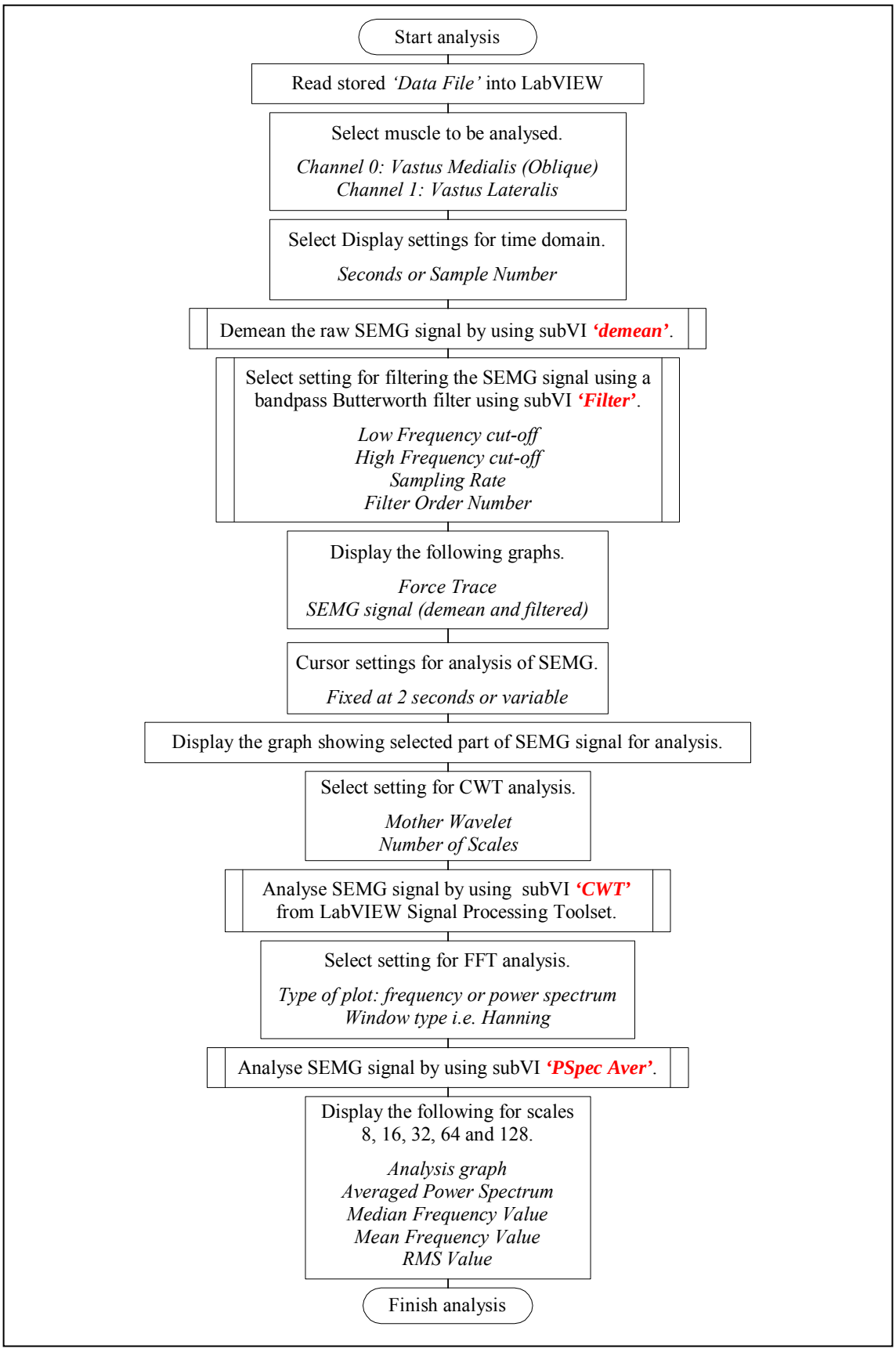

Figure 3.18 LabVIEW development flowchart for final analysis and displaying the results of SEMG signal using Continuous Wavelet Transform (CWT).

3.5 Feature Extraction and Selection

This section covers the stage 4 of this research as illustrated in the Figure 3.1. This was one of the main parts of this study, which were the core of processing and analysing of the data. The signal features were extracted using the most suitable analysis scheme determined in section 3.4, the CWT.

The feature selection was aimed to determine the RMS values of the signals, mean and median frequencies from the average power spectrum for each signal at 25%, 50% and 75% of the MVIC of the right leg's vastus lateralis for the Artificial Neural Network (ANN). Although recorded, data from the maximum strength 100% or the MVIC value was not included in the analysis and ANN classification as they were mainly used to guide the subject to exert the right amount of force for the 25%, 50% and 75% of the MVIC. Data from the left legs and vastus medialis were also recorded for future research purposes.

The output of CWT analysis using Morlet mother wavelet was used to produce a scalogram which includes scale indexes. The acquired data was transferred into the LabVIEW's VI design of the CWT enclosed in the Appendix D. This VI design is built based on the design of the CWT analyser in the Appendix B5 but had been functionally extended to improve presentation of the results display panel. The detailed specification of settings used to process using CWT VI is listed in Table 3.3.

Table 3.3 List of specifications required to process data signal using CWT.

Sampling frequency	2048 Hz
Scales	8, 16, 32, 64, 128, 256
Time	2 seconds
Mother wavelet	Morlet
Wavelet Centre Frequency, F_c	0.8125 Hz

The SEMG signal data files employed for feature extraction and analysis process using CWT analysis technique built in the Appendix D. The results were in the form of RMS values of the signal, and mean and median frequencies from the average power spectrum where they were trained and validated in the ANN in chapter 4.

For the feature extraction process, a part of the raw SEMG signals was selected. The selected region is a four second interval after the first peak signal activation. The first two seconds were not processed and analysed to allow changes in the muscle tension at the beginning of the muscle contraction. The next two seconds was the region to be processed and analysed [55, 60]. This region was where there was no muscle fatigue present and assumed to be quasi-stationary, that is stationary during short time intervals. Under this assumption spectral analysis for feature extraction can be applied [55, 60]. Figure 3.19 illustrates the regions of signals to be processed.

Within this 2-second region, the initial scalogram was produced. As explained in chapter 2, the scalogram shows lower scale numbers as for the narrow version of the wavelet window which represent high frequencies, and the higher scale numbers for the wider windows represent as low frequencies. The conversion of scale index numbers to frequencies or *pseudo frequencies* were then carried out using the centre frequency of the mother wavelet, which in this case was the Morlet. A frequency-time based spectrum was plotted as a result of this conversion. A range of dominant frequencies could also be viewed from the frequency-time spectrum.

The information detected from the scalogram gave an overview of which scale indexes would provide better features for the signal classification using ANN. These scale indexes were selected from the scalogram and the 2-second region of the SEMG signal was reproduced at each of these selected scales using the designed CWT virtual instrument as shown in Appendix D.

These reproduced signals were set with the sampling frequency at 2048 Hz. Hence within the quasi-stationary region of two seconds, there were 4096 data. Within this 2-second region, the *average* power spectrum was produced by applying the Fast Fourier Transform. Different from the 'regular' power spectrum, the *average* power spectrum is the average of a number of combined power spectrums.

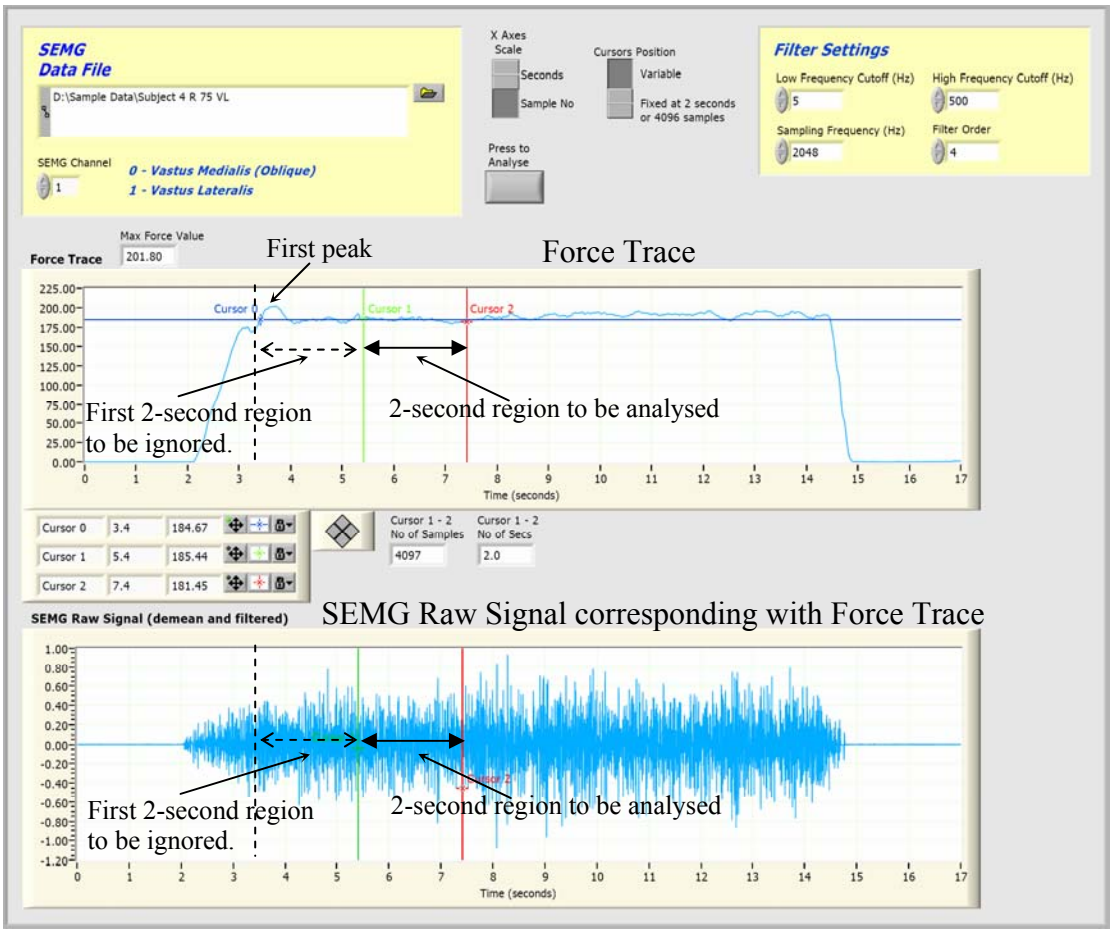

Figure 3.19 Graph of force trace and raw signal showing the region for processing and analysing

Power spectrum was produced from every 1024 samples or 0.5 seconds interval with an overlap of 50%. With an overlap of 50%, it created a total of seven 0.5 second intervals. The *average* of the power spectrum was formed from these 0.5 second intervals by averaging all of the spectra lying within the region. This method was used to reduce the variance in the spectrum estimates and create the characteristic values of the power distribution [60]. From this, the average of the spectrum, the mean and median frequencies were calculated. The spectral bandwidth was restricted to 5 to 500 Hz. This process was executed for each of the selected scales to determine the RMS values of the signal, mean and median frequencies from the average power spectrum. The concept of the averaging method in spectral analysis is illustrated in Figure 3.20.

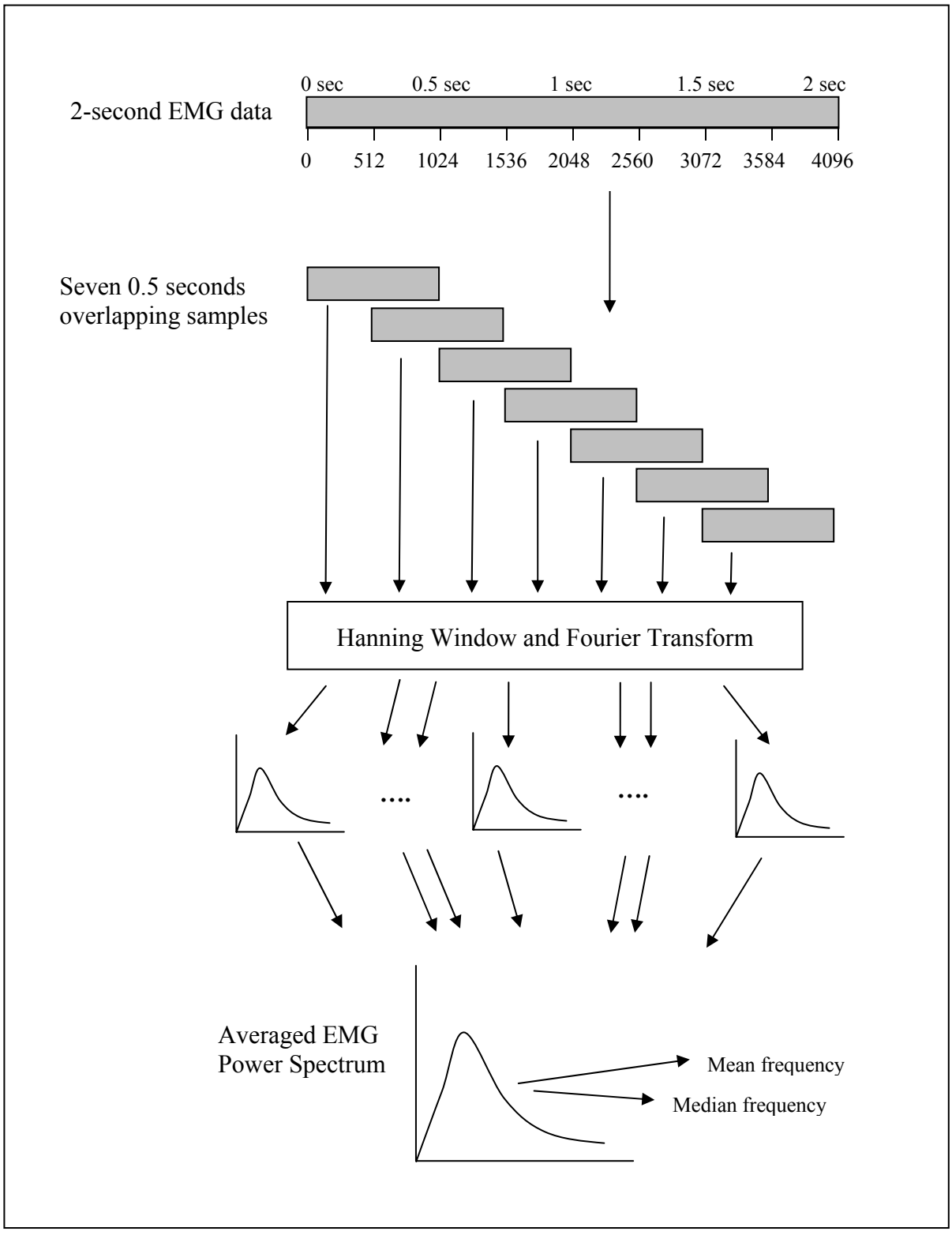

Figure 3.20 Schematic diagram of EMG processing procedure in the frequency domain by analysing the EMG spectrum

Hence, in summary the feature extraction analysis process was as follows:

1. Selection of 2-second quasi-stationary region from the acquired raw signals,
2. Formation of the scalogram using the CWT,
3. Conversion of the scale numbers to frequencies or the formation of the frequency-time based spectrum plot. General dominant frequencies were viewed,
4. Selection of scale index numbers,
5. Signal reproduction using each of the scale index number,
6. Formation of average power spectrum from each of reproduced signal of each scale,
7. Determination of the RMS values, mean and median frequencies of each scale.

The stage 3 of this research finished with the actual values determined for the RMS, mean and median frequencies for 25%, 50% and 75% of the MVIC muscle contraction at each scale level from each participant. These data are to be put through an ANN in chapter 4 of this thesis. The next section presents the actual results from this experimental investigation showing graphs and values from one typical sample.

3.6 Results of One Typical Output Signals

This section covers the results of the experimental investigation, showing one of the typical data obtained from forty five subjects. This includes the presentation of force trace along with the raw signals, the scalogram by the CWT and its inversion to frequency plot, scales selection, signal reconstruction using the selected scales, the formation of average power spectrum and the determined values of the RMS, the mean and median frequencies for each of the selected scales.

From the initial scalogram, the scales selected were 8, 16, 32, 64 and 128. For every one of these scales, data from 25%, 50% and 75% of the MVIC on the right legs were processed to determine the RMS value, the mean and the median frequencies.

The following diagrams are one of the typical results of a male subject who exerted 75% of the MVIC from his right leg's vastus lateralis. Figure 3.21 shows the force trace and the SEMG raw data. The 2-seconds quasi-stationary region to be analysed was indicated between Cursor 1 in green and Cursor 2 in red. Figure 3.22 illustrates the magnified version of the quasi-stationary region analysed (blue plot) with the power spectrum plot at its right hand side (red plot). It also shows the scalogram which was produced by using the CWT analysis. It was converted to frequencies shown by the following frequency-time based spectrum plot, which shows the dominant frequencies in white streaks which were mainly below 200 Hz.

The quasi-stationary signals were reproduced using the selected scales of 8, 16, 32, 64 and 128 and for each reproduced signals, the average power spectrum were formed. These are illustrated in Figure 3.23. The RMS value, mean and median frequencies of each scale are shown on the right hand side of the average power spectrum and also on the Table 3.4.

Table 3.4 Extracted features from the right leg's vastus lateralis of a male subject at 75% of MVIC (Subject No.4).

Scales	Mean frequencies (Hz)	Median frequencies (Hz)	RMS (mV)
8	168.83	167.12	0.0839
16	95.47	94.21	0.3886
32	51.70	50.59	0.6281
64	26.77	26.25	0.4095
128	14.93	13.89	0.3265

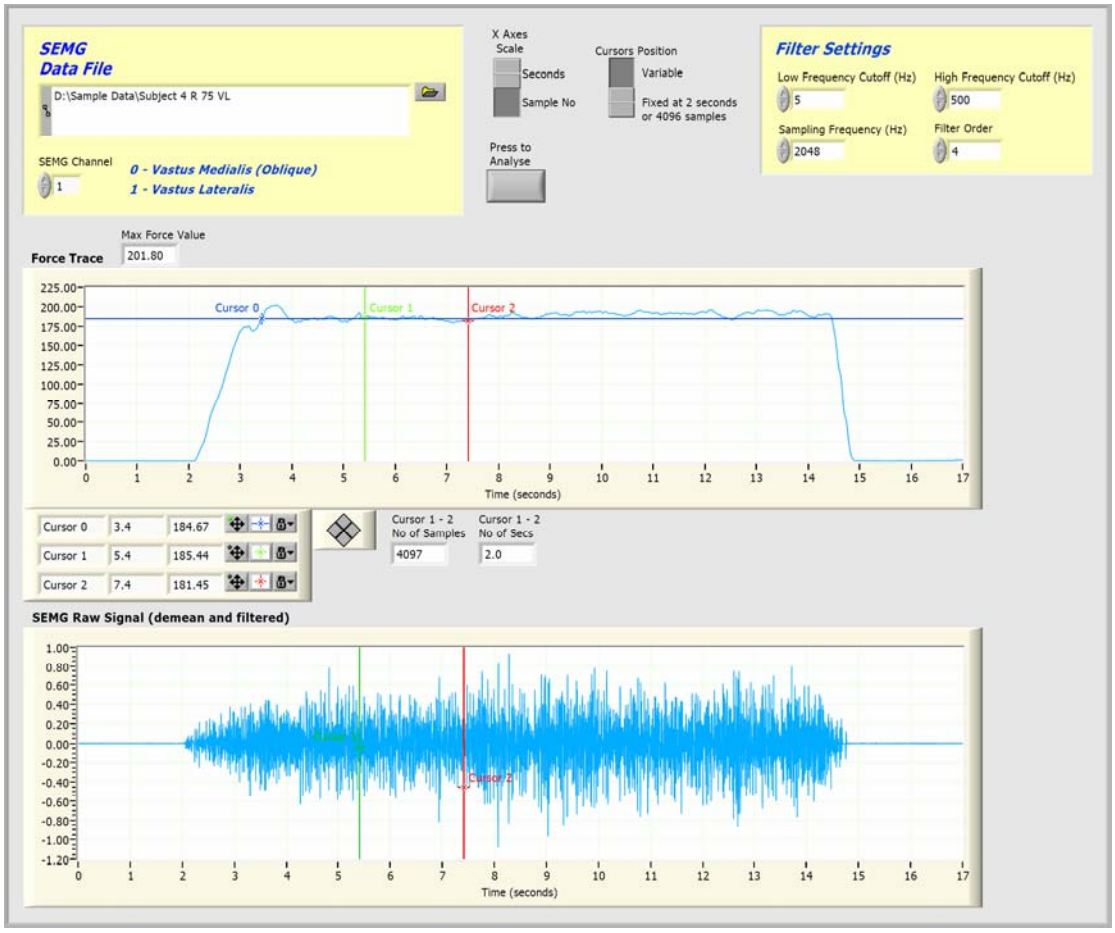

Figure 3.21 Force trace and the SEMG raw data of 75% of MVIC from right leg's vastus lateralis of a male subject (Subject No.4).

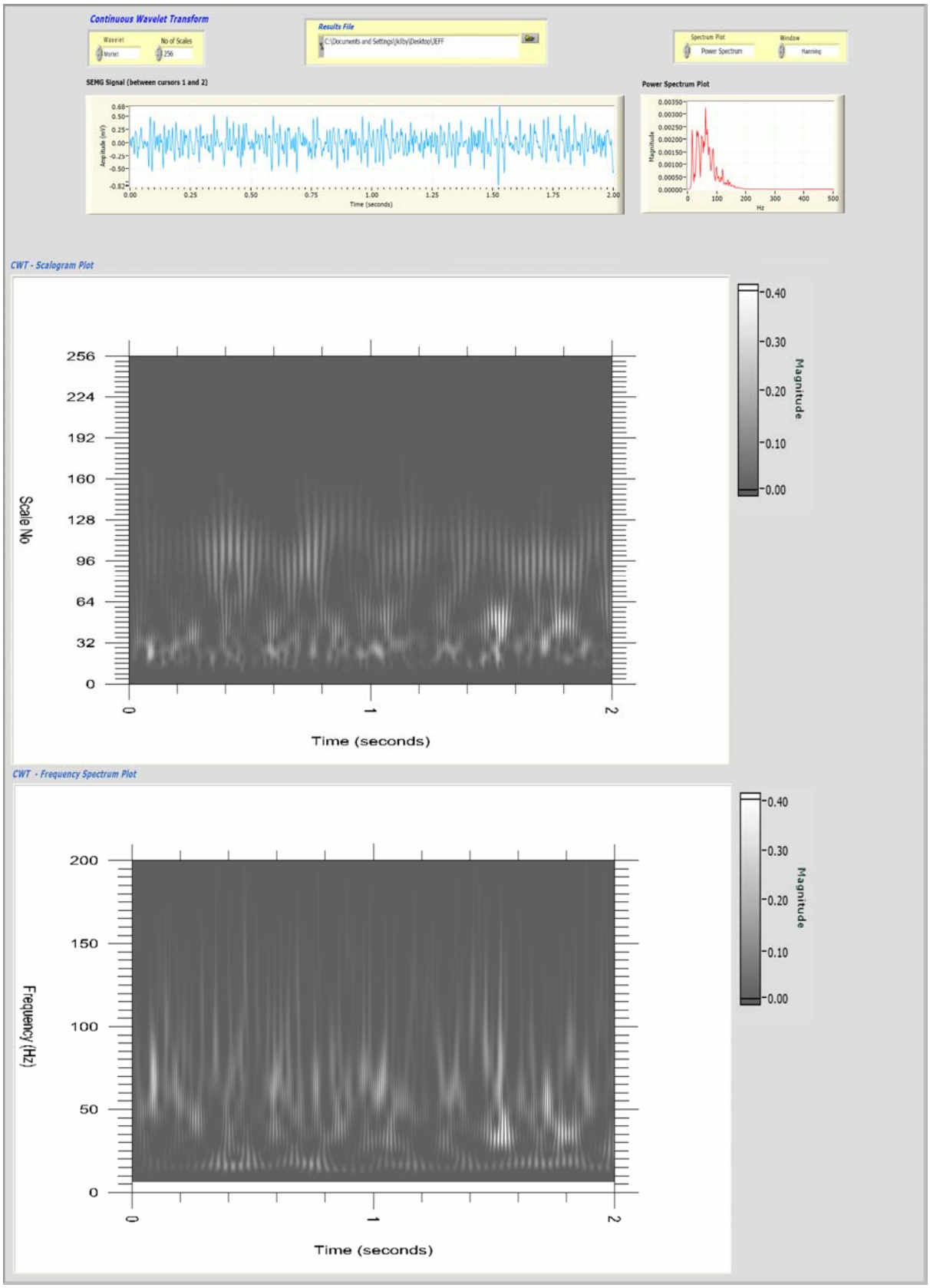

Figure 3.22 The quasi-stationary region analysed (blue plot) with the power spectrum plot at its right hand side (red plot), and below them is the scalogram which were converted to frequencies shown by the following frequency-time based spectrum plot. Data are of 75% of MVIC from right leg's vastus lateralis of a male subject (Subject No.4).

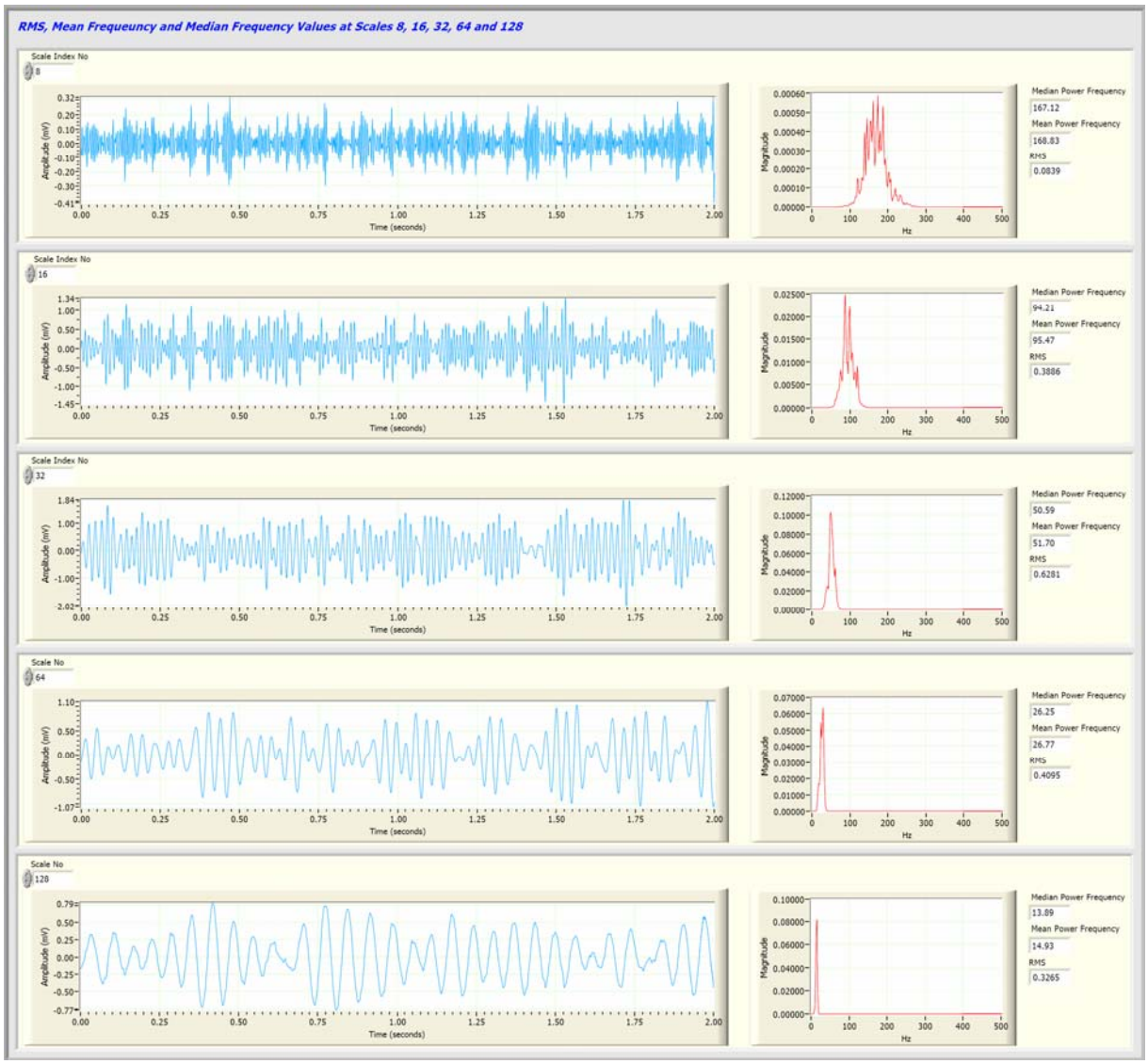

Figure 3.23 The reproduced quasi-stationary signals with the scales of 8, 16, 32, 64 and 128 in blue plots. The average power spectrum corresponding to each scale is in the red plots. The RMS values, mean and median frequencies of each scale are shown on the right side of the average power spectrums.

Chapter 4
SEMG Signal Classification Using Artificial Neural Network

4.1 Introduction

This chapter covers the brief fundamentals of Artificial Neural Network (ANN) and the use of it within this research. As part of an ongoing research, the aim of this exercise is to form a reliable methodology for developing an intelligent SEMG signals classifier. Other than investigating the possibility of using wavelet analysis to extract features from muscle contractions, the use of ANN was also explored. This research also aims to investigate the possibility and the use of ANN in training and validation as a base methodology for classifying and recognising patterns for normal muscle signals.

Traditionally, practical methodologies for pattern classification are the *statistical* and the *syntactic* approaches [45, 61-63]. Much early research on EMG signals classification found many difficulties associated with the statistical method of instrumenting many channels of the signal. The *learning* or *neural* approach in ANN is the most recent established type of pattern classifier which is a matured form of adaptive linear elements in learning algorithms [45, 64-66]. The first ANN began to appear in the mid 1980s where it could be a powerful method for classifying EMG signals. It is the *feature set* or data itself that is crucial to the overall performance of the classifier [45], which comes down to the selecting of the signal features that produce the best performance in terms of accuracy and efficiency [1]. Hence, a substantial set of database with sufficient quantity and effective selected features, may improve the classification of the EMG signals. As the latest classification method, ANN's potential ability as a powerful tool is yet required to be investigated for the classification purposes in this research. Research by Englehart et al [1] showed an effective representation for classification using ANN.

The objective of this chapter is to execute the last stage of this research which was to train an ANN with 35 sets of the selected features from signals extracted in Chapter 3. The ANN was then validated with ten sets of untrained features-extracted previously. The ultimate purpose

of this exercise is to develop an ANN classifier that will differentiate the abnormal from the normal muscles. To build a normative database from normal muscle signals is essential for differential diagnosis of neurological and musculoskeletal disorders. By validating ANN using the ten sets of untrained data, it was to test and prove that the ANN developed was able to classify the untrained data as normal muscle signal. This should be a base methodology for further research in training and validating data for different muscle conditions and ultimately, for diagnosing whether an individual may have a specific neurological and or musculoskeletal disorder. Existing research evidence clearly indicates that when any type of neurological or muscle injury occurs the recruitment and electrophysiology of the muscle is altered [30-32].

A commercially available database on normal muscle signals is not available at this stage. An established database will become very useful for further use and research in designing an EMG signal analyser to compare and diagnose normal or abnormal muscles. Hence, signals were necessary to be collected manually in this research.

4.2 Neural Network Fundamentals

An ANN is a computer program that can recognise patterns in a given collection of data and produce a model for that data. It performs similarly to artificial intelligence and approximation algorithms for smart approximation. It resembles the brain in two respects, knowledge is acquired by the network through a learning process of trial and error as well as its interneuron connection strengths known as *synaptic weights* which are used to store the knowledge. It is a tool that is capable of learning from its environment and finding non-evident dependencies between data [67].

The ANN algorithms are modelled after the brain and how it processes the information. The brain is a multi layer structure with 10^{11} neurons interconnected to each other. It grows new neural links between neurons when learning from the 'feedback' it receives from the world as input maps to the output. In this research the data obtained from the muscle signal were being trained or put through neural network as inputs. These inputs create an environment which has its own typical features or patterns in the layer called the *hidden layer* of the

network. Every time a new input is being trained, the hidden layer readjusts the previous features to be the more updated version of it, which becomes the output layer of the network. This process is iterative until all the data is trained and the output target is reached [67].

This type of iterative process or learning rule is referred to as *backpropagation*, which is a generalisation of the Widrow-Hoff learning rule to multiple-layer networks and non-linear differentiable transfer functions [67]. Input vectors and the corresponding target vectors are used to train a network until it can approximate a function, associate input vectors with specific output vectors or classify input vectors in an appropriate way as defined by users. Networks with biases, a sigmoid layer and a linear output layer, are capable of approximating any function with a finite number of discontinuities. Hence, backpropagation is a gradient descent algorithm used for processing non-linear multilayer networks to compute negative gradients of the performance function.

Properly trained backpropagation networks tend to give reasonable answers when testing with new similar sourced inputs that they have never seen [67]. This is a way of validating whether the new inputs belong to a certain group or are classified as the target of the output. In other words, a new input leads to an output similar to the correct output for inputs used in training that are similar to the new input being presented. This generalisation property in ANN makes it possible to train a network on a set of input or target pairs and get sufficient representative results without training the network on all possible input or output pairs [67].

Basically there are four general steps in the training process [67]:

1. Assemble the training data – which have been already gathered in Chapter 3.
2. Create the network object – design and initialise the neural network.
3. Train the network – also called as batch training.
4. Simulate the network response to new inputs – this is also to compare results of the computed output of the network with training data and validation data.

A single layer neuron by itself is not a very useful pattern recognition tool. The real power of ANN comes when neurons are combined into the multilayer structures called the neural networks. The structure of a neural network is based on a single layer neuron model interconnected to each other to form multilayer network [67]. A single layer neuron model with R inputs is shown in Figure 4.1. Each input is weighted with an appropriate w. The sum

of the weighted inputs and the bias forms the input to transfer function *f*. Neurons may use differentiable transfer function *f* to generate their input.

There are three transfer functions commonly used for backpropagation for multilayer networks [67]. Multilayer network often use the log-sigmoid transfer function as in Figure 4.2. The function log-sigmoid generates outputs between 0 and 1 as the neuron's net input goes from negative to positive infinity. In MATLAB neural network toolbox used in this thesis, the notation program is written as

$$a = logsig(n) \tag{4.1}$$

which is equivalent to the mathematical expression

$$a = \frac{1}{1+e^{-n}} \tag{4.2}$$

where *n* is the input to the transfer function and *a* is the output data.

Alternatively, multilayer networks may use the tan-sigmoid transfer function as in Figure 4.3. The linear transfer function as in Figure 4.4 is also occasionally used in backpropagation networks. Both MATLAB program notations and mathematical expressions for Figure 4.3 and 4.4 are shown in the diagram boxes [67].

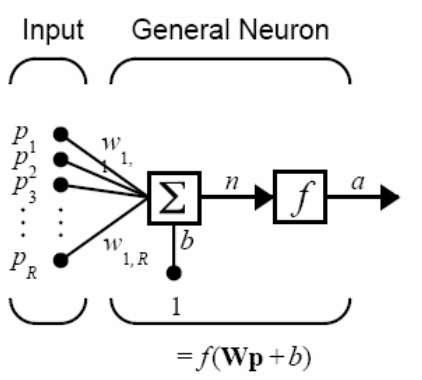

where R = number of elements in input vector

Figure 4.1 Single-layer neuron model.

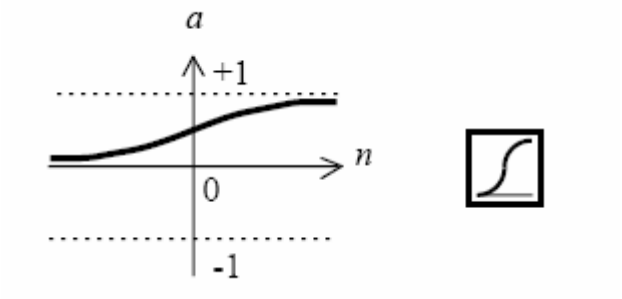

MATLAB notation a=logsig(n)

Mathematical expression $a = \frac{1}{1+e^{-n}}$

Figure 4.2 Log-sigmoid transfer function.

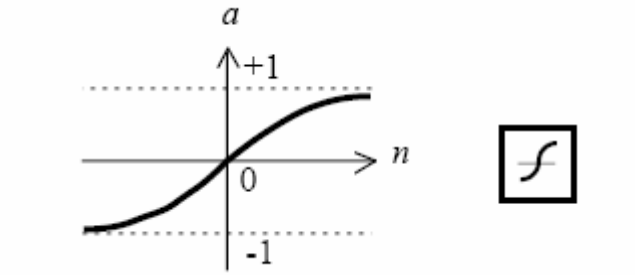

MATLAB notation a=tansig(n)

Mathematical expression $a = \frac{1-e^{-n}}{1+e^{-n}}$

Figure 4.3 Tan-sigmoid transfer function.

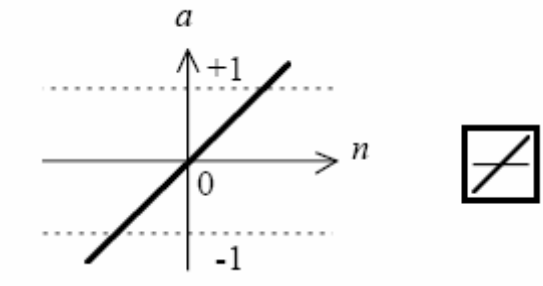

MATLAB notation a=purelin(n)

Mathematical expression $a = f(n) = n$

Figure 4.4 Linear transfer function.

If the last layer of a multilayer network has sigmoid neurons, then the outputs of the network are limited to a small range. If linear output neurons are used, the network outputs can take on any value. The structure of multilayer neurons is illustrated in Figure 4.5.

In backpropagation, it is important to be able to calculate the derivatives of any transfer functions used. Each of the transfer functions has a corresponding derivative function. However, these differentiable transfer functions are not commonly used and can be created and used with backpropagation if desired.

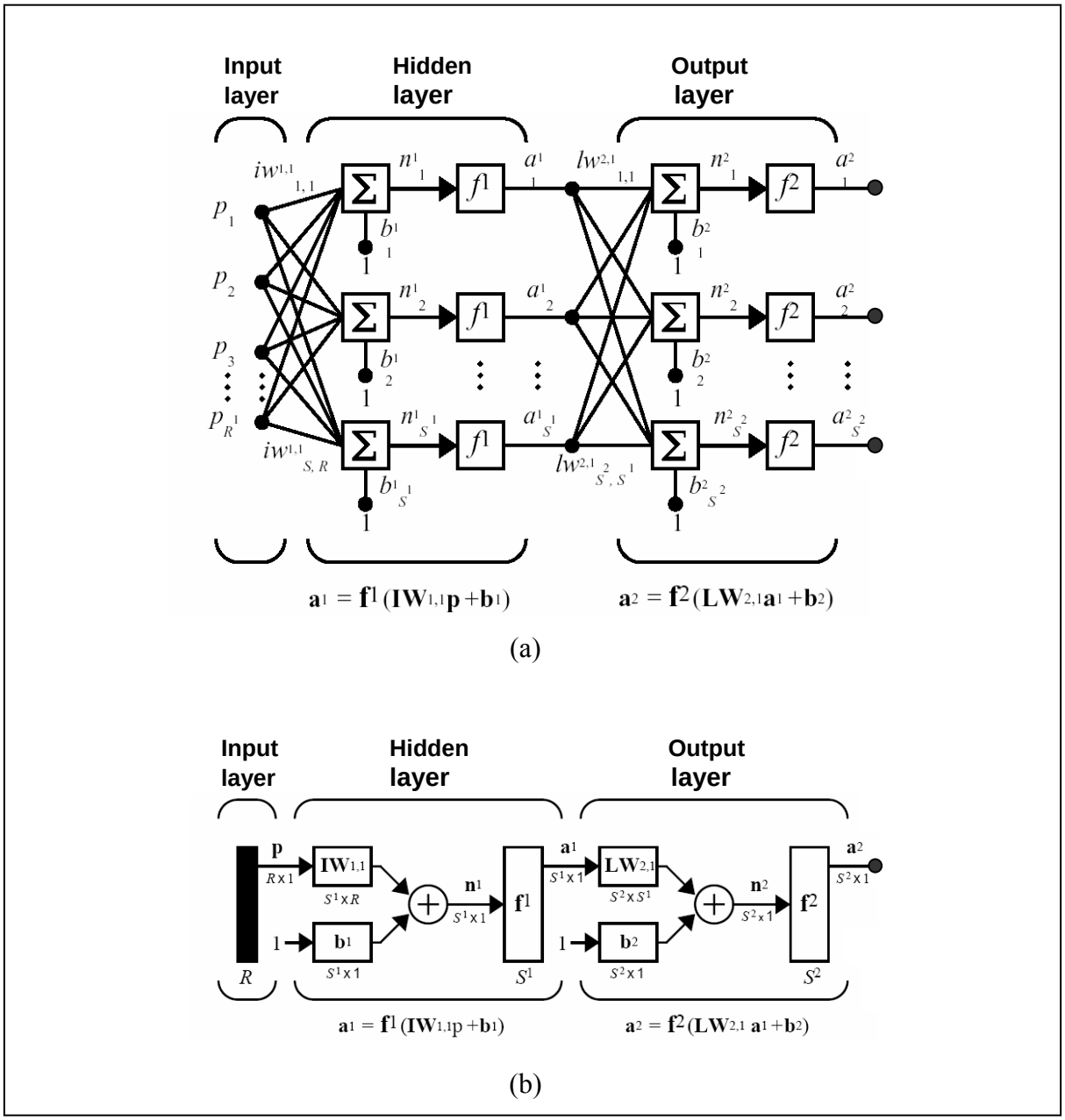

Figure 4.5 Multilayer neuron model. (a) Three layers multilayer version. (b) Abbreviated notation of (a).

Feedforward networks, or *forward pass* where information is flowing forward through the network, often have one or more hidden layers of sigmoid neurons followed by an ouput layer of linear neurons. Multiple layers of neurons with nonlinear transfer functions allow the network to learn nonlinear and linear relationships between input and output vectors. The linear output layer lets the network produce values outside the range of -1 to +1 [67].

The next section covers the four steps of the training process involved in this research. Section 4.3 includes the assembling of the data discussing the array, feature and target management. Section 4.4 describes and illustrates the design of the ANN and section 4.4 covers the validation result.

4.3 Data Assembling and Array Management

The data were required to be organised according to the nature or architectural structure of the neural network program. The ANN requires the structure of the target to be assigned or set in the form of output vector based on the Boolean notation. Depending on the data gathered and how they can be classified, the output vectors should be set accordingly to the research needs and efficiency of the operation.

The data assembled for the training of the neural network were from thirty five subjects exerting 25%, 50% and 75% of MVIC from right vastus lateralis leg muscles. The extracted features from 25%, 50% and 75% of MVIC become the target vector or the main output vector formed as

$$a = \begin{bmatrix} 1 & 0 & 0 \\ 0 & 1 & 0 \\ 0 & 0 & 1 \end{bmatrix} \tag{4.3}$$

where the first column is the target for 25%, the second for 50% and the third 75% of MVIC data. Each target column consisted of 15 features from each subject which included the mean and median frequencies from the average power spectrum and the RMS values of the wavelet coefficients at different scales of 8, 16, 32, 64 and 128. The structure of the array is drawn up in Figure 4.6. With the total of 35 subjects, there will be one target vector representing 35 data in each column.

No	Features	Subject 1			Subject 2			…	Subject 35		
	Median frequency at scale:	**25%** MVIC	**50%** MVIC	**75%** MVIC	**25%** MVIC	**50%** MVIC	**75%** MVIC		**25%** MVIC	**50%** MVIC	**75%** MVIC
1	8										
2	16										
3	32										
4	64										
5	128										
	Mean frequency at scale:										
6	8										
7	16										
8	32										
9	64										
10	128										
	RMS at scale:										
11	8										
12	16										
13	32										
14	64										
15	128										

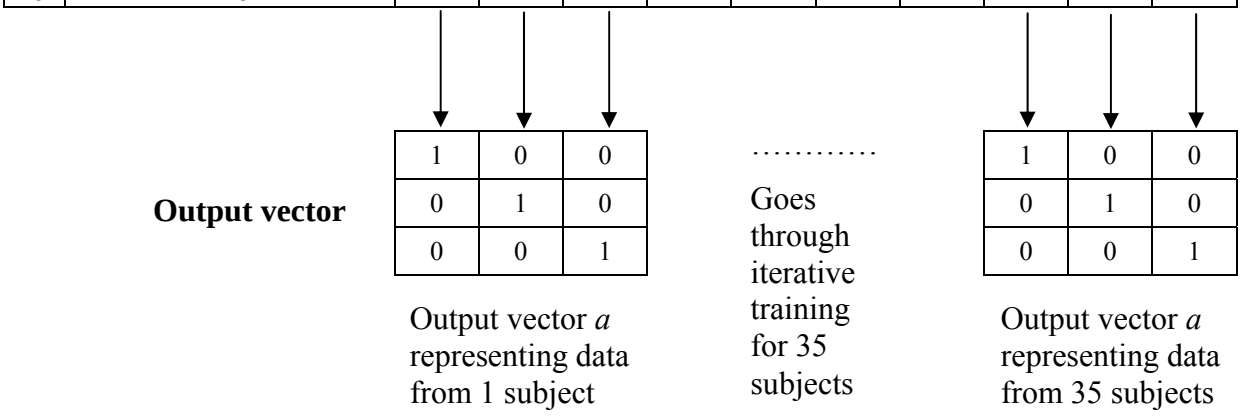

Figure 4.6 Array management of input data to the output vector.

4.4 Designing and Training of the Neural Network

The network architecture for this research consisted of an input layer, one hidden layer and an output layer or target as depicted in Figure 4.7. As previously explained in section 4.3, 15 features which included the RMS values, mean and median frequencies from the average power spectrum at wavelet scales of 8, 16, 32, 64 and 128 from the 35 subjects were in the input layer. These 15 input features from the 35 subjects were the data to be trained in the ANN.

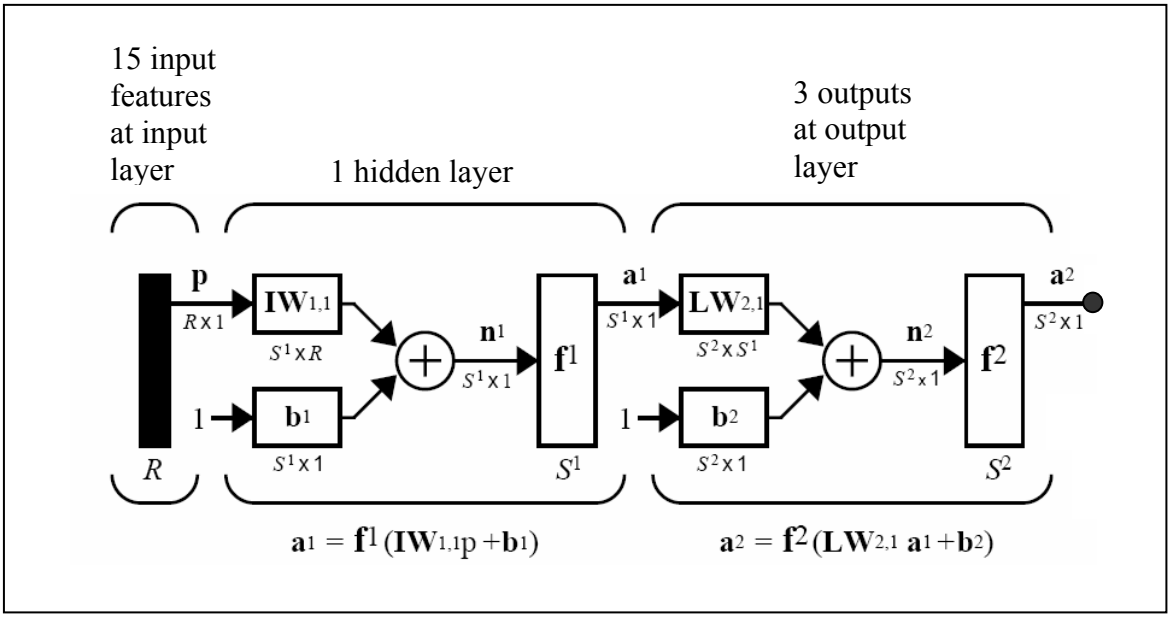

Figure 4.7 Network architecture built for this research.

A hidden layer in an ANN consists of a number of neurons. The number of neurons in the hidden layer needs to be selected based on the overall performance in reaching the target upon validation. Apart from the number of neurons, two transfer functions of log-sigmoid and tan-sigmoid were also used. Linear transfer function was not selected as it did not represent the nature of the SEMG data which are non-linear. Several trainings and validations are executed using different number of neurons and the two types of transfer functions. Validations were executed with ten sets of untrained data, each containing 15 features which similarly included the RMS values, mean and median frequencies from the average power spectrum at scales 8, 16, 32, 64 and 128 from the 10 subjects. The ANN with the number of neurons and the type of transfer function which met the performance goal with least errors was the selected one for a base classifier in further research and development of SEMG signal classifier.

The network architecture built for this research is illustrated in the Figure 4.7 where 15 features from 35 subjects in the input layer were trained for 3 targets of 25%, 50% and 75% MVIC in the output layer as described in section 4.3. In the hidden layer, the neuron numbers tested are from 3 to 10 to start with. The lower the number of neurons selected, the more efficient the training process is. This means with less iterations the faster the

processing is. The ANN program notations by MATLAB that represent the architecture are enclosed in the Appendix E.

With both transfer functions, tan-sigmoid and log-sigmoid, parameters were set as follows:

1. Training algorithm: Levenberg-Marquardt [67]
2. No. of epochs or iterations: 1000
3. Performance goal: 0.001 or 0.1% error
4. Maximum performance gradient: 1×10^{-10}

Using the two transfer functions, tan-sigmoid and log-sigmoid, and the neuron numbers in the hidden layer set between 3 and 10, hence there were 16 different ANNs to be trained. After the training, the 16 ANNs went through the validation process using the untrained data from ten subjects. The performance goal or the error results between the 16 ANNs were then compared.

4.5 Validation, Results and Analysis

After training and validation, the transfer function which met the network target vector was the tan-sigmoid transfer function with neuron numbers 4, 5, 6 or 7 in the hidden layer. None of the log-sigmoid transfer function networks met the target after validation. The tan-sigmoid ANNs with the mentioned neuron numbers produced more comparable results in terms of meeting the performance goal. ANNs with neuron numbers 3, 8, 9 and 10 did not meet the target with some number of epochs or iterations being too great compared to the ANNs with neuron numbers 4, 5, 6 and 7.

The network with neuron number 4 in the hidden layer is named as '*net1*', the one with neuron number 5 is '*net2*' and so on. Ten sets of untrained data from ten subjects were validated, 15 input features were tested for three targets from each subject. With ten subjects, 10 validations with Boolean notation results were produced for each of the three output targets, which are 25%, 50% and 75% MVIC, totalling 30 validation results. Details of Boolean results from ten validating data for three outputs are shown in Figure 4.8 to 4.11. Figure 4.12 shows the comparison between training curves of the different neuron numbers in

the hidden layer showing efficiency in reaching the performance goal. The summary of results of the ANNs which met the target were listed in Table 4.1.

Parameters

Inputs	15
Hidden (neuron number)	4
Outputs	3
Function	tansig

net1 Architecture

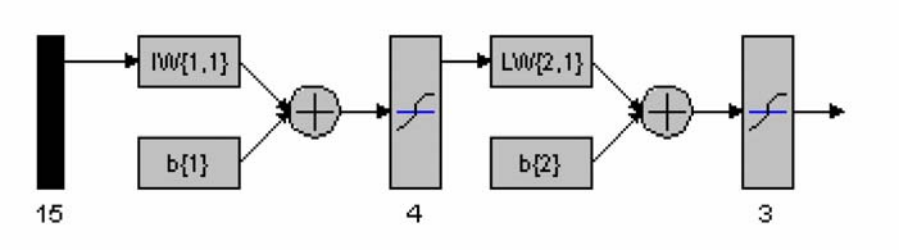

net1 Training Curve

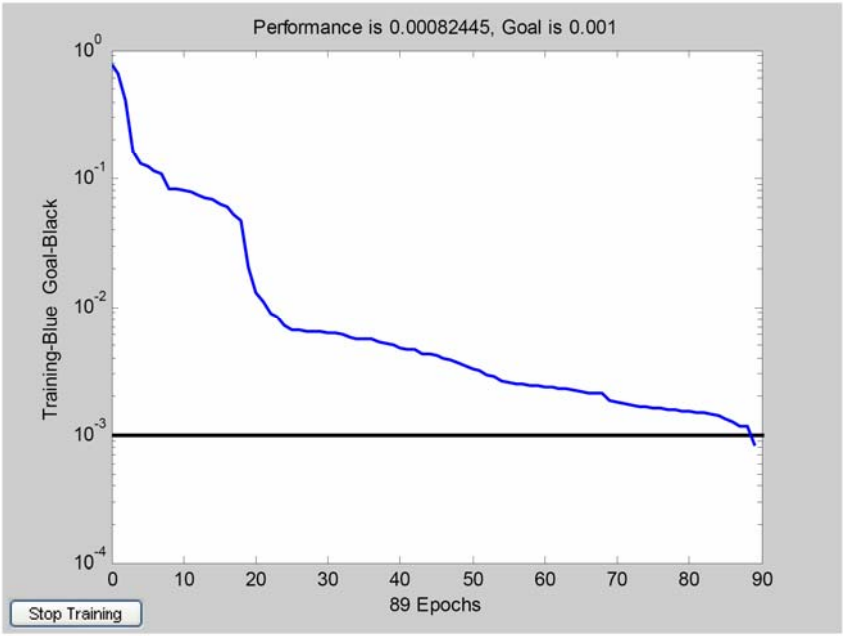

Figure 4.8 ANN net1 parameter setting, architecture and training curve.

net1 Validation Data Results

25%	50%	75%	25%	50%	75%	25%	50%	75%	25%	50%	75%	25%	50%	75%
1	0	0	1	0	0	1	1	0	1	0	0	1	0	0
0	1	0	0	1	1	0	1	1	0	1	0	0	1	0
0	0	1	0	0	1	0	0	1	0	0	1	0	0	1
Data No.1			Data No.2			Data No.3			Data No.4			Data No.5		

25%	50%	75%	25%	50%	75%	25%	50%	75%	25%	50%	75%	25%	50%	75%
1	0	0	1	0	0	1	0	0	1	0	0	1	0	0
0	1	0	0	1	1	0	1	0	0	1	1	1	1	0
0	0	1	0	0	1	0	0	1	0	0	1	0	0	1
Data No.6			Data No.7			Data No.8			Data No.9			Data No.10		

Figure 4.8 (Continued) ANN net1 validation data results.

The orange shaded areas in the validation data results in Figure 4.8 indicate the output column vector that did not meet the output target $a = \begin{bmatrix} 1 & 0 & 0 \\ 0 & 1 & 0 \\ 0 & 0 & 1 \end{bmatrix}$. These occur with data No.2 at the third column, data No.3 at the second and third column, data No.7 at the third column, data No.9 at the third column and data No.10 at the first column. The total unmet targets are six columns data out of 30 columns. Therefore the error of net1 is 6 out of 30 or 20%.

Parameters

Inputs	15
Hidden (neuron number)	5
Outputs	3
Function	tansig

net2 Architecture

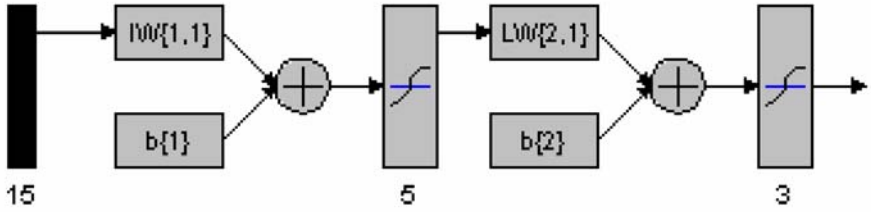

Figure 4.9 ANN net2 parameter setting and architecture.

net2 Training Curve

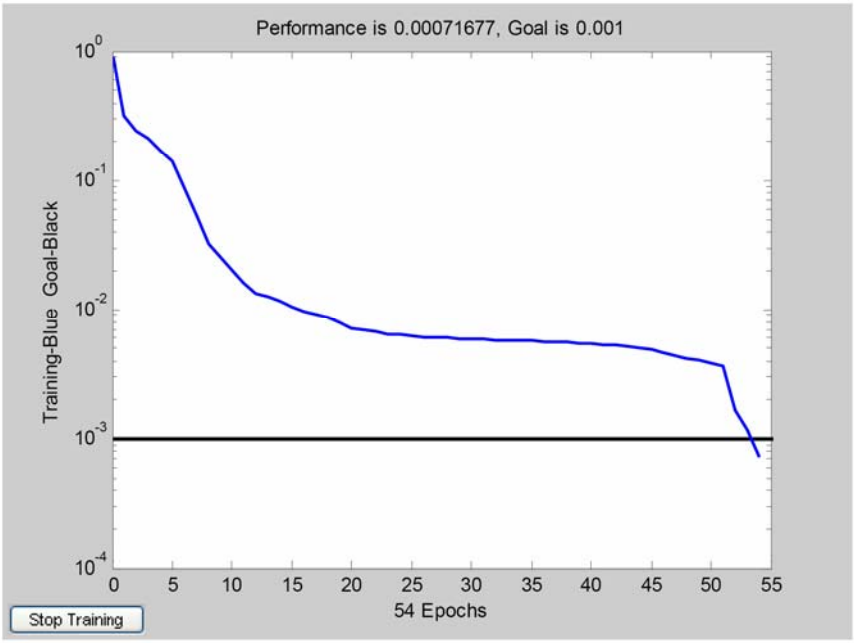

net2 Validation Data Results

25%	50%	75%	25%	50%	75%	25%	50%	75%	25%	50%	75%	25%	50%	75%
1	0	0	1	0	0	1	0	0	1	0	0	1	0	0
0	1	0	0	1	0	0	1	0	0	1	0	0	1	0
0	1	1	0	0	1	0	0	1	0	0	1	0	0	1
	Data No.1			Data No.2			Data No.3			Data No.4			Data No.5	

25%	50%	75%	25%	50%	75%	25%	50%	75%	25%	50%	75%	25%	50%	75%
1	0	0	1	0	0	1	0	0	1	0	0	1	0	0
0	1	0	0	1	0	1	1	0	0	1	0	0	1	0
0	0	1	0	0	1	0	0	1	0	0	1	0	0	1
	Data No.6			Data No.7			Data No.8			Data No.9			Data No.10	

Figure 4.9 (Continued) ANN net2 training curve and validation data results.

The orange shaded areas in the validation data results in Figure 4.9 indicate the output column vector that did not meet the output target $a = \begin{bmatrix} 1 & 0 & 0 \\ 0 & 1 & 0 \\ 0 & 0 & 1 \end{bmatrix}$. These occur with data No.1 at the second column and data No.8 at the first column. The total unmet targets are two columns data out of 30 columns. Therefore the error of net2 is 2 out of 30 or 6.67%.

Parameters

Inputs	15
Hidden (neuron number)	6
Outputs	3
Function	tansig

net3 Architecture

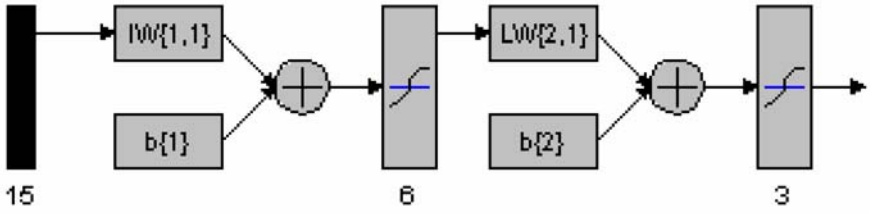

net3 Training Curve

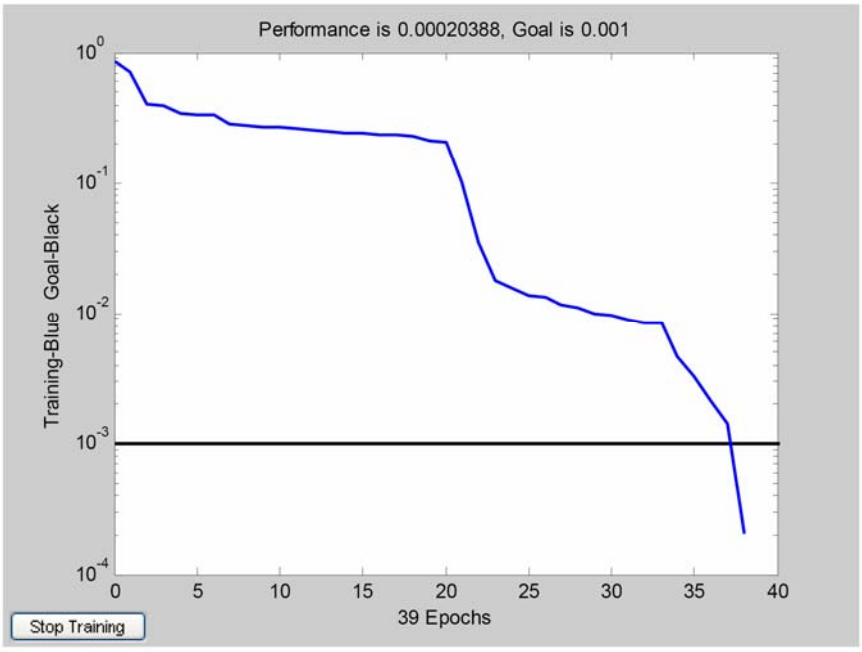

Figure 4.10 ANN net3 parameter setting, architecture and training curve.

net3 Validation Data Results

25%	50%	75%	25%	50%	75%	25%	50%	75%	25%	50%	75%	25%	50%	75%
1	0	0	1	0	0	1	0	0	1	0	0	1	0	0
0	1	0	0	1	0	0	1	0	0	1	0	0	1	0
0	1	1	0	0	1	0	0	1	0	0	1	0	0	1
Data No.1			Data No.2			Data No.3			Data No.4			Data No.5		

25%	50%	75%	25%	50%	75%	25%	50%	75%	25%	50%	75%	25%	50%	75%
1	0	0	1	0	0	1	0	0	1	0	0	1	0	0
0	1	0	0	1	0	0	1	0	0	1	0	0	1	0
0	0	1	0	0	1	0	0	1	0	0	1	0	0	1
Data No.6			Data No.7			Data No.8			Data No.9			Data No.10		

Figure 4.10 (Continued) ANN net3 validation data results.

The orange shaded areas in the validation data results in Figure 4.10 indicate the output column vector that did not meet the output target $a = \begin{bmatrix} 1 & 0 & 0 \\ 0 & 1 & 0 \\ 0 & 0 & 1 \end{bmatrix}$. This occurs with data No.1 at the second column. The total unmet target is one column data out of 30 columns. Therefore the error of net3 is 1 out of 30 or 3.33%.

Parameters

Inputs	15
Hidden (neuron number)	7
Outputs	3
Function	tansig

net4 Architecture

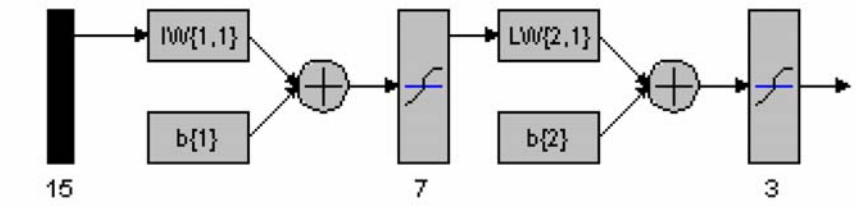

Figure 4.11 ANN net4 parameter setting and architecture.

net4 Training Curve

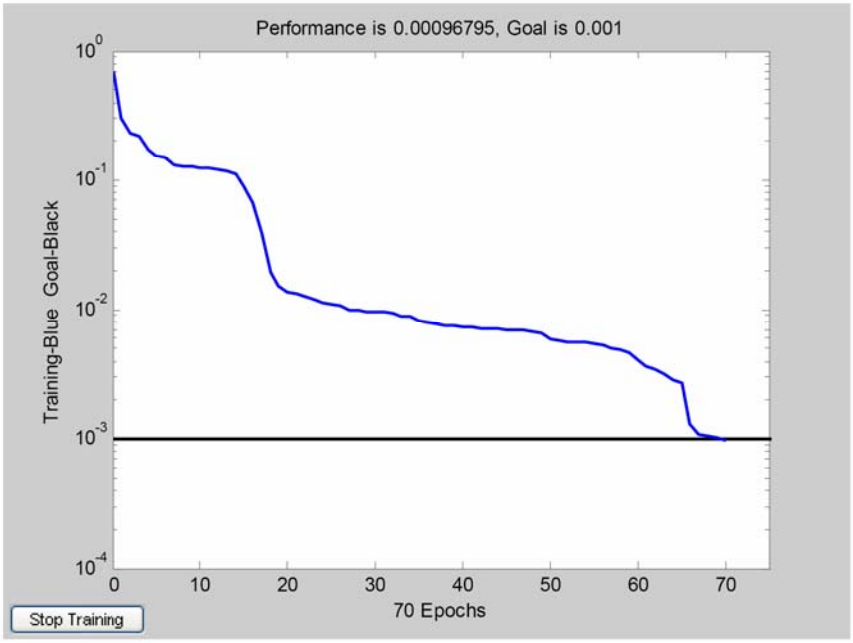

net4 Validation Data Results

25%	50%	75%	25%	50%	75%	25%	50%	75%	25%	50%	75%	25%	50%	75%
1	0	0	1	0	0	1	0	0	1	0	0	1	0	0
0	1	1	0	1	1	0	1	1	0	1	0	0	1	1
0	0	1	0	0	1	0	0	1	0	0	1	0	0	1
Data No.1			Data No.2			Data No.3			Data No.4			Data No.5		

25%	50%	75%	25%	50%	75%	25%	50%	75%	25%	50%	75%	25%	50%	75%
1	0	0	1	0	0	1	1	0	1	0	0	1	0	0
0	1	1	0	1	0	0	1	0	0	1	0	0	1	1
0	0	1	0	0	1	0	0	1	0	0	1	0	0	1
Data No.6			Data No.7			Data No.8			Data No.9			Data No.10		

Figure 4.11 (Continued) ANN net4 training curve and validation data results.

The orange shaded areas in the validation data results in Figure 4.11 indicate the output column vector that did not meet the output target $a = \begin{bmatrix} 1 & 0 & 0 \\ 0 & 1 & 0 \\ 0 & 0 & 1 \end{bmatrix}$. These occur with data No.1 at the third column, data No.2 at the third column, data No.3 at the third column, data No.5 at the third column, data No.6 at the third column, data No.8 at the second column and data

No.10 at the third column. The total unmet targets are seven columns data out of 30 columns. Therefore the error of net4 is 7 out of 30 or 23.33%.

Comparison of efficiency in reaching the performance goal between different neuron numbers in the hidden layer is shown in the Figure 4.12.

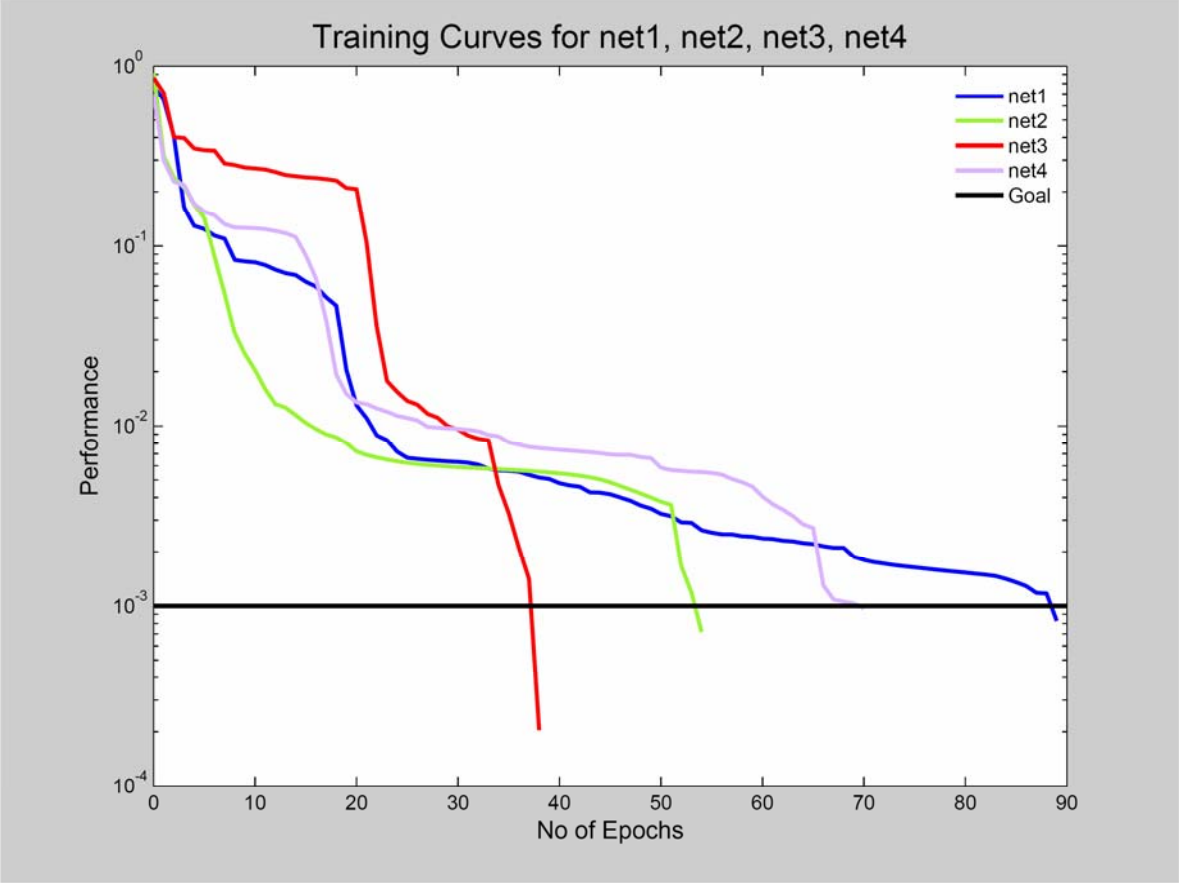

Figure 4.12 Training curves of net1, net2, net3 and net 4 showing efficiency in reaching performance goal.

Table 4.1 Summary of results of training and validating neural networks using tan-sigmoid transfer function.

Network name	Neuron number at Hidden layer	Error	Error Percentages
net1	4	6/30	20
net2	5	2/30	6.67
net3	6	1/30	3.33
net4	7	7/30	23.33

The third column of Table 4.1 lists the summary of errors resulting from the validation process out of 30 data and the fourth column shows in terms of percentages. The error indicated the number of times out of 30 that did not meet or reach the target vector *a*. From Table 4.1, the network which produced the least error number from the ten validating data is net3 which has 6 neurons in its hidden layer.

The efficiency performance can be determined from the training curves of net1, net2, net3 and net4 which are illustrated in Figure 4.12. The black line is the performance goal of 0.1% error. The network which reached the goal with the least number of epochs is also net3, at 39 iterations when reaching the performance goal. The next best network is net2, which reached the performance goal at 54 epochs and 6.67% error as listed in Table 4.1. net2 is network with neuron number 5. net4 with neuron number 7 produced the greatest error of 23.33% with 71 epochs and net1 produced 20 % error with 89 epochs.

Therefore, from this comparison, ANN net3 with the tan-sigmoid transfer function and 6 neurons in the hidden layer is the most suitable network that can be used for training and validating the data of this research.

The outcome of this research stage showed that the methodology of using ANN was able to predict the untrained data classified as normal muscle which underwent 25%, 50% and 75% of MVIC with minimal error. Hence, this technique is concluded to be a strong base method for further study in this research of developing muscle signal classifier.

Chapter 5
Discussion and Conclusions

5.1 Introduction

This chapter covers the discussions on all of the stages undertaken in this research. Comparative analysis is presented particularly on the software development and the pre-processing stage which used different analysis schemes for feature extractions. Other findings on the practical aspects of data collection and acquisition are commented in this chapter. Outcomes or results from the final selected feature extraction process and signal classification using Artificial Neural Network (ANN) are further analysed and discussed. The pros and cons of each stage are described with some potential work extension which can be implemented for further research.

This research undertook many aspects, ranging from software development, data acquisition, pre-processing, feature extraction to the ANN. Every stage contributes strengths and flaws in its own specific parameters which may be carried through to the next stage. It was challenging to control every aspect that was involved, and this research has made every effort to minimise any biases or flaws which could greatly affect the results.

5.2 Software Development

The software development stage involved two major software programs, LabVIEW and MATLAB, which contributed a crucial part of this research as processing and analysing tools. All efforts have been made in learning the rigorous LabVIEW and MATLAB programming codes in order to build the signal processing tools for analysing and extracting features of the Surface Electromyography (SEMG) signals using different analysis schemes, which were the Fast Fourier Transform (FFT), Short Time Fourier Transform (STFT), Continuous Wavelet Transform (CWT), Discrete Wavelet Transform (DWT) and the Discrete Wavelet Packet Transform (DWPT).

The software development stage required a sample or pilot signal in order to test the programs as they were being written. In reality, some data needed to be collected at the same time as the building of the software programs. Hence, data collection and acquisition were carried out alongside the completion of the programs.

LabVIEW programs provide a user-friendly interface to the user in terms of output display as well as data management and the core design of the programming code. It uses the system of block diagrams and flowcharts in designing the required processing tools or so called the virtual instruments (VIs). It resembles the 'G' programming language where the blocks are for processing operation and the lines for data flow. It was found that the LabVIEW programming code is more versatile and easier to learn, especially for anyone with the least familiarity of the popular programming codes or language such as 'C' or 'Visual Basic'.

Another advantage of LabVIEW is that it enables users to change, manipulate or select any features on the interface or front display panel without entering back to the core programming codes to make the change. These were such as entering a new input on the interface VI panel to produce a different value or visual output, or selecting parts of the output graph for determining various values related to the graph. Programming errors were minimised as users did not need to return to the core design to make input changes. These manipulation capabilities within the LabVIEW programming give more control, flexibility and versatility to the users, minimising errors in programming.

On the other hand, the MATLAB programming system is consisted of commands and codes similar to a conventional programming language such as 'C' which needed to be written in a logical manner. Most of the commands and other calculation codes are often the common signs and codes which are familiar to the mathematicians, scientists and engineers. This makes MATLAB also a powerful and versatile tool in this field. The MATLAB programming system could be more suitable for users who are familiar with computer programming codes, whereas LabVIEW provides the visual aid in programming as it uses block diagrams and flowcharts.

Many signal processing programs were built using different analysis schemes, which were FFT, STFT, CWT, DWT and DWPT, with both LabVIEW and MATLAB programs. The

development of these numerous programs was for comparison purposes. It was thought to be a necessary part of the research process in this field undertaken by the university, which is still at a very early stage. This process provided comparisons to validate which programs to use and to evaluate which format would be the most efficient and useful.

Both results by LabVIEW and MATLAB programs shown in Table 3.1 were close to each other. MATLAB is no less superior to LabVIEW in terms of signal processing accuracy and efficiency. Both programs are valid to be used for the purpose of this research.

In summary, programming by LabVIEW is found to be more flexible and efficient for signal processing, analysis and feature extraction of the SEMG signals. The reason for this claim is the versatility of being able to control more from the front display panel without going into the core programming chart, hence minimising programming error. Depending on the users' background and programming style or preference, whether they are visually or logically driven, or which programs they are initially familiar with, or whether they are willing to learn new programming system, LabVIEW and MATLAB can both be used for this purpose.

5.3 Data Collection and Signal Acquisition

The collection of the data was a massive operation to undertake. Ethical approval was required before the data collection as it involved live human subjects as the participants. The other major aspect was to find the proper protocols or procedures during data collection. As it involved physiological information and research, proper consultation and management with the related professionals from the Physical and Rehabilitation Research Centre at Akoranga Campus of AUT were extremely crucial. This process was to ensure that the protocols, data collectors and participants were all as consistent and uniform as each other, minimising any manual bias or human error that could easily occur during data collection.

The equipment and the process used in signal acquisition also played an important role in obtaining the data signals. All practicable or common steps were accounted for the aspects of signal acquisition, amplification and conditioning to eliminate any signal biases and artifacts. Prior to the data collection, the equipment was checked by carrying out trial runs to view the

signals obtained. Some offset or bias component from the main supply that showed on the signals were rectified accordingly. The types of amplification and signal conditioning procedures were chosen based on the common practice of SEMG signal acquisition taken from some literature sources [17, 20, 68]. When there were several settings or methods to choose from, selections were made based on the suitability of the practice or nature of this research. Therefore, there is always room to investigate more on different settings, equipment or setups for viewing how they influence the overall results. These are sampling rate, filter settings, amplification and so on.

Collecting SEMG data from forty five subjects were repetitive and laborious tasks performed often by the same person as the data collector. The location of the surface electrodes placed on the muscle could not be exactly accurate for every single subject who participated in the data collection. A different data collector may carry out the protocols slightly different from another data collector. These are the human errors which can contribute to the signal characterisation results which could be minimised as much as possible by carrying strict uniformed instructions for the participants to follow.

5.4 Signal Pre-processing

As the five programs were built using FFT, STFT, CWT, DWT and DWPT analysis schemes with LabVIEW programming code, this stage of pre-processing used a set of sample signals to analyse and extract features to produce outputs for each of the program. A comparison was made of which analysis scheme provided the most suitable features or parameters which can be useful for the development of ANN at the later stage.

From five of these programs built in stage 1, the one that produced the most satisfactory results for signal classification in the ANN was the Continuous Wavelet Transform or CWT. CWT was the most satisfactory analysis tool for this research purpose as it produced a better display of the wavelet transform. It produced the most detailed information in the range of frequencies for each scale used. The transformation of scales to frequencies was one of the useful procedures that could be used throughout the research in this field. CWT provided clearer visual output on where in time the dominant scales were located. Thus the

transformation of the dominant scales into frequencies could be calculated along with the further processing on feature extraction and selection, determining the mean and median frequencies of the power spectrum and the RMS value of the signal.

DWT and DWPT provided more detailed signal information for every breakdown of the time period resulting from the multiresolution analysis using a particular dominant scale index number. Investigating more outcomes from DWT and DWPT analysis can be a form of future work in this field. DWT and DWPT analysis can be used to investigate further into each level of scale index to gain detailed characterisation of the signal.

By using DWT and DWPT, although they could be used to focus on characters at particular scale index level, they did not give the overall outlook of the transform to start with, which was essential for the initial attempt to view what scales and when the dominant transform occurred. Hence, analysis using CWT is an appropriate step for the initial outlook of the dominant scales before selecting the scale number for the multiresolution analysis if any further research is carried out using the DWT and DWPT analysis.

Obviously time localisation of the dominant frequency was not available by using FFT analysis alone. The FFT analysis was used at the later stage in the software design, after signal processing using CWT analysis, to calculate and determine the mean and median of the average power spectrum and RMS values of the signals. STFT is also limited by the size of the window which has to be uniform throughout the duration of the signal. Many signals require a more flexible approach in window sizing which have been catered for by the wavelet transform analysis. The flexibility of window sizing or the compression and dilation of the mother wavelet provides accuracy in determining the time-frequency component of the signals.

This research, hence, adopted the CWT analysis in the signal processing for feature extraction and developed it further to a final program using FFT as an extension to calculate and determine the feature selected for this research, the mean and median frequencies of the average power spectrum and the RMS values of the signals.

5.5 Feature Extraction and Selection

The feature extraction stage implemented a selection of techniques which were chosen based not only on common practices but also on a sound judgement for assumptions that were considered relevant to the case in this research. This was reflected by one of the procedures in selecting the relevant part of the 10-second signals for feature extraction using CWT analysis. The 2-second region described in chapter 3.5 and Figure 3.19 was considered and selected as a prime location for feature extraction due to the stability of the muscle signal from the contraction, stabilising after the initial period when the muscle started to contract. This practice was quoted by Merletti et al [55, 60] and Luttmann et al [55, 60] for extracting features on SEMG signals.

Extracting feature from the whole 10-second signal would be an ideal as it may show more variants of the signal characteristics. Processing the whole duration at one time would require a vast amount of power from the computer and disk-space to run. Such facilities are not available at this stage. Breaking the signals into short time durations would be more achievable for feature extraction, but a laborious task. At this stage, processing the 2-second region is sufficient to represent the signal characterisation [55, 60]. This 2-second region is assumed to be quasi-stationary. Although it is sufficient and had been previously used by Luttmann et al [60], performing a further test of stationarity could be carried out in order to determine the longest stationary period where signal length region can be selected for more accuracy in stationarity. Researching into extracting the features from the whole signal duration could also be expanded for the future work in this research.

After applying the CWT analysis to this 2-second quasi-stationary region, a scalogram was formed presenting the scale and time-based plot. This plot showed which scale at particular time was dominant indicated by the amplitude. The technique of scales to frequencies conversion is relatively new, and found to be a powerful way of portraying scales, which are less familiar parameters, to frequencies which are more common and meaningful parameters. This technique is indeed one of the major procedures in this research, as it leads to the selection of the scale index number from the corresponding dominant frequencies, which would largely impact the whole signal characterisation.

Selecting the scale index numbers was carried out by visually viewing the scalogram and the frequency-time based spectrum plot. The dominant regions were noted with the corresponding scale numbers which were chosen. This technique required sound judgement and accuracy as it was done manually. Hence, the results can still be subjected by human error. Although, whichever index scale number is chosen, as long as the same ones are being used throughout the rest of the research process, the end results should give the same consistency. This is due to the nature of the values from any parameter being relative rather than absolute. Future work to develop an extension programming code for selecting dominant scale index numbers can be done to eliminate or minimise error.

5.6 SEMG Signal Classification Using Artificial Neural Network

The outcome of this research stage managed to show that the methodology of using Artificial Neural Network (ANN) was able to predict the untrained data classified as normal muscle which underwent 25%, 50% and 75% of Maximum Voluntary Isometric Contraction. This was shown in the results with the minimum error of 3.33% from data of the most suitable ANN, net3, with tan-sigmoid transfer function and neural number 6 in the hidden layer.

There was no specific rule in setting the target vector. Hence, it required a sound judgement to set and form one based on the nature of the data and how the data was managed. Array management for the data is therefore an essential part of achieving strong performance of the ANN.

The error in the ANN validation process was caused by an overlap in the target vector. In Figure 4.10, showing net3 validation results, some of the data in the second column from data No.1 was classified as 50% and 75% MVIC instead of just 50% MVIC. This may due to the fact that there may be a close range of values between features, particularly the mean and median frequencies of the average power spectrum. Having both in the same unit of Hz and close statistical position, thus give them more possibilities of being in the close range of values. Hence, due to the overlapping effect, using a combination of features in a similar unit such as the mean and median frequencies of the power spectrum may add more complexity in setting the target vector. A combination of features with different units such as the RMS

value of the signal and either the mean or median frequencies, and some other parameters which differ in units, may improve the performance of the ANN, producing less error and add more certainties. This way of investigation may be carried out for the future research in refining the use of ANN for improving efficiency, accuracy and overall performance.

As mentioned before, literature review claimed that the overall performance of the ANN depends on the quality and quantity of the selected feature set or data itself rather than just having a powerful classifier [45]. Therefore, collecting more data is also another way to improve the ANN performance. The drawback of this is that it is a laborious task but it is one of the major contributions for developing a powerful classifier.

Collecting data from abnormal muscles can be carried out where they can be used to test and validate the existing classifier which was built to classify for normal muscle. This technique can be executed for validating various classifiers that can be built for different muscles. It is the amount of database of muscle signal data which is again a laborious task that is required to be built for this purpose.

So far, the ANN stage has produced satisfactory results with minimal error in terms of classifying the untrained normal muscle data as 'normal'. This showed that the basic procedure developed using ANN can be further utilised and refined for future work by collecting more data and investigating into setting features in different units. This technique is concluded to be a strong base method for further study in this research of developing muscle signal classifier.

5.7 Conclusions

In summary, this research has investigated aspects involved in the digital signal processing using wavelet and Fourier analysis for extracting features of SEMG signals, the signal collection from forty five males with normal leg muscles, and the use of ANN for developing a signal classifier. As a beginning research area in the faculty, various aspects were developed more in an outlined manner rather than a strong focus in one area, using

techniques used in the literature review. More focused works on a particular area can be done in future work of this research.

The area which had been covered in this research included:

- Software development which used the principles of digital signal processing using different analysis schemes of FFT, STFT, CWT, DWT and DWPT to extract features of the SEMG signals.
- Understanding the SEMG signals and the procedures or protocols in collecting them.
- Designing an Artificial Neural Network which trained data and validated the network that it is capable of classifying the data for a certain category.

This research has produced results which were satisfactory, and hence the methodology developed is potentially promising and can be used as a basis of practice for future work in developing a SEMG signal classifier.

5.8 Recommendations

- Data Acquisition, apparatus and setups – more investigation can be carried out focusing on different settings, equipment or setups to view how they influence the overall results.

- Feature extraction and analysis schemes
  - Performing a further test of stationarity to determine the longest stationary period where signal length region can be selected for more accuracy in stationarity. Researching into extracting the features from the whole signal duration could also be expanded for the future work in this research.
  - Continuous Wavelet Transform can remain to be the first or overall basic analysis scheme for feature extraction. For future work, the Discrete Wavelet Transform and Discrete Wavelet Packet Transform analysis can be utilised to analyse focusing more into each level of scale index in order to gain detailed characterisation of the signals.

- Developing an extension programming code for selecting dominant scale index numbers from the scalogram to minimise or eliminate error when it is done manually.

- Feature selection – different sets of features can be further investigated other than the ones that were determined in this research. RMS value of the signals was an efficient feature that can be used in combination with other features like the mean frequency of the average power spectrum and some other features which are not the same in unit or close range in values.

- Artificial Neural Network – more data can be obtained and employed for training ANN to establish a more powerful and accurate classifier. Data from abnormal muscles can be collected and used to test and validate the existing classifier for accuracy.

- Future Classifiers – By building a substantial database of SEMG muscle signals of different conditions, which are normal and abnormal with various ailments, classifiers can be further developed into recognising these conditions.

Appendix A

Factors of SEMG Signal Measurement Complexity

The factors that gives rise to the complexity of SEMG signal measurement were discussed and classified in depth by De Luca [20] and identified in the following categories

- Causative
- Intermediate
- Deterministic

The interrelationships of the factors and effects on the EMG signal and subsequent interpretation of the signal characteristics are displayed in the following.

The *causative* factors have a basic effect on the signal, split into two groups:

- Extrinsic factors: those associated with electrode structures and its placement/orientation on the surface of the skin above the muscle.
- Intrinsic factors: the physiological, anatomical and biochemical characteristics of the muscle. Unlike the extrinsic factors associated with the electrodes, these factors cannot be easily controlled because they involves:
    - the number of active motor units at any particular time of the contraction
    - fibre composition of the muscle which determine change in the pH during contraction
    - Blood flow in the muscle which determine the rate of metabolism during contraction
    - Fibre diameter
    - Depth and location of the active fibres
    - The amount of tissue between the surface of the muscle and the electrode which affects the spatial filtering of the signal.

The *intermediate* factors represent physical and physiological phenomena that are influenced by one or more of the causative factors and in turn influence the deterministic factors, which include:

- Band-pass filtering aspects of the electrode, an inherent characteristic of a differential electrode configuration.

- Detection volume of the electrode which determine the number and weight of a motor unit action potential (MUAP) that composes the signal.
- Superposition of action potentials in the detected EMG signal which influence the characteristics of the amplitude and frequency of the signal.
- Crosstalk from nearby muscle, which contaminates the signal and may mislead interpretation of the signal information.
- Conduction velocity of the action potentials that propagate along the muscle fibre membrane; the conduction velocity affects amplitude and frequency characteristics of the signal.
- The spatial filtering effect due to relative position of the electrode and the active muscle fibres.

The *deterministic* factors have a direct bearing on the information in the EMG signal and the recorded force, these includes:

- The number of active motor units
- Motor unit force-twitch
- Mechanical interaction between muscle fibres
- Motor unit firing rate
- The number of detected motor units
- Amplitude, duration and shape of the MUAPs
- Recruitment stability of motor units

Appendix B1

Signal Processing Program using Fast Fourier Transform (FFT) Analysis by LabVIEW

Block Diagram

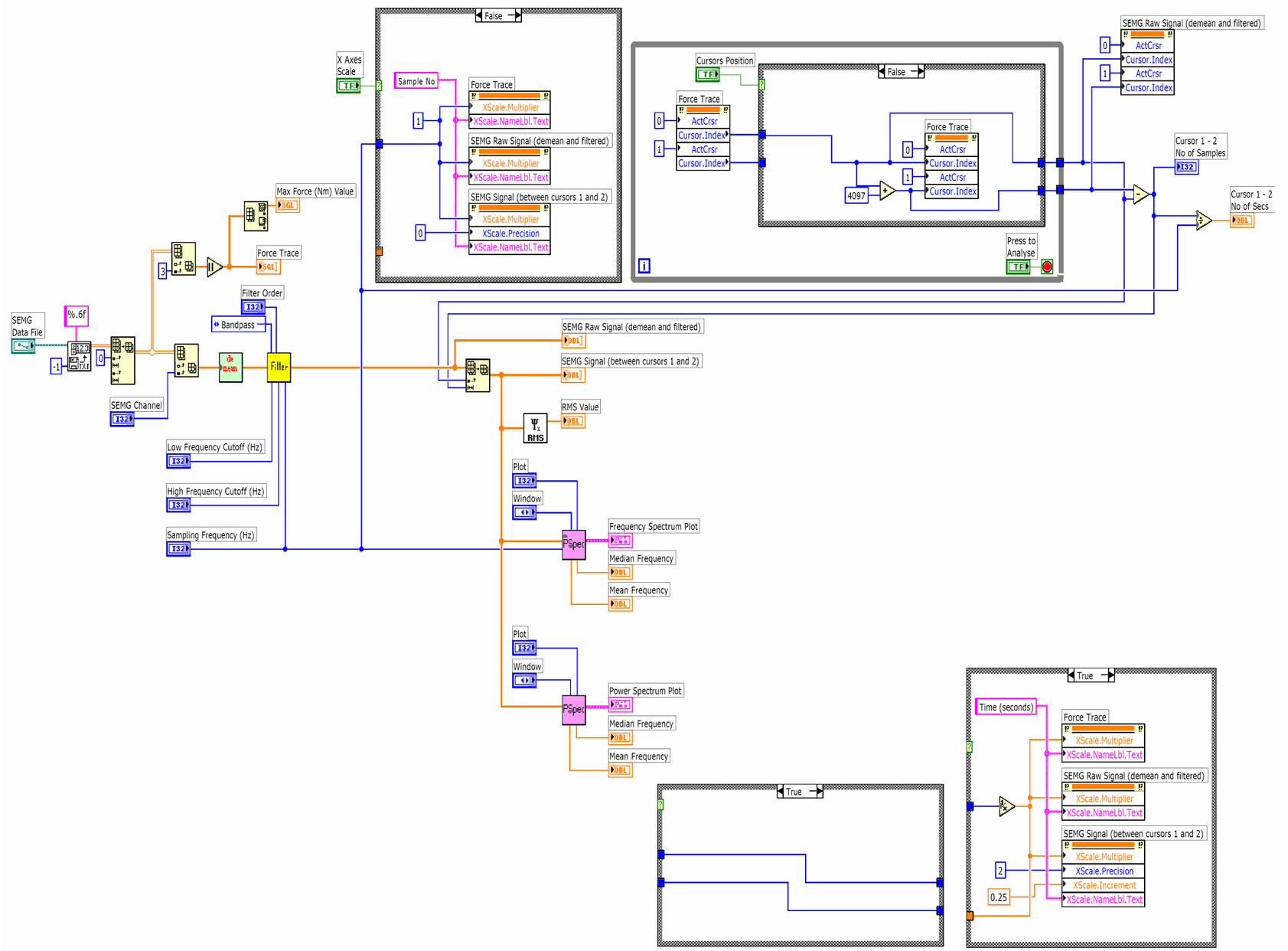

Front Panel

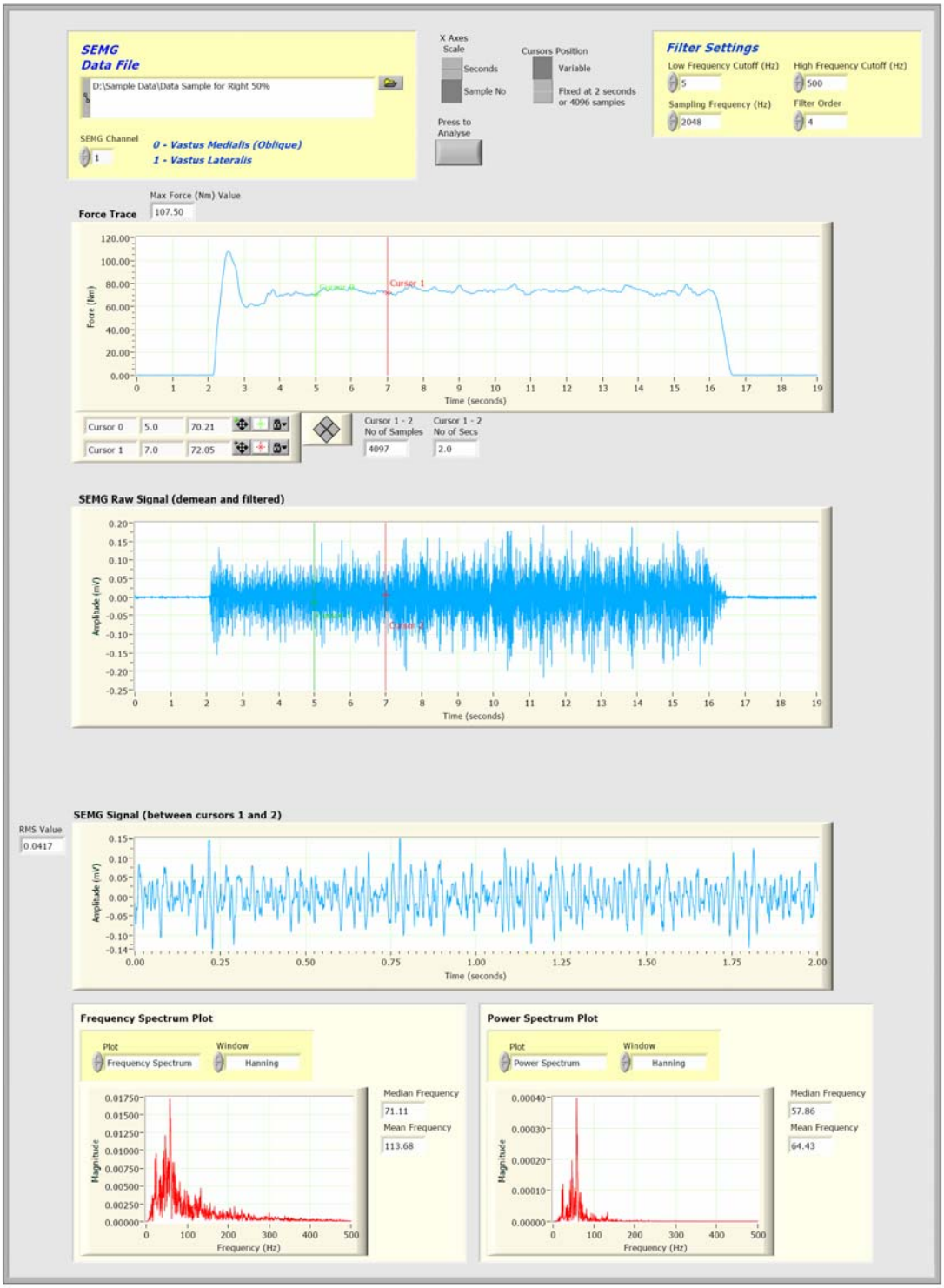
SEMG
Data File
D:\Sample Data\Data Sample for Right 50%
SEMG Channel
1
0 - Vastus Medialis (Oblique)
1 - Vastus Lateralis
X Axes Scale
Seconds
Sample No
Press to Analyse
Cursors Position
Variable
Fixed at 2 seconds or 4096 samples
Filter Settings
Low Frequency Cutoff (Hz)
5
High Frequency Cutoff (Hz)
500
Sampling Frequency (Hz)
2048
Filter Order
4
Max Force (Nm) Value
107.50
Force Trace
Force (Nm)
Time (seconds)
Cursor 1
Cursor 0 5.0 70.21
Cursor 1 7.0 72.05
Cursor 1 - 2 No of Samples
4097
Cursor 1 - 2 No of Secs
2.0
SEMG Raw Signal (demean and filtered)
Amplitude (mV)
Time (seconds)
RMS Value
0.0417
SEMG Signal (between cursors 1 and 2)
Amplitude (mV)
Time (seconds)
Frequency Spectrum Plot
Plot
Frequency Spectrum
Window
Hanning
Magnitude
Frequency (Hz)
Median Frequency
71.11
Mean Frequency
113.68
Power Spectrum Plot
Plot
Power Spectrum
Window
Hanning
Magnitude
Frequency (Hz)
Median Frequency
57.86
Mean Frequency
64.43

Appendix B2

Signal Processing Program Using Fast Fourier Transform (FFT) Analysis by MATLAB

```
1 % This program produces the FFT (Frequency and Power Spectrum) of a 2 second period of an SEMG Signal
2 %(Written by Jeff Kilby)
3
4 % Data File (Raw Data)
5 load data50r;
6
7 % Force Trace
8 force=data50r(:,1);
9
10 %SEMG Signal
11 emg=data50r(:,2);
12
13 % SEMG Signal (demean and filtered using a Butterworth Filter Order=4, LF=5Hz and HF=500Hz)
14 mn=mean(emg);
15 emgmn=emg-mn;
16 n=4;
17 Wn=[5 500]/1024;
18 [b,a]=butter(n, Wn);
19 emgmnfl=filtfilt(b,a,emgmn);
20
21 % Plot of
22 % Force
23 % SEMG Signal
24 % 2 seconds of data
25 %FFT Spectrum Plots
26
```

```
27 subplot(4,1,1);
28 plot(force)
29 ylabel('Force (Nm)')
30 xlabel('Sample No')
31 title('Force Trace')
32
33 subplot(4,1,2);
34 plot(emgmnfl)
35 ylabel('Amplitude (mV)')
36 xlabel('Sample No')
37 title('SEMG Signal (demeaned and filtered)')
38
39 subplot(4,1,3);
40 plot(emgmnfl(10223:14319))
41 ylabel('Amplitude (mV)')
42 xlabel('Sample No')
43 title('2 sec SEMG Signal (Sample No 10223 to 14319)')
44
45 % FFT Frequency and Power Spectum Plots
46 Y=fft(emgmnfl(10223:14319),2048);
47 Pyy=Y.*conj(Y)/2048;
48 f=2048*(0:1024)/2048;
49
50 subplot(4,2,7);
51 plot(f,abs(Y(1:1025)))
52 ylabel('Magnitude')
53 xlabel('Frequency')
54 title('Frequency Spectrum Plot of 2 sec SEMG Signal')
55
56 subplot(4,2,8);
57 plot(f,Pyy(1:1025))
58 ylabel('Magnitude')
59 xlabel('Frequency')
60 title('Power Spectrum Plot of 2 sec SEMG Signal')
```

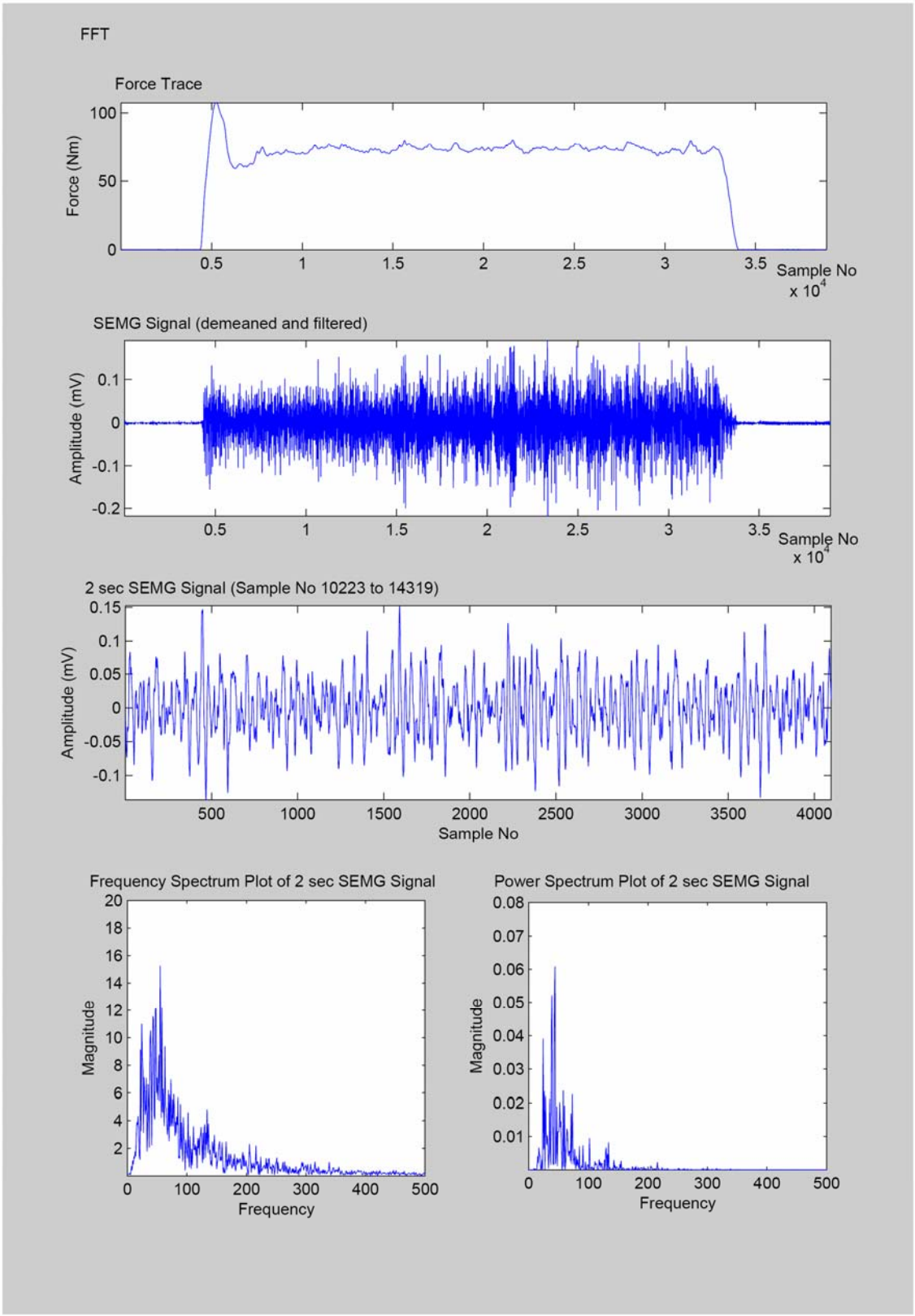
FFT
Force Trace
Force (Nm)
100
50
0
0.5
1
1.5
2
2.5
3
3.5
Sample No
x 10^4
SEMG Signal (demeaned and filtered)
Amplitude (mV)
0.1
0
-0.1
-0.2
0.5
1
1.5
2
2.5
3
3.5
Sample No
x 10^4
2 sec SEMG Signal (Sample No 10223 to 14319)
Amplitude (mV)
0.15
0.1
0.05
0
-0.05
-0.1
500
1000
1500
2000
2500
3000
3500
4000
Sample No
Frequency Spectrum Plot of 2 sec SEMG Signal
Magnitude
20
18
16
14
12
10
8
6
4
2
0
100
200
300
400
500
Frequency
Power Spectrum Plot of 2 sec SEMG Signal
Magnitude
0.08
0.07
0.06
0.05
0.04
0.03
0.02
0.01
0
100
200
300
400
500
Frequency

Appendix B3

Signal Processing Program using Short Time Fourier Transform (STFT) Analysis by LabVIEW

Block Diagram

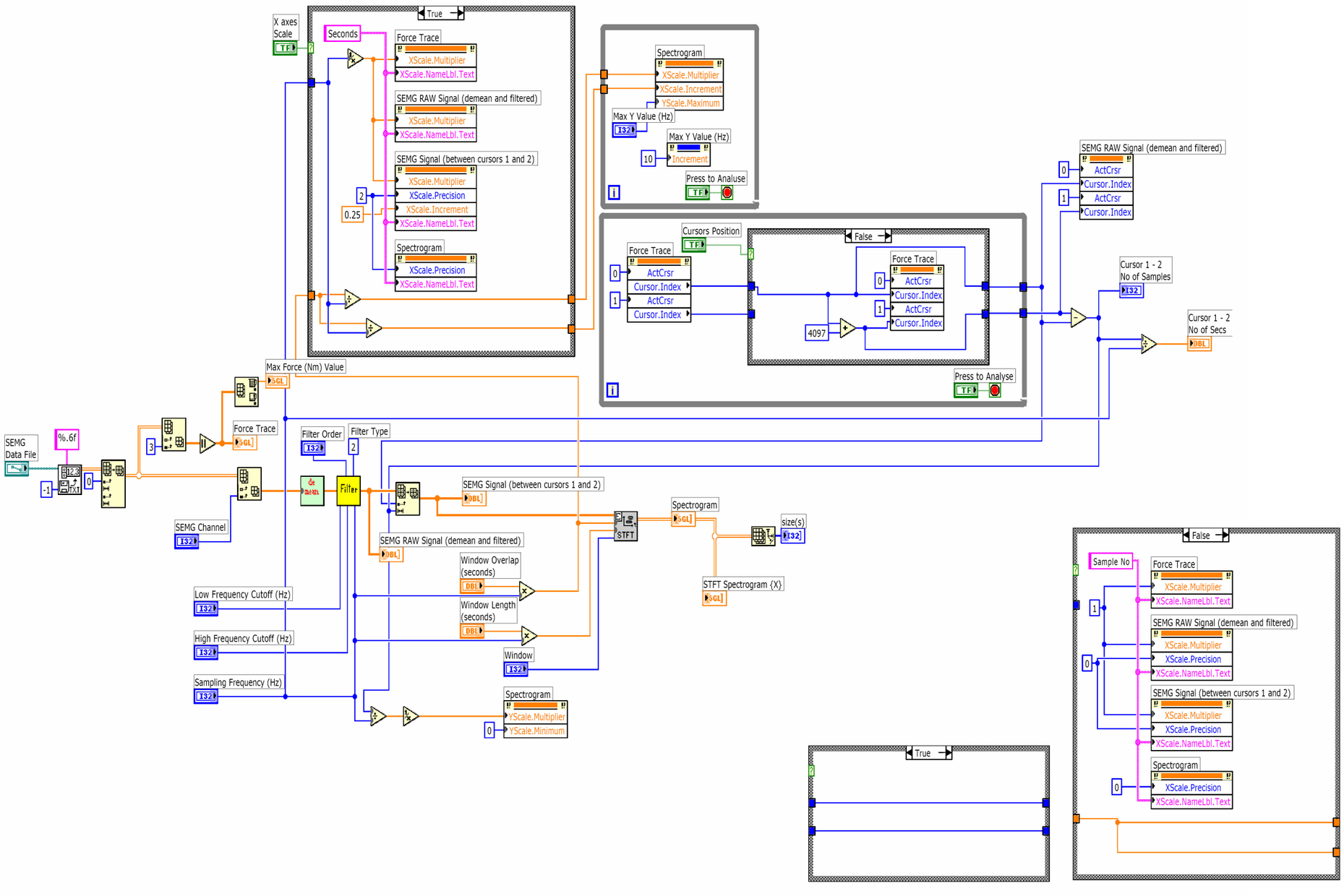

Front Panel

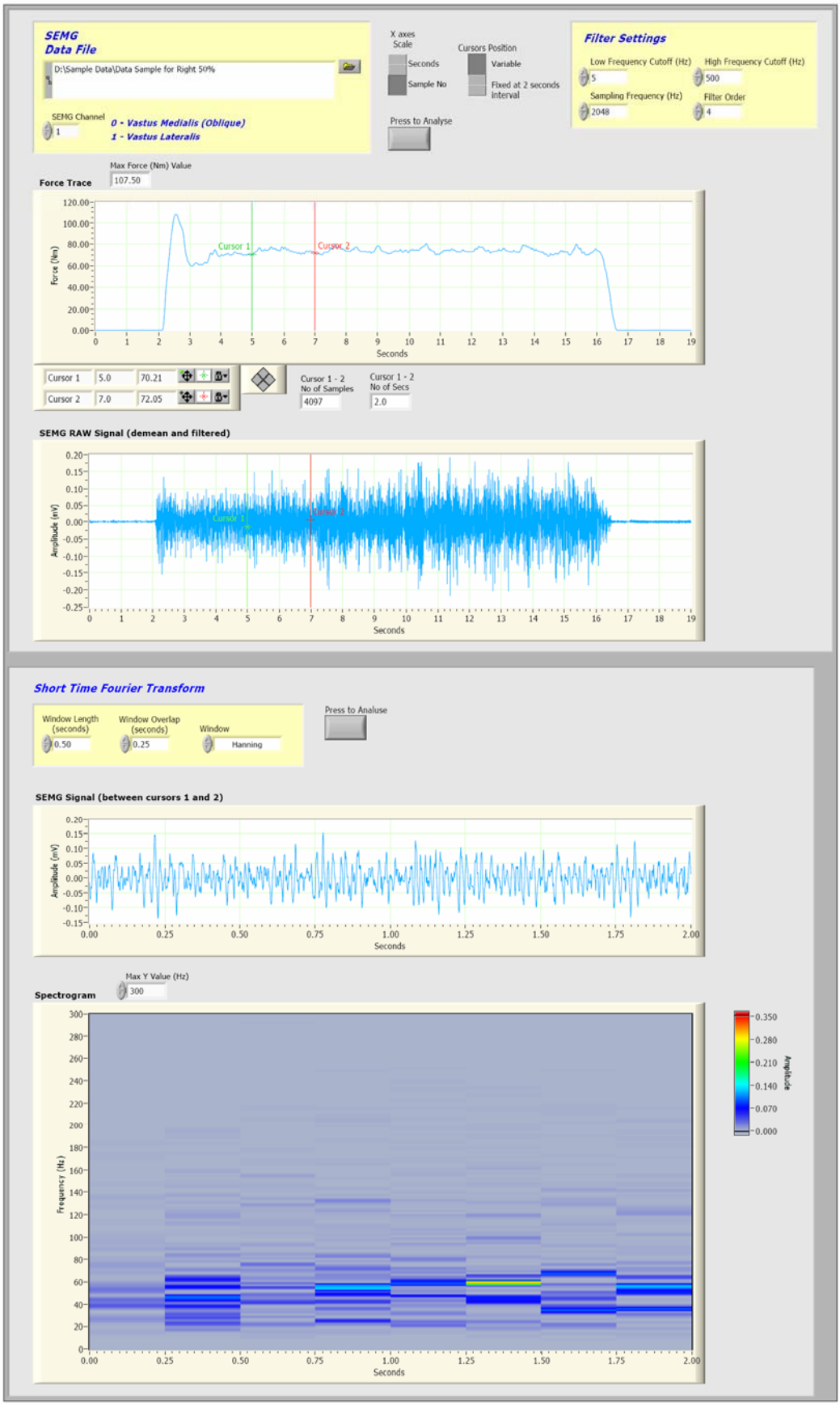
SEMG
Data File
D:\Sample Data\Data Sample for Right 50%
SEMG Channel
1
0 - Vastus Medialis (Oblique)
1 - Vastus Lateralis
X axes Scale
Seconds
Sample No
Cursors Position
Variable
Fixed at 2 seconds Interval
Press to Analyse
Filter Settings
Low Frequency Cutoff (Hz)
5
High Frequency Cutoff (Hz)
500
Sampling Frequency (Hz)
2048
Filter Order
4
Max Force (Nm) Value
107.50
Force Trace
Force (Nm)
Seconds
Cursor 1
Cursor 2
Cursor 1 5.0 70.21
Cursor 2 7.0 72.05
Cursor 1 - 2 No of Samples
4097
Cursor 1 - 2 No of Secs
2.0
SEMG RAW Signal (demean and filtered)
Amplitude (mV)
Seconds
Short Time Fourier Transform
Window Length (seconds)
0.50
Window Overlap (seconds)
0.25
Window
Hanning
Press to Analuse
SEMG Signal (between cursors 1 and 2)
Amplitude (mV)
Seconds
Max Y Value (Hz)
300
Spectrogram
Frequency (Hz)
Seconds
Amplitude
0.350
0.280
0.210
0.140
0.070
0.000

Appendix B4

Signal Processing Program Using Short Time Fourier Transform (STFT) Analysis by MATLAB

```
% This program produces a Spectrogram of a 2 second period of an SEMG Signal
% (Written by Jeff Kilby)

% Data File (Raw Data)
load data50r;

% Force Trace
force=data50r(:,1);

% SEMG Signal
emg=data50r(:,2);

% SEMG Signal (demean and filtered using a Butterworth Filter Order=4, LF=5Hz and HF=500Hz)
mn=mean(emg);
emgmn=emg-mn;
n=4;
Wn=[5 500]/1024;
[b,a]=butter(n, Wn);
emgmnfl=filtfilt(b,a,emgmn);

% Plot of
% Force
% SEMG Signal
% 2 seconds of data
% STFT Spectogram

subplot(4,1,1);
```

```
28 plot(force)
29 ylabel('Force (Nm)')
30 xlabel('Sample No')
31 title('Force Trace')
32
33 subplot(4,1,2);
34 plot(emgmnfl)
35 ylabel('Amplitude (mV)')
36 xlabel('Sample No')
37 title('SEMG Signal (demeaned and filtered)')
38
39 subplot(4,1,3);
40 plot(emgmnfl(10223:14319))
41 ylabel('Amplitude (mV)')
42 xlabel('Sample No')
43 title('2 sec SEMG Signal (Sample No 10223 to 14319)')
44
45 % STFT Analysis (Window 0.5sec with 0.25sec overlap)
46
47 subplot(4,1,4);
48 specgram(emgmnfl(10223:14319),1024,2048,HANN(1024),512)
49 title('Spectogram');colorbar
```

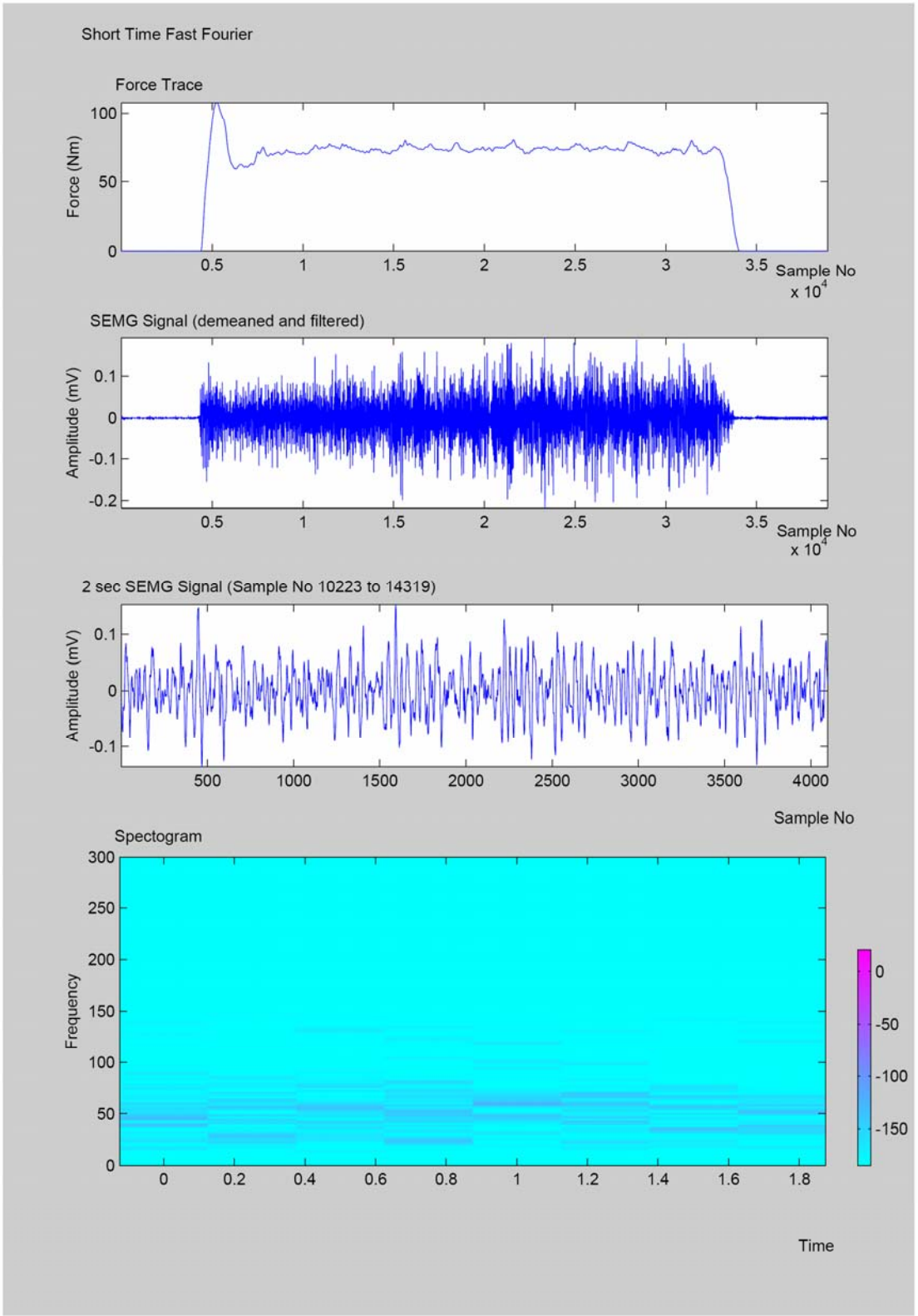
Short Time Fast Fourier
Force Trace
Force (Nm)
100
50
0
0.5
1
1.5
2
2.5
3
3.5
Sample No
x 10^4
SEMG Signal (demeaned and filtered)
Amplitude (mV)
0.1
0
-0.1
-0.2
0.5
1
1.5
2
2.5
3
3.5
Sample No
x 10^4
2 sec SEMG Signal (Sample No 10223 to 14319)
Amplitude (mV)
0.1
0
-0.1
500
1000
1500
2000
2500
3000
3500
4000
Sample No
Spectogram
Frequency
300
250
200
150
100
50
0
0
0.2
0.4
0.6
0.8
1
1.2
1.4
1.6
1.8
Time
0
-50
-100
-150

Appendix B5

Signal Processing Program using Continuous Wavelet Transform (CWT) Analysis by LabVIEW

Block Diagram

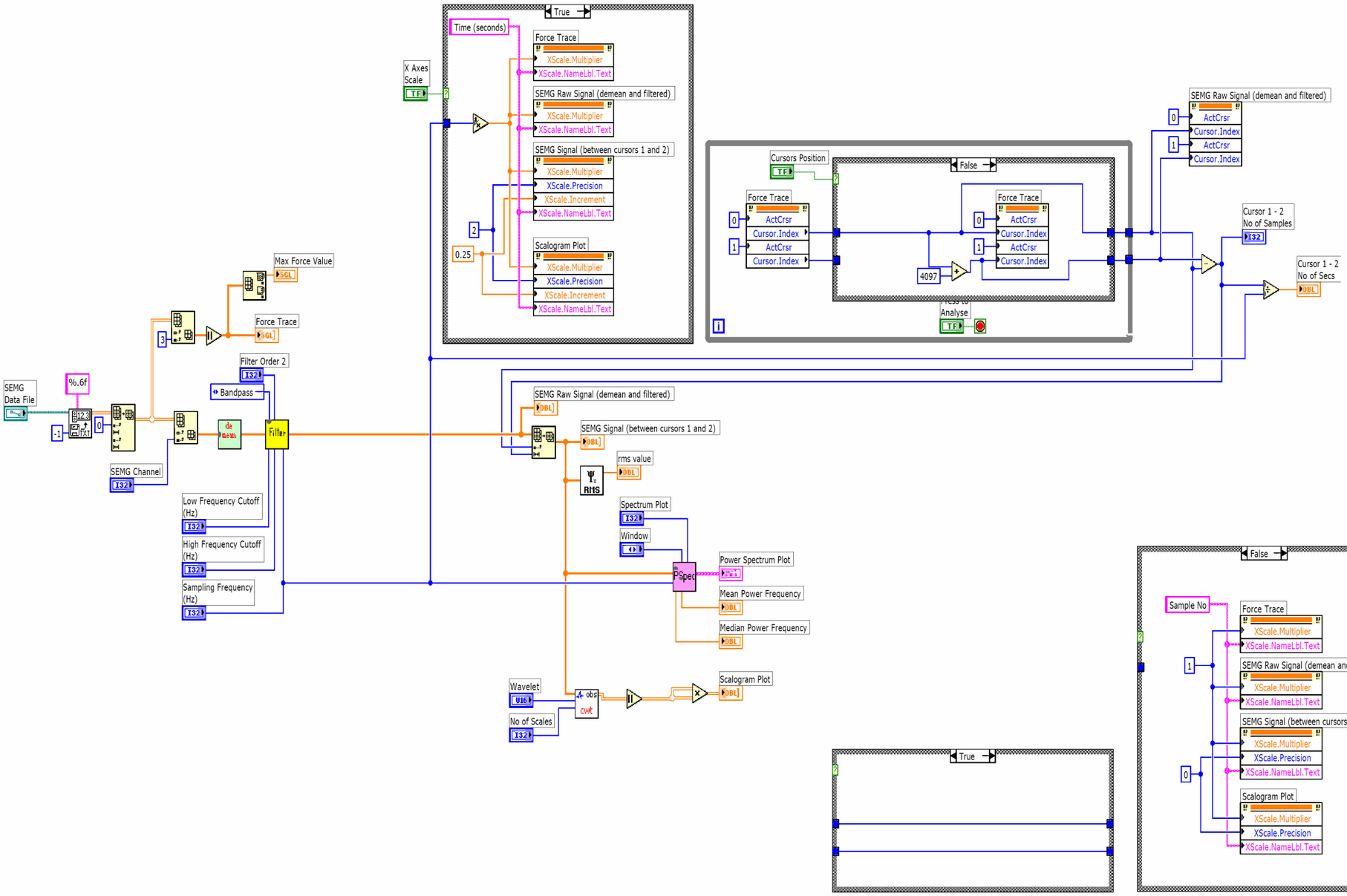

Front Panel

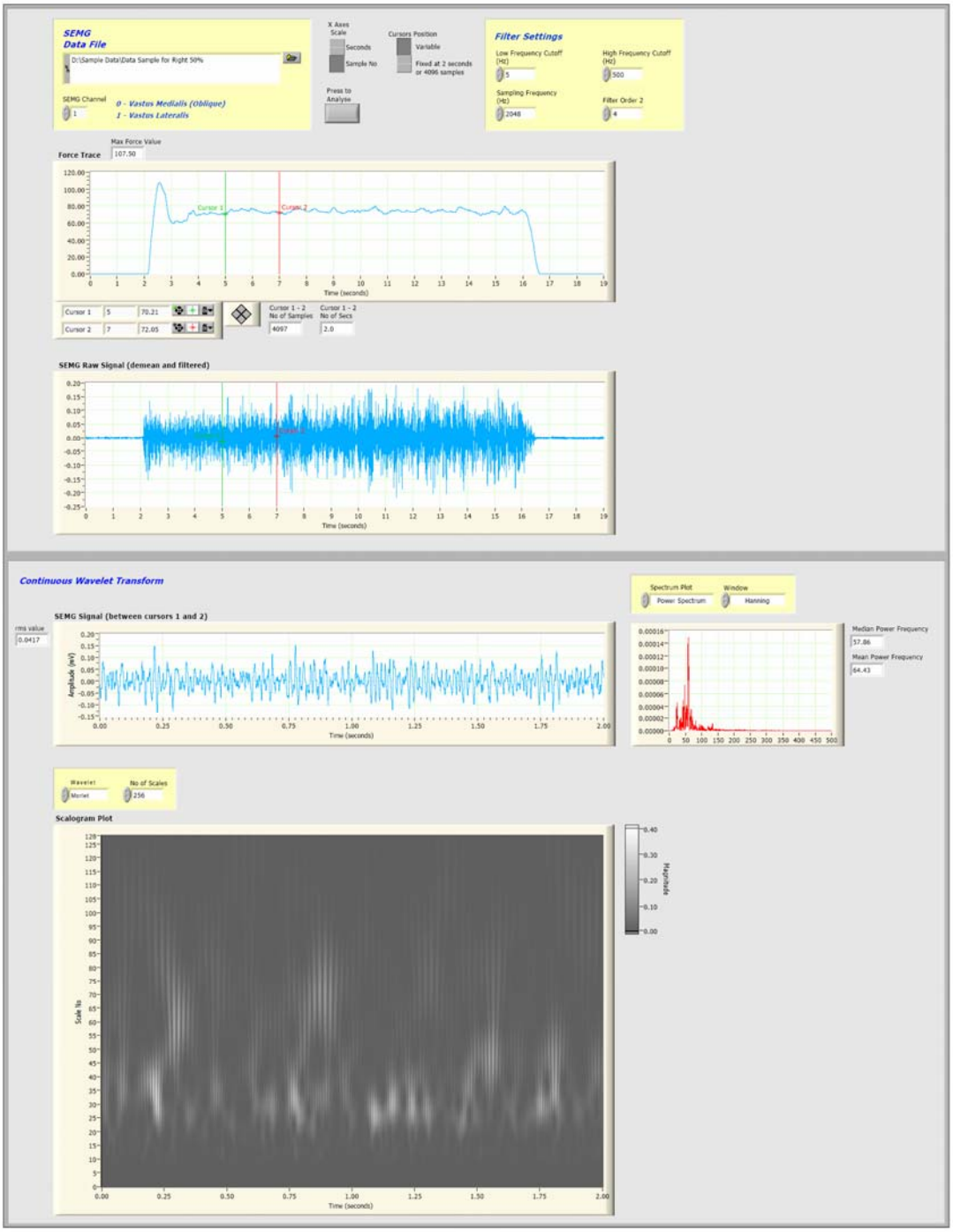
SEMG
Data File
D:\Sample Data\Data Sample for Right 50%
SEMG Channel
0 - Vastus Medialis (Oblique)
1 - Vastus Lateralis
X Axes Scale
Seconds
Sample No
Cursors Position
Variable
Fixed at 2 seconds or 4096 samples
Press to Analyse
Filter Settings
Low Frequency Cutoff (Hz)
High Frequency Cutoff (Hz)
Sampling Frequency (Hz)
Filter Order 2
Force Trace
Max Force Value
107.50
Time (seconds)
SEMG Raw Signal (demean and filtered)
Continuous Wavelet Transform
Spectrum Plot
Power Spectrum
Window
Hanning
SEMG Signal (between cursors 1 and 2)
rms value
0.0417
Amplitude (mV)
Median Power Frequency
57.86
Mean Power Frequency
64.43
Wavelet
Morlet
No of Scales
256
Scalogram Plot
Scale No
Magnitude

Appendix B6

Signal Processing Program Using Continuous Wavelet Transform (CWT) Analysis by MATLAB

```
%This program produces a Continuous Wavelet Transform (CWT) Scalogram of a 2 second
period of an SEMG Signal
%(Written by Jeff Kilby)

%Data File (Raw Data)
load data50r;

%Force Trace
force=data50r(:,1);

%SEMG Signal
emg=data50r(:,2);

%SEMG Signal (demean and filtered using a Butterworth Filter Order=4, LF=5Hz and HF=500Hz)
mn=mean(emg);
emgmn=emg-mn;
n=4;
Wn=[5 500]/1024;
[b,a]=butter(n, Wn);
emgmnfl=filtfilt(b,a,emgmn);

%Plot of
%Force
%SEMG Signal
%2 seconds of data
%CWT Spectogram
```

```
26
27 subplot(4,1,1);
28 plot(force)
29 ylabel('Force (Nm)')
30 xlabel('Sample No')
31 title('Force Trace')
32
33 subplot(4,1,2);
34 plot(emgmnfl)
35 ylabel('Amplitude (mV)')
36 xlabel('Sample No')
37 title('SEMG Signal (demeaned and filtered)')
38
39 subplot(4,1,3);
40 plot(emgmnfl(10223:14319))
41 ylabel('Amplitude (mV)')
42 xlabel('Sample No')
43 title('2 sec SEMG Signal (Sample No 10223 to 14319)')
44
45 %CWT Scalogram (Mother Wavelet - Morlet, No of Scales - 256)
46
47 subplot(4,1,4);
48 cwt(emgmnfl(10223:14319),1:257,'morl' ,'plot');colorbar
49 ylabel('Scale No')
50 xlabel('Sample No')
51 title('Scalogram')
```

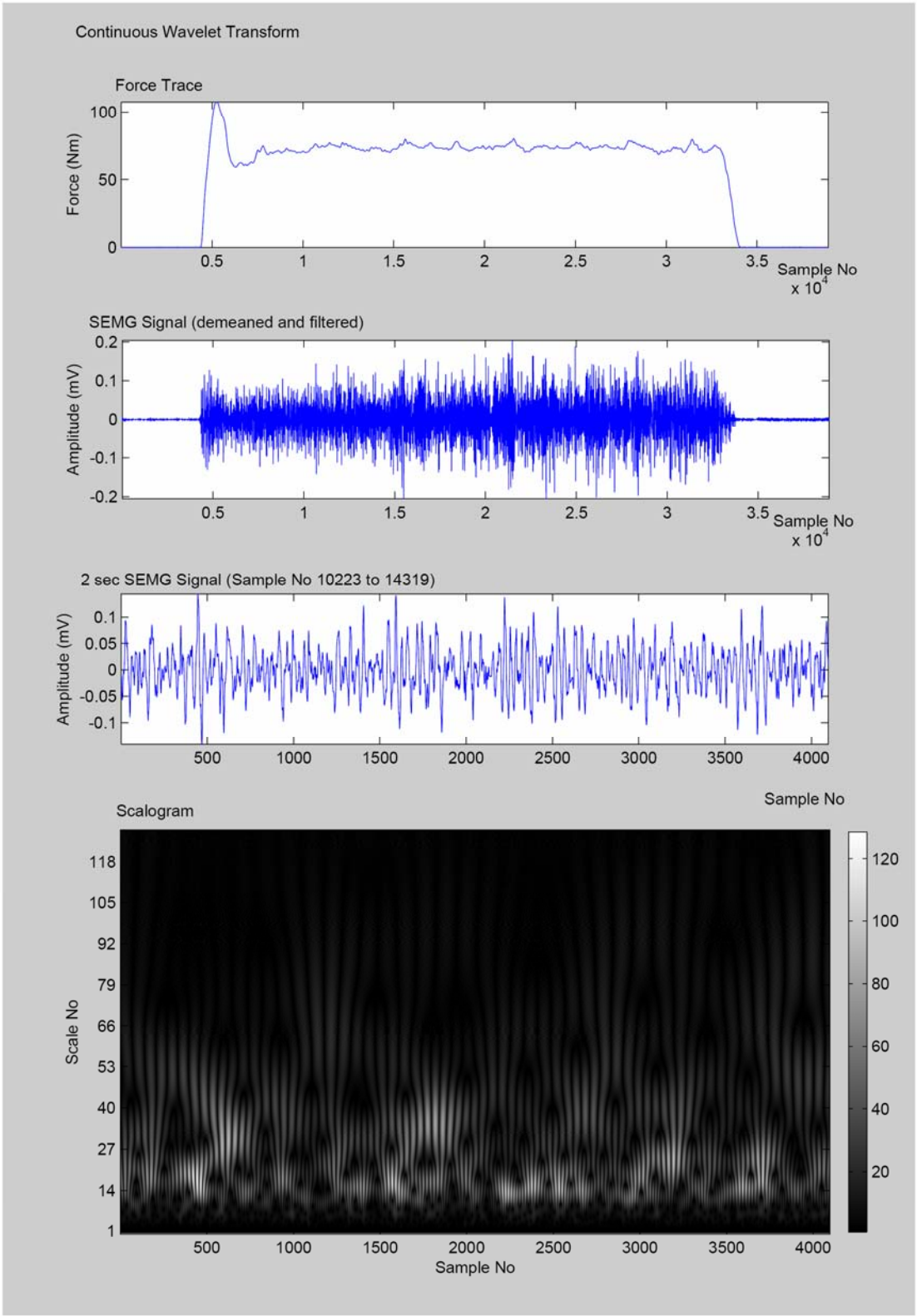
Continuous Wavelet Transform
Force Trace
Force (Nm)
100
50
0
0.5
1
1.5
2
2.5
3
3.5
Sample No
x 10^4
SEMG Signal (demeaned and filtered)
Amplitude (mV)
0.2
0.1
0
-0.1
-0.2
0.5
1
1.5
2
2.5
3
3.5
Sample No
x 10^4
2 sec SEMG Signal (Sample No 10223 to 14319)
Amplitude (mV)
0.1
0.05
0
-0.05
-0.1
500
1000
1500
2000
2500
3000
3500
4000
Scalogram
Sample No
Scale No
118
105
92
79
66
53
40
27
14
1
500
1000
1500
2000
2500
3000
3500
4000
Sample No
120
100
80
60
40
20

Appendix B7

Signal Processing Program using Discrete Wavelet Transform (DWT) Analysis by LabVIEW

Block Diagram

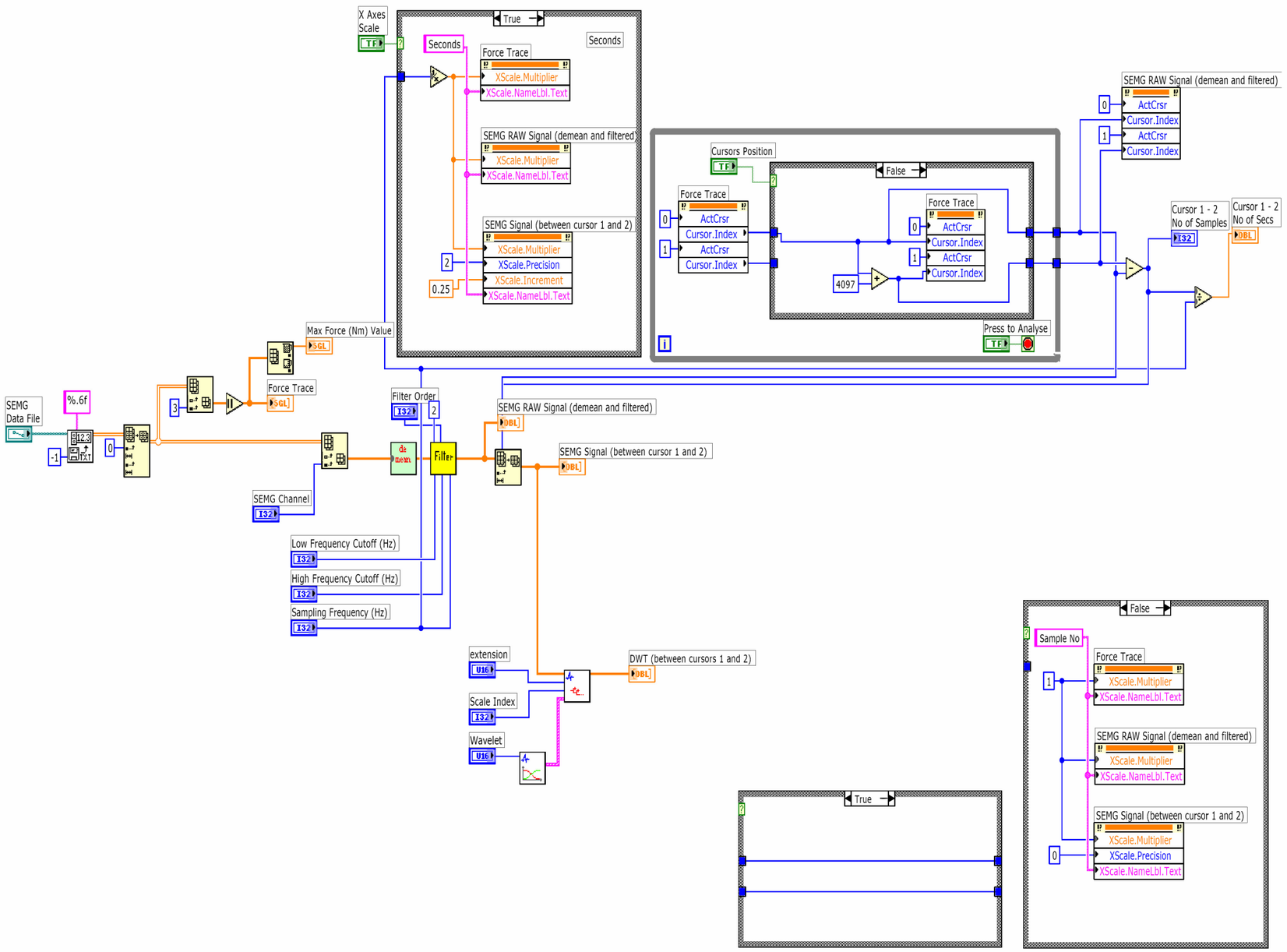

Front Panel

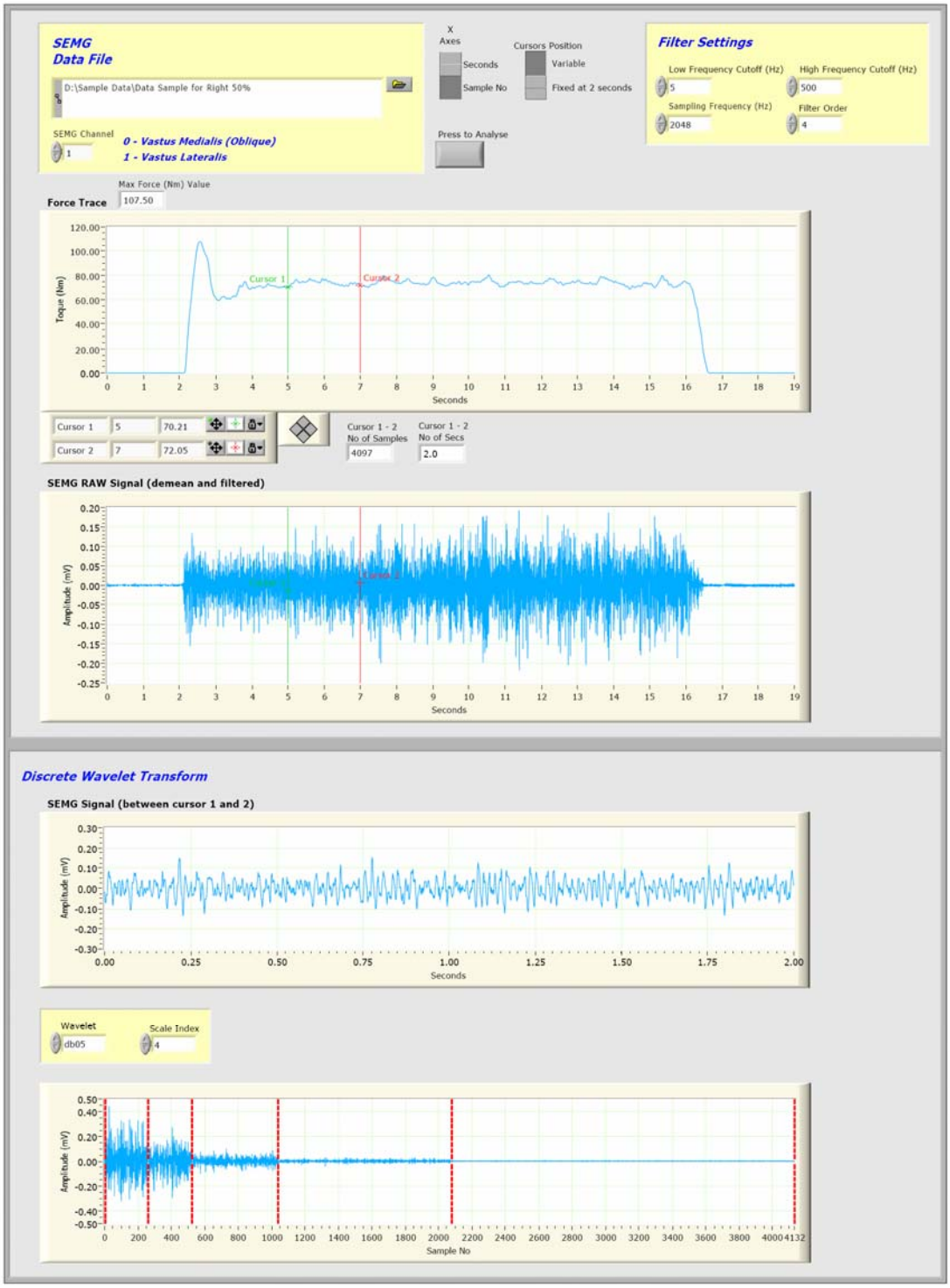
SEMG
Data File
D:\Sample Data\Data Sample for Right 50%
SEMG Channel
1
0 - Vastus Medialis (Oblique)
1 - Vastus Lateralis
X Axes
Seconds
Sample No
Cursors Position
Variable
Fixed at 2 seconds
Press to Analyse
Filter Settings
Low Frequency Cutoff (Hz)
5
High Frequency Cutoff (Hz)
500
Sampling Frequency (Hz)
2048
Filter Order
4
Max Force (Nm) Value
107.50
Force Trace
Torque (Nm)
Seconds
Cursor 1
Cursor 2
Cursor 1 5 70.21
Cursor 2 7 72.05
Cursor 1 - 2 No of Samples
4097
Cursor 1 - 2 No of Secs
2.0
SEMG RAW Signal (demean and filtered)
Amplitude (mV)
Seconds
Discrete Wavelet Transform
SEMG Signal (between cursor 1 and 2)
Amplitude (mV)
Seconds
Wavelet
db05
Scale Index
4
Amplitude (mV)
Sample No

Appendix B8

Signal Processing Program Using Discrete Wavelet Transform (DWT) Analysis by MATLAB

```
1 % This program produces the Discrete Wavelet Transform (DWT) of a 2 second period of and SEMG Signal
2 % (Written by Jeff Kilby)
3
4 % Data File (Raw Data)
5 load data50r;
6
7 % Force Trace
8 force=data50r(:,1);
9
10 % SEMG Signal
11 emg=data50r(:,2);
12
13 % SEMG Signal (demean and filtered using a Butterworth Filter Order=4, LF=5Hz and HF=500Hz)
14 mn=mean(emg);
15 emgmn=emg-mn;
16 n=4;
17 Wn=[5 500]/1024;
18 [b,a]=butter(n, Wn);
19 emgmnfl=filtfilt(b,a,emgmn);
20
21 %Plot of
22 % Force
23 % SEMG Signal
24 % 2 seconds of data
25 % DWT
26
```

```
27 subplot(4,1,1);
28 plot(force)
29 ylabel('Force (Nm)')
30 xlabel('Sample No')
31 title('Force Trace')
32
33 subplot(4,1,2);
34 plot(emgmnfl)
35 ylabel('Amplitude (mV)')
36 xlabel('Sample No')
37 title('SEMG Signal (demeaned and filtered')
38
39 subplot(4,1,3);
40 plot(emgmnfl(10223:14319))
41 ylabel('Amplitude (mV)')
42 xlabel('Sample No')
43 title('2 sec SEMG Signal (Sample No 10223 to 14319)')
44
45 % DWT Analysis (Mother Wavelet - db05, Scale Index - 256)
46
47 dwt=emgmnfl(10223:14319);
48 subplot(4,1,4);
49 plot(wavedec(dwt,4,'db05'));
50 ylabel('Amplitude (mV)')
51 xlabel('Sample No')
52 title('DWT')
```

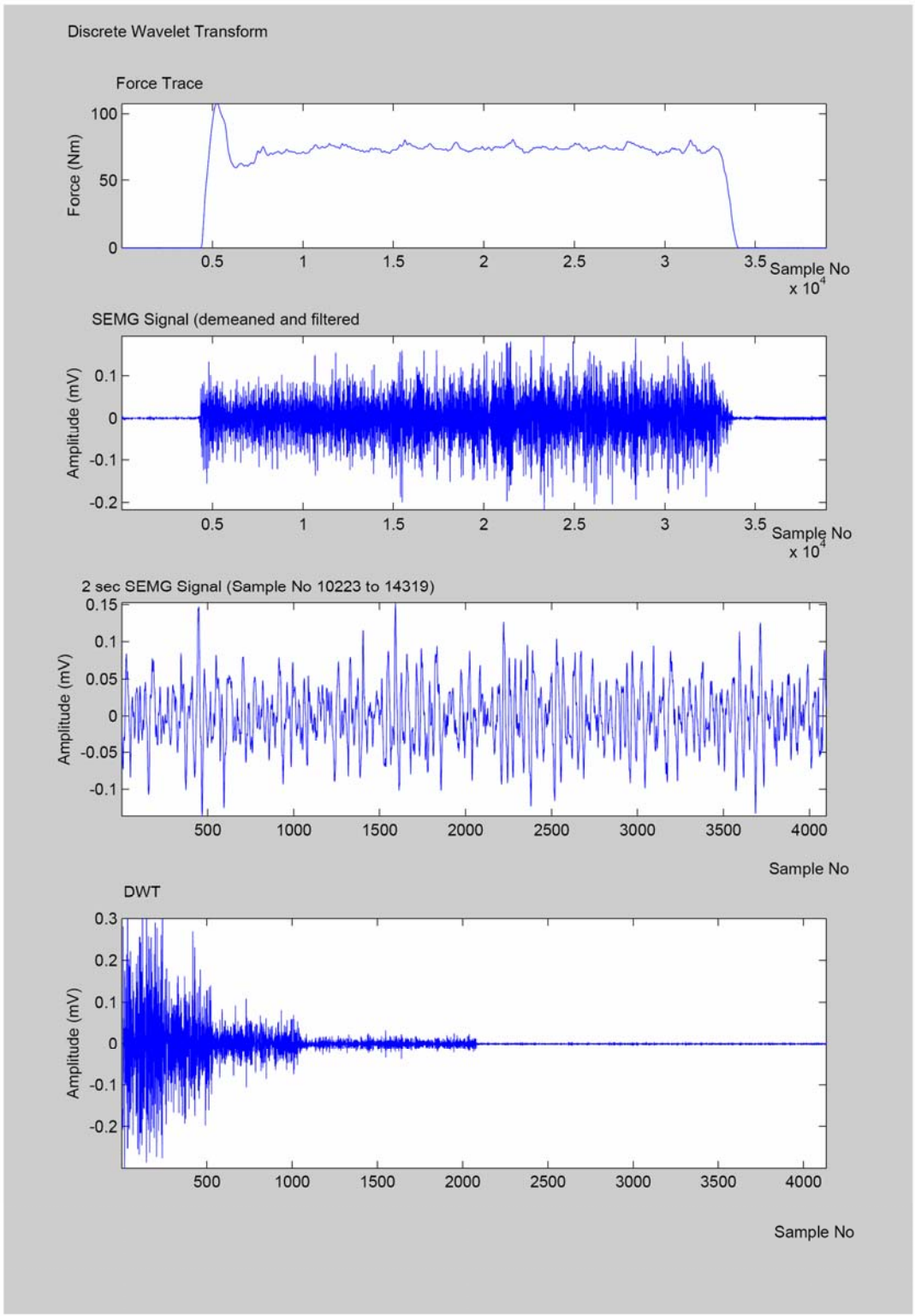
Discrete Wavelet Transform
Force Trace
Force (Nm)
100
50
0
0.5
1
1.5
2
2.5
3
3.5
Sample No
x 10^4
SEMG Signal (demeaned and filtered
Amplitude (mV)
0.1
0
-0.1
-0.2
0.5
1
1.5
2
2.5
3
3.5
Sample No
x 10^4
2 sec SEMG Signal (Sample No 10223 to 14319)
Amplitude (mV)
0.15
0.1
0.05
0
-0.05
-0.1
500
1000
1500
2000
2500
3000
3500
4000
Sample No
DWT
Amplitude (mV)
0.3
0.2
0.1
0
-0.1
-0.2
500
1000
1500
2000
2500
3000
3500
4000
Sample No

Appendix B9

Signal Processing Program using Discrete Wavelet Packet Transform (DWPT) Analysis by LabVIEW

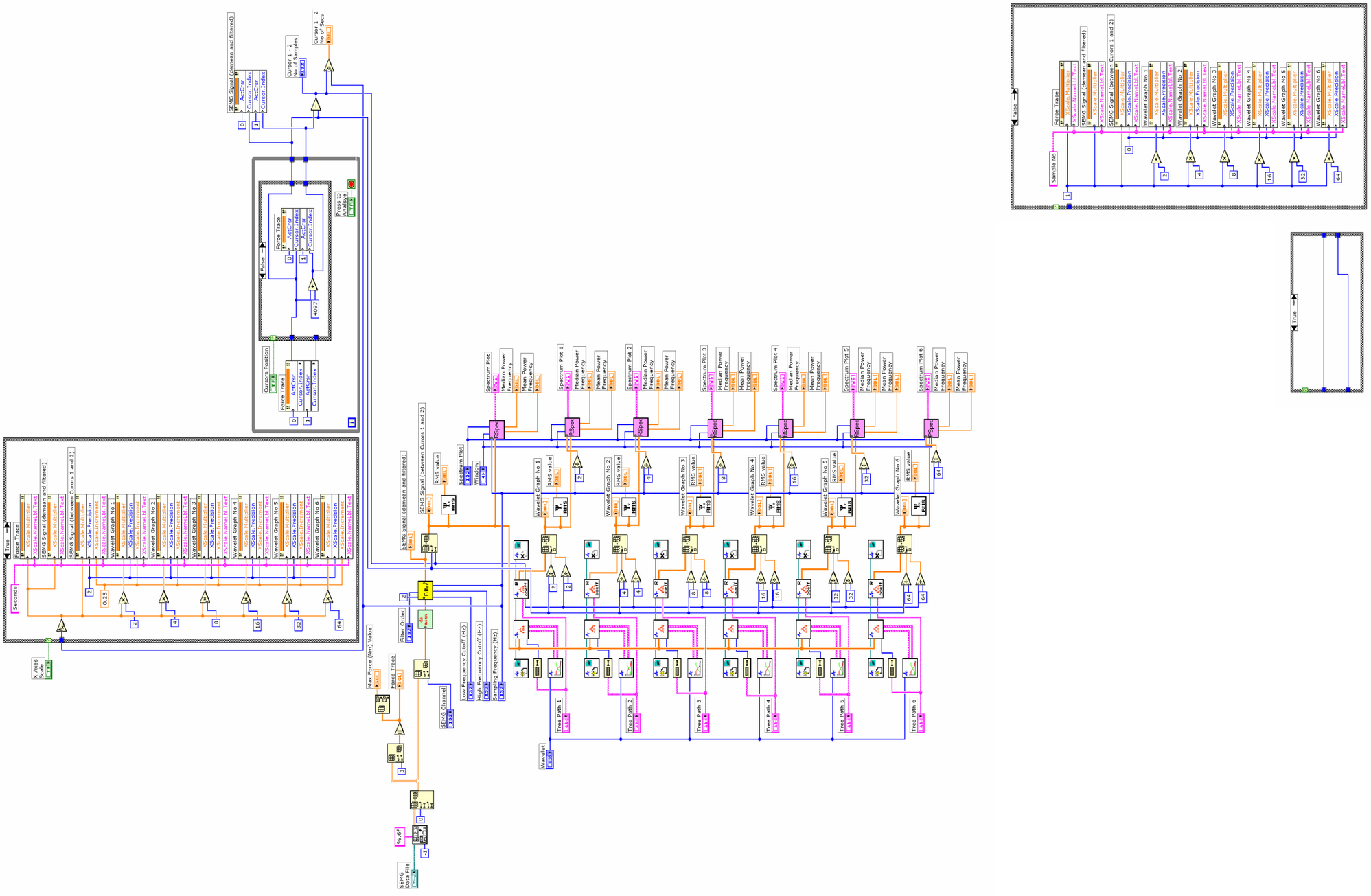

Front Panel

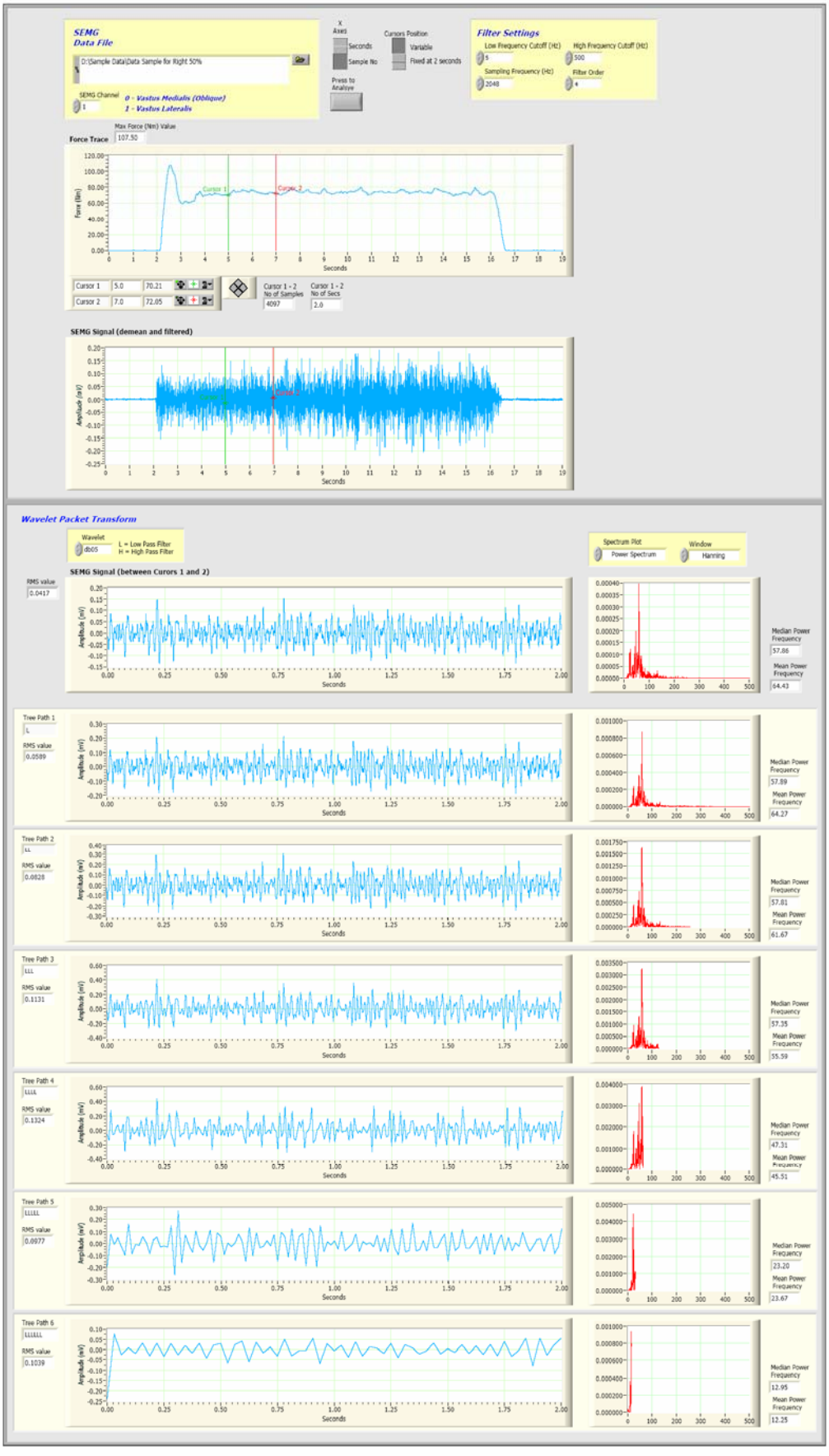
SEMG
Data File
D:\Sample Data\Data Sample for Right 50%
SEMG Channel
0 - Vastus Medialis (Oblique)
1 - Vastus Lateralis
Filter Settings
Low Frequency Cutoff (Hz)
High Frequency Cutoff (Hz)
Sampling Frequency (Hz)
Filter Order
Force Trace
Max Force (Nm) Value
107.50
Force (Nm)
Seconds
Cursor 1
Cursor 2
SEMG Signal (demean and filtered)
Amplitude (mV)
Wavelet Packet Transform
Wavelet
db05
L = Low Pass Filter
H = High Pass Filter
Spectrum Plot
Power Spectrum
Window
Hanning
SEMG Signal (between Curors 1 and 2)
RMS value
Tree Path 1
Tree Path 2
Tree Path 3
Tree Path 4
Tree Path 5
Tree Path 6
Median Power Frequency
Mean Power Frequency

Appendix B10

Signal Processing Program Using Discrete Wavelet Packet Transform (DWPT) Analysis by MATLAB

```
1 %This program produces the Discrete Wavelet Packet Transform to Level 6 (Low Filter Path) of a 2 second period of an SEMG Signal
2 %(Written by Jeff Kilby)
3
4 %Data File (Raw Data)
5 load data50r;
6
7 %Force Trace
8 force=data50r(:,1);
9
10 %SEMG Signal
11 emg=data50r(:,2);
12
13 %SEMG Signal (demean and filtered using a Butterworth Filter Order=4, LF=5Hz and HF=500Hz)
14 mn=mean(emg);
15 emgmn=emg-mn;
16 n=4;
17 Wn=[5 500]/1024;
18 [b,a]=butter(n, Wn);
19 emgmnfl=filtfilt(b,a,emgmn);
20
21 %Plot of
22 %Force
23 %SEMG Signal
24 %2 seconds of data
25 %DWPT Scales 1-6 Low Filter Path
26
```

```
27 subplot(9,1,1);
28 plot(force)
29 ylabel('Force (Nm)')
30 xlabel('Sample No')
31 title('Force Trace')
32
33 subplot(9,1,2);
34 plot(emgmnfl)
35 ylabel('Amplitude (mV)')
36 xlabel('Sample No')
37 title('SEMG Signal (demeaned and filtered)')
38
39 subplot(9,1,3);
40 plot(emgmnfl(10223:14319))
41 ylabel('Amplitude (mV)')
42 xlabel('Sample No')
43 title('2 sec SEMG Signal (Sample No 10223 to 14319)')
44
45 %DWPT Analysis
46 %Mother Wavelet - db05
47
48 dwt=emgmnfl(10223:14319);
49 [C,L]=wavedec(dwt,6, 'db05');
50
51 waveL1=appcoef(C,L, 'db05',1);
52 waveL2=appcoef(C,L, 'db05',2);
53 waveL3=appcoef(C,L, 'db05',3);
54 waveL4=appcoef(C,L, 'db05',4);
55 waveL5=appcoef(C,L, 'db05',5);
56 waveL6=appcoef(C,L, 'db05',6);
57
58 subplot(9,1,4);
59 plot(waveL1)
60 title('Scale 1 (L)')
```

```
61 ylabel('Amplitude (mV)')
62 xlabel('Sample No')
63
64 subplot(9,1,5);
65 plot(waveL2)
66 title('Scale 2 (LL)')
67 ylabel('Amplitude (mV)')
68 xlabel('Sample No')
69
70 subplot(9,1,6);
71 plot(waveL3)
72 title('Scale 3 (LLL)')
73 ylabel('Amplitude (mV)')
74 xlabel('Sample No')
75
76 subplot(9,1,7);
77 plot(waveL4)
78 title('Scale 4 (LLLL)')
79 ylabel('Amplitude (mV)')
80 xlabel('Sample No')
81
82 subplot(9,1,8);
83 plot(waveL5)
84 title('Scale 5 (LLLLL)')
85 ylabel('Amplitude (mV)')
86 xlabel('Sample No')
87
88 subplot(9,1,9);
89 plot(waveL6)
90 title('Scale 1 (LLLLLL)')
91 ylabel('Amplitude (mV)')
92 xlabel('Sample No')
```

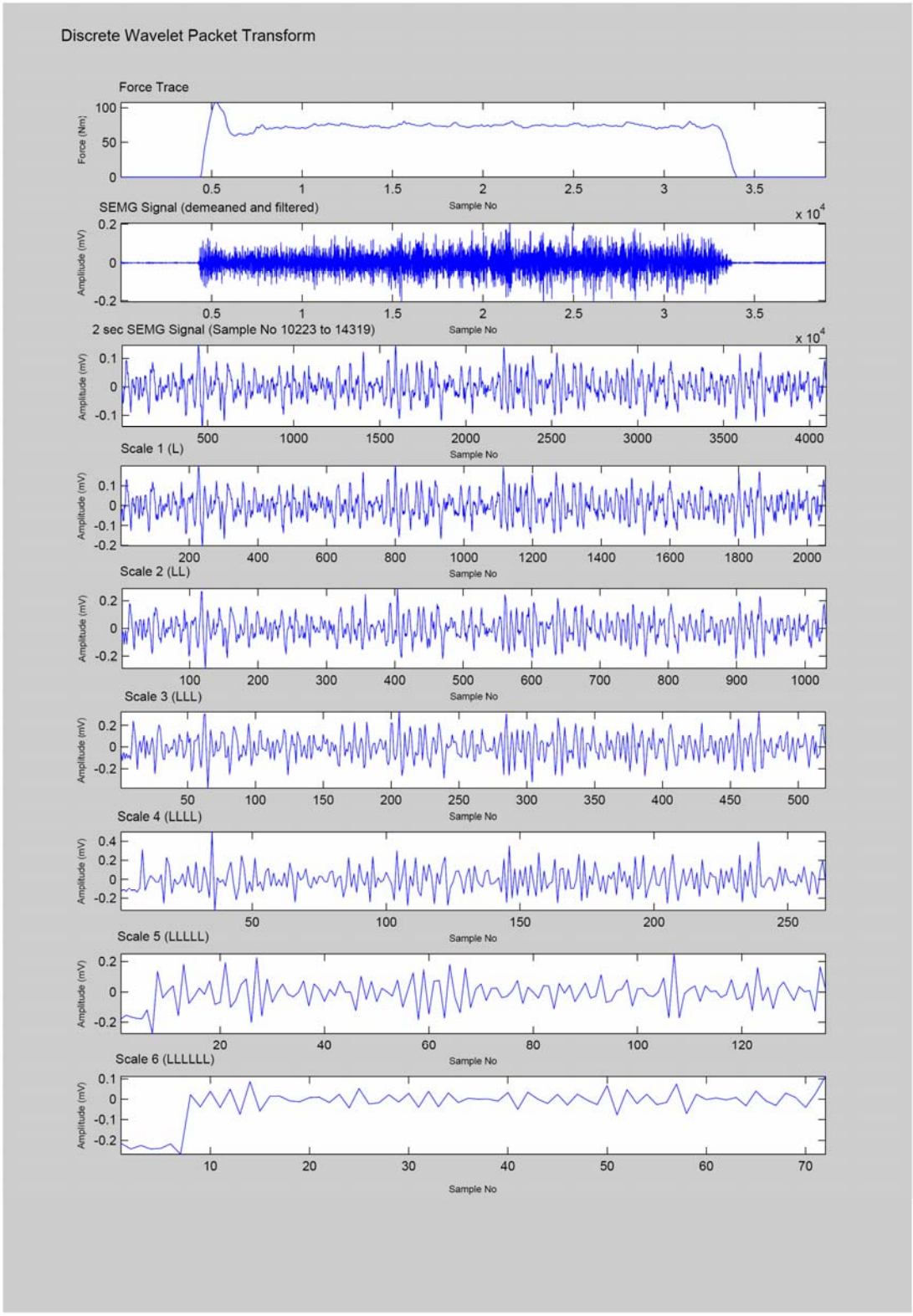
Discrete Wavelet Packet Transform
Force Trace
Force (Nm)
Sample No
SEMG Signal (demeaned and filtered)
Amplitude (mV)
x 10^4
2 sec SEMG Signal (Sample No 10223 to 14319)
Scale 1 (L)
Scale 2 (LL)
Scale 3 (LLL)
Scale 4 (LLLL)
Scale 5 (LLLLL)
Scale 6 (LLLLLL)

Appendix B11

Sub-VIs Designs of *'demean'*, *'Filter, and 'PSpec'* by LabVIEW

subVI – *demean*

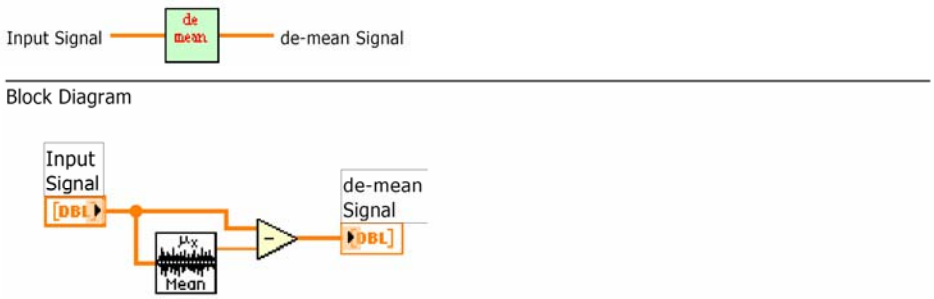

subVI - *Filter*

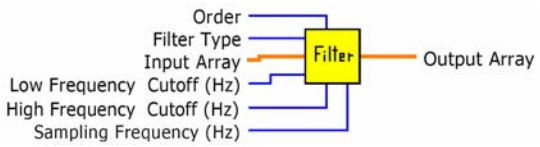

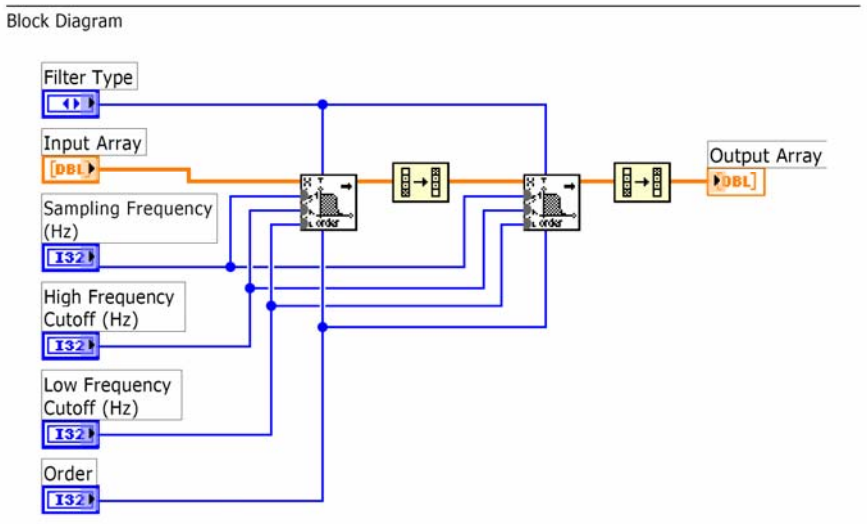

subVI – *PSpec*

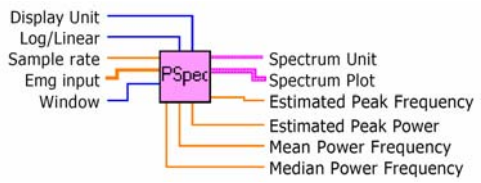

Block Diagram

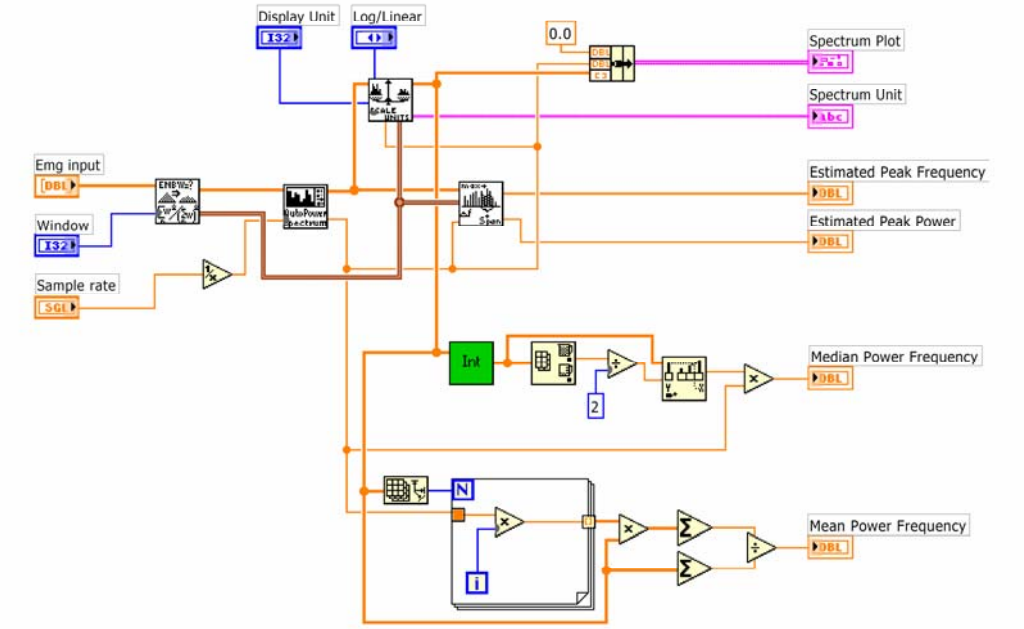

Appendix C1

Recommendation for Sensor Locations in Hip or Upper Leg Muscles – Vastus Lateralis

Muscle

Name	Quadriceps Femoris
Subdivision	vastus lateralis

Muscle Anatomy

Origin	Proximal parts of intertrochanteric line, anterior and inferior orders of greater trochanter, lateral lip of gluteal tuberosity, proximal half of lateral lip of linea aspera, and lateral intermuscular septum
Insertion	Proximal border of the patella and through patellar ligament
Function	Extension of the knee joint

Recommended sensor placement procedure

Starting posture	Sitting on a table with the knees in slight flexion and the upper body slightly bend backward.
Electrode size	Maximum size in the direction of the muscle fibres: 10 mm
Electrode distance	20 mm

<u>Electrode placement</u>

- location	Electrodes need to be placed at 2/3 on the line from the anterior spina iliaca superior to the lateral side of the patella
- orientation	In the direction of the muscle fibres
- fixation on the skin	(Double sided) tape / rings or elastic band
- reference electrode	On / around the ankle or the proc. spin of C7

Clinical test	Extend the knee without rotating the thigh while applying pressure against the leg above the ankle in the direction of flexion.
Remarks	The SENIAM guidelines include also a separate sensor placement procedure for the vastus medialis and the rectus femoris muscle.

Appendix C2

Recommendation for Sensor Locations in Hip or Upper Leg Muscles – Vastus Medialis

Muscle

Name	Quadriceps Femoris
Subdivision	vastus medialis

Muscle Anatomy

Origin	Distal half of the intertrochanteric line, medial lip of line aspera, proximal part of medial supracondylar line, tendons of adductor longus and adductor magnus and medial intermuscular septum
Insertion	Proximal border of the patella and through patellar ligament
Function	Extension of the knee joint

Recommended sensor placement procedure

Starting posture	Sitting on a table with the knees in slight flexion and the upper body slightly bend backward.
Electrode size	Maximum size in the direction of the muscle fibres: 10 mm.
Electrode distance	20 mm.

<u>Electrode placement</u>

- location	Electrodes need to be placed at 80% on the line between the anterior spina iliaca superior and the joint space in front of the anterior border of the medial ligament.
- orientation	Almost perpendicular to the line between the anterior spina iliaca superior and the joint space in front of the anterior border of the medial ligament.
- fixation on the skin	(Double sided) tape / rings or elastic band.
- reference electrode	On / around the ankle or the proc. spin. of C7.

Clinical test	Extend the knee without rotating the thigh while applying pressure against the leg above the ankle in the direction of flexion.
Remarks	The SENIAM guidelines include a separate sensor placement procedure for the vastus lateralis and the rectus femoris muscle.

Appendix D

Final Version of Signal Processing Program using Continuous Wavelet Transform (CWT) Analysis by LabVIEW

Block Diagram of the Main CWT Analysis Program

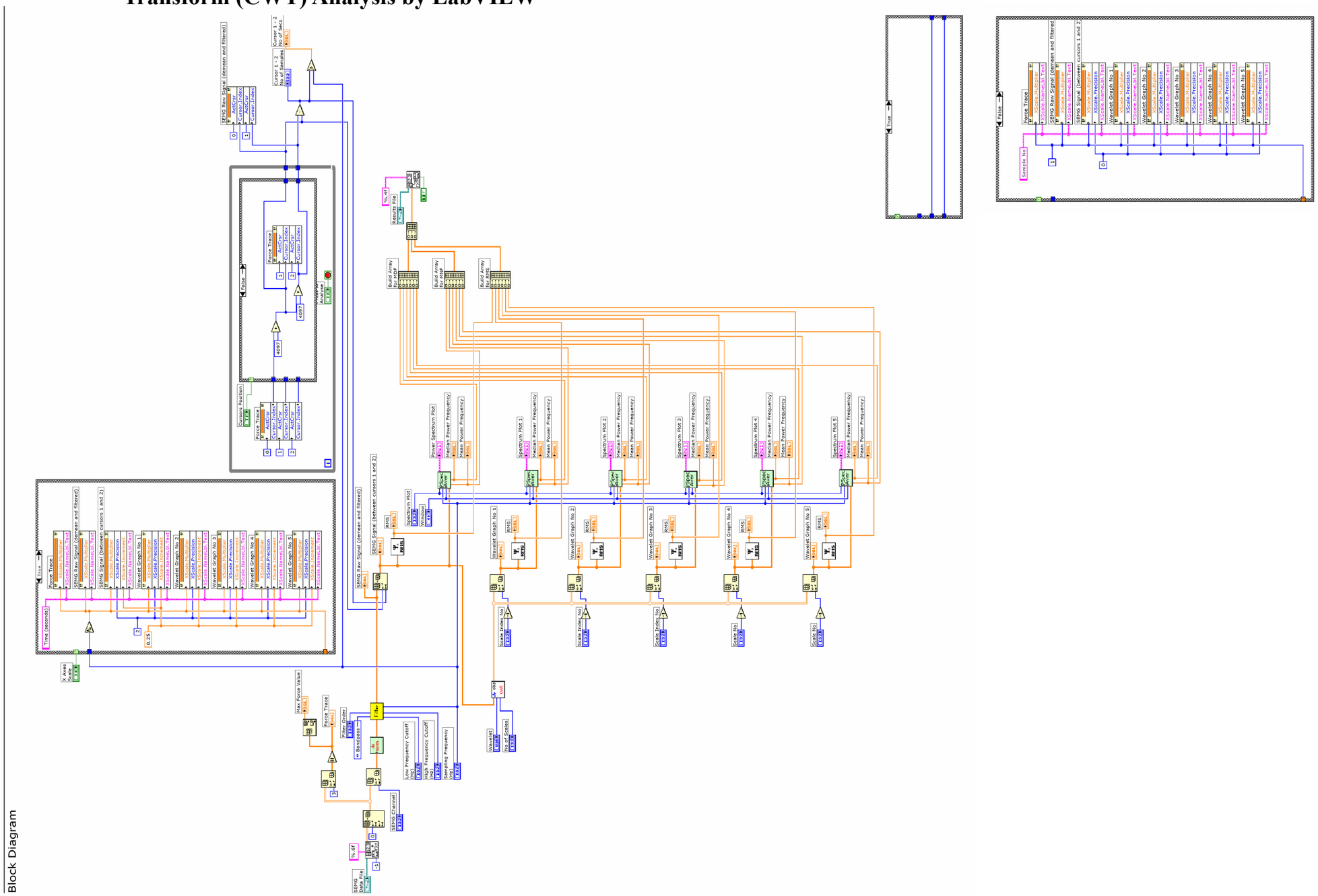

Block Diagram of the SubVI *PSpec* Program

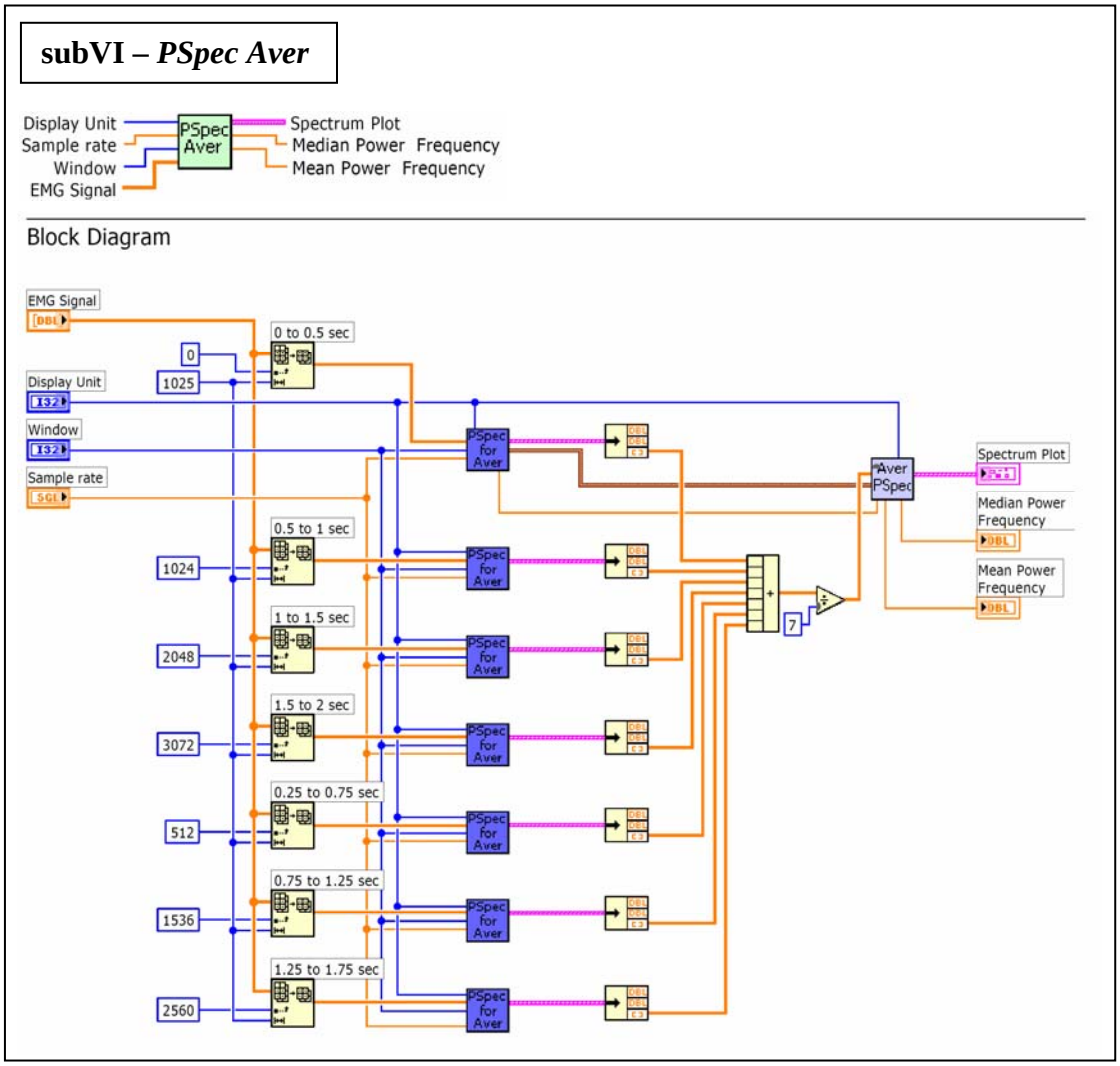

Front Panel Showing the Results of One Set of Typical Signals

Front Panel

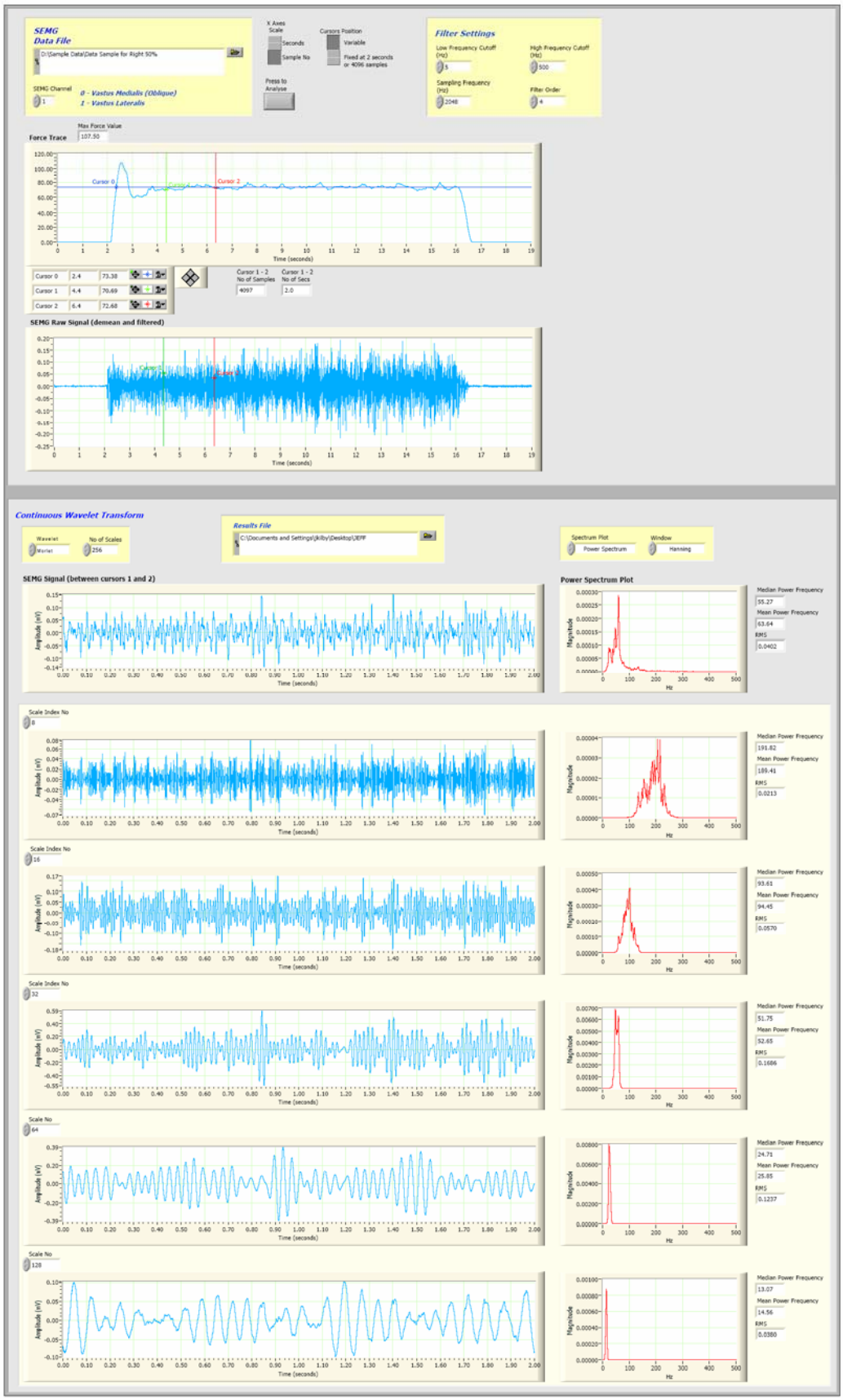

Appendix E

Program Notation for Training Using Artificial Neural Network (ANN) by MATLAB

```
% This program produces an Artificial Neural Network (ANN) for Classification of SEMG Signals by Force
% (Written by Jeff Kilby)


% This part of the program reads the data into Matlab
p=xlsread('data_train');


% This part of the program sets up targets for training the ANN
n=35;
t25=[1;0;0];
t50=[0;1;0];
t75=[0;0;1];
a=[t25 t50 t75];
t=repmat(a,1,n);


% This part of the program trains and creates the ANN
net1=newff(minmax(p),[4,3],g,'trainlm');
net1.trainParam.show=50;
net1.trainParam.epochs=1000;
net1.trainParam.goal=0.001;
[net1,tr1]=train(net1,p,t)
```

References

1. Englehart, K., Hudgins, B., Parker, P. A., Stevenson, M. 1999. Classification of the Myoelectric Signal using Time-Frequency Based Representations. *Med Eng Phys*, **21**, 431-438.

2. Constable, R., Thornhill, R. J. 1993. Using the Discrete Wavelet Transform For Time-Frequency Analysis of the Surface EMG Signal. *ISA*, **16**, 121-127.

3. Sparto, P. J., Jagadeesh J. M., Parnianpour, M. 1997. Wavelet Analysis of Electromyography for Back Muscle Fatigue Detection During Dynamic Constant-Torque Exertions. *ISA*, **33**, 82-87.

4. Crowe, J. A., Gibson, M. S., Woolfson, M. S., Somekh, M. G. 1992. Wavelet Transforms as a Potential Tool for ECG Analysis and Compression. *J Biomed Eng*, **14,** 268-272.

5. Kieft, B. 2005. *A Brief History of Wavelets*. Retrieved from the World Wide Web on 2 March 2005: http://www.gvsu.edu/math/student_work/Kieft/Wavelets%20-%20Main%20Main%20Page.html.

6. Drost, G., Stegeman, D. F., Schillings, M. L., Horemans, H. L. D., Janssen, H. M. H., Massa, M., Nollet, F., Zwarts, M. J. 2004. Motor Unit Characteristics in Healthy Subjects and Those with Postpoliomyelitis Syndrome: A High Density Surface EMG Study. *Muscle Nerve*, **30,** 269-276.

7. Kamen, G. 2005. *Frequently Asked Questions About Electromyography (EMG)*. Retrieved from the World Wide Web on 2 March 2005: http://vuiis.vanderbilt.edu/~nins/EMG_FAQ.htm.

8. Bullock, J., Boyle, J., Wang, M. B. 1995. *Physiology*. Williams & Wilkins, Philadelphia. pp. 35-47.

9. BioControl Systems. 2003. *EMG Biocontrol Technology and Applications*. Retrieved from the World Wide Web on 3 March 2004: http://www.biocontrol.com/emg.html.

10. Wynne, N. 2005. *Electromyograph: an Example of a Biomedical Signal Processor*. Retrieved from the World Wide Web on 2 March 2005: http://www.bae.ncsu.edu/research/blanchard/www/465/textbook/otherprojects/1999/Biosignal_Processing/group1/project/emg/emg.

11. Noraxon. 2004. *What is SEMG?* Retrieved from the World Wide Web on 27 May 2004: http://www.noraxon.com/semg/whatissemg.php3.

12. Basmajian, J. V., De Luca C. J. 1985. *Muscles alive: their functions revealed by electromyography*. Williams and Wilkins, Baltimore.

13. Brody, L. R., Pollock, M. T., Roy, S. H., De Luca, C. J., Celli, B. 1991. pH-induced effects on median frequency and conduction velocity of the myoelectric signal. *J Appl Physiol*, **71**(5), 1878-1885.

14. Karlsson, S., Gerdle, B. 2001. Mean frequency and signal amplitude of the surface EMG of the quadriceps muscles increase with increasing torque--a study using the continuous wavelet transform. *J Electromyogr Kinesiol*, **11**(2), 131-140.

15. Knaflitz, M., Bonato, P. 1999. Time-frequency methods applied to muscle fatigue assessment during dynamic contractions. *J Electromyogr Kinesiol*, **9**(5), 337-350.

16. De Michele, G., Sello, S., Carboncini, M. C., Rossi, B., Strambi, S. K. 2003. Cross-correlation time-frequency analysis for multiple EMG signals in Parkinson's disease: a wavelet approach. *Med Eng Phys*, **25**(5), 361-369.

17. De Luca, G. 2003. *Fundamental Concepts in EMG Signal Acquisition*. DelSys Inc. Retrieved from the World Wide Web on 11 January 2005: http://www.noraxon.com/semg/whatissemg.php3.

18. Pattichis, C. S., Pattichis, M. S. 1999. Time-Scale Analysis of Motor Unit Action Potentials. *IEEE Trans BME*, **46**(11), 1320-1329.

19. Zwarts, M. J., Drost, G., Stegeman, D. F. 2000. Recent Progress in the Diagnostic Use of Surface EMG for Neurological Diseases. *J Electromyogr Kinesiol*, **10**, 287-291.

20. De Luca, C. J. 1997. The Use of Surface Electromyography in Biomechanics. *J Appl Biomech*, **13**(2), 135-163.

21. Farina, D., Merletti, R., Enoka, R. M. 2004. The Extraction of Neural Strategies From the Surface EMG. *J Appl Physiol*, **96**, 1486-1495.

22. Anctil, B., Slawnych, M. P. 1998. An Efficient Method for Modelling EMG Potentials as Recorded Using Surface Electrodes in *Proceedings 20th Annual International Conference IEEE/EMB*. Hong Kong.

23. Thakor, N. V., Zhu Y. -S. 1991. Applications of Adaptive Filtering to ECG Analysis: Noise Cancellation and Arryhthmia Detection. *IEEE Trans BME*, **18**(8), 785-794.

24. Chu, D. P. K., Luk, T. C., Hong, Y. 1998. EMG Activities Between Sit-and-Reach and Stand-and-Reach: a Pilot Study in *Proceedings 20th Annual International Conference IEEE/EMB*. Hong Kong.

25. Wang, L., Buchanan, T. S. 2002. Prediction of Joint Moments Using a Neural Network Model of Muscle Activations From EMG Signals. *IEEE Trans Syst Rehabil Eng*, **10**(1), 30-37.

26. Ksiezyk, R., Blinowska, K., Durka, P. 2005. *Neural Networks with Wavelet Preprocessing in EEG Artifact Recognition.* Retrieved from the World Wide Web on 2 March 2005: http://www.brain.fuw.edu.pl/~durka/papers/medicon98_arif.pdf.

27. Birkedal, L., Collet, T., Dagilis, S. 2002. *Pattern Recognition of Upper-body Electromyography for Control of Lower-limb Prostheses.* Retrieved from the World Wide Web on 2 March 2005: http://www.miba.auc.dk/~sdag01/8semester.

28. Ferguson, S., Dunlop, G. R. 2002. Grasp Recognition From Myoelectric Signals in *Australasian Conference on Robotics and Automation*. Auckland, New Zealand.

29. Moshou, D., Hostens, I., Papaioanou, G., Ramon, H. 2000. Wavelets and Self-organising Maps in Electromyogram (EMG) Analysis in *ESIT 2000*. Aachen, Germany.

30. Hodges, P. W., Richardson, C. A. 1999. Altered trunk muscle recruitment in people with low back pain with upper limb movement at different speeds. *Arch Phys Med Rehabil*, **80**(9), 1005-1012.

31. Mannion, A. F. 1999. Fibre type characteristics and function of the human paraspinal muscles: normal values and changes in association with low back pain. *J Electromyogr Kinesiol*, **9**(6), 363-377.

32. Riley, N. A., Bilodeau, M. 2002. Changes in upper limb joint torque patterns and EMG signals with fatigue following a stroke. *Disabil Rehabil*, **24**(18), 961-969.

33. Panagiotacopulos, N. D., Lee, J. S., Pope, M. H., Friesen, K. 1998. Evaluation of EMG signals from rehabilitated patients with lower back pain using wavelets. *J Electromyogr Kinesiol*, **8**(4), 269-278.

34. Strambi, S. K., Rossi, B., De Michele, G., Sello, S. 2004. Effect of medication in Parkinson's disease: a wavelet analysis of EMG signals. *Med Eng Phys*, **26**(4), 279-290.

35. Kilby, J., Gholam Hosseini, H. 2004. Wavelet Analysis of Electromyography Signals in *Proceedings 26th Annual International Conference IEEE/EMB.* San Franscisco, US.

36. Cohen, A. 1986. *Biomedical Signal Processing: Volume 1 Time and Frequency Domain Analysis*. CRC Press, Boca Raton, FL.

37. Young, M. T., Lucas, C. L., Blanchard, S. M., Enderle, J. D. (ed), Blanchard, S. M. (ed), Bronzino, J. D. (ed). 2000. *Biosignal Processing* in *Introduction to Biomedical Engineering*. Academic Press, San Diego, CA. pp. 233-278.

38. Misiti, M., Misiti. Y., Oppenheim, G., Poggi, J. 2000. *Wavelet Toolbox For Use with MATLAB*. The MathWorks Inc., Natick, MA, 1.1-2.56.

39. BioControl Systems. 2003. *Bio-Signal Processing*. Retrieved from the World Wide Web on 3 March 2004: http://www.biocontrol.com/biosignalprocessing.html.

40. Day, S. 2005. *Important Factors in Surface EMG Measurement*. Bortec Biomedical Ltd. Retrieved from the World Wide Web on 2 March 2005: http://www.bortec.ca.

41. Sloboda, W. M., Zatsiorsky, V. M. 1997. Wavelet Analysis of EMG Signals in *21st Annual Meeting of the American Society of Biomechanics*. Clemson University, South Carolina, US.

42. Fahy, K., Perez, E. 1993. *Fast Fourier Transforms and Power Spectra in LabVIEW*, in *Application Note 040*. National Instruments Corporation.

43. Hagg, G. M. 1992. Interpretation of EMG Spectral Alterations and Alteration Indexes at Sustained Contraction. *J Appl Physiol*, **73**(4), 1211-1217.

44. Vegte, J. V.d. 2002. *Fundamentals of Digital Signal Processing*. Prentice Hall, Sydney.

45. Merletti, R., Parker, P. A. 2004. *Electromyography*. John Wiley & Sons, Hoboken, New Jersey. pp. 259-304.

46. Mertins, A. 1999. *Signal Analysis*. John Wiley & Sons, Chichester.

47. Karlsson, S., Yu, J., Akay, M. 2000. Time-Frequency Analysis of Myoelectric Signals During Dynamic Contractions: A Comparative Study. *IEEE Trans BME*, **47**(2), 228-238.

48. Smalling III, E. 2005. *Wavelets*. Retrieved from the World Wide Web on 2 March 2005: http://home.texoma.net/~smalling/wavelet.htm.

49. Addison, P. S. 2002. *The Illustrated Wavelet Transform Handbook*. Institute of Physics Publishing, Bristol.

50. Sparto, P. J., Parnianpour, M., Barria, E. A., Jagadeesh, J. M. 2000. Wavelet and Short-Time Fourier Transform Analysis of Electromyography for Detection of Back Muscle Fatigue. *IEEE Trans Rehab Eng*, **8**(3), 433-436.

51. *Wavelets*. 2005. Retrieved from the World Wide Web on 3 October 2005: http://www.resonancepub.com/wavelets.com

52. Hostens, I., Seghers, J., Spaepen, A., Ramon, H. 2004. Validation of the wavelet spectral estimation technique in Biceps Brachii and Brachioradialis fatigue assessment during prolonged low-level static and dynamic contractions. *J Electromyogr Kinesiol*, **14,** 205-215.

53. Karlsson, J. S., Ostlund, N., Larsson, B., Gerdle, B. 2003. An estimation of the influence of force decrease on the mean power spectral frequency shift of the EMG during repetitve maximum dynamic knee extensions. *J Electromyogr Kinesiol*, **13,** 461-468.

54. Department of Health and Human Services U.S. 1992. *Selected Topics in Surface Electromyography for Use in the Occupational Setting: Expert Perspectives*. National Institute for Occupational Safety and Health, US.

55. Merletti, R., Lo Conte, L. R. 1997. Surface EMG Signal Processing During Isometric Contractions. *J Electromyogr Kinesiol*, **7**(4), 241-250.

56. Hermens, H. J., Freriks, B., Disselhorst-Klug, C., Rau, G. 2000. Development of recommendations for SEMG sensor and sensor placement procedures. *J Electromyogr Kinesiol*, **10,** 361-374.

57. Cram, J. R., Kasman, G. S., Holtz, J. 1998. *Introduction to Surface Electromyography*. Aspen Publishers, Gaithersburg, Maryland, USA. p. 49.

58. Surface Electromyography for Noninvasive Assessment of Muscle (SENIAM). 2005. *Recommendations for sensor locations in hip or upper leg muscles - vastus lateralis*. Retrieved from the World Wide Web on 4 August 2005: http://www.seniam.org/quadricepsfemorisvastuslateralis.html.

59. Surface Electromyography for Noninvasive Assessment of Muscle (SENIAM). 2005. *Recommendations for sensor locations in hip or upper leg muscles - vastus medialis*. Retrieved from the World Wide Web on 4 August 2005: http://www.seniam.org/quadricepsfemorisvastusmedialis.html.

60. Luttmann, A., Jager, M., Sokeland, J., Laurig, W. 1996. Electromyographical study on surgeons in urology - II. Determination of muscular fatigue. *Ergonomics*, **39**(2), 298-313.

61. Duda, R. O., Hart, P. E. 1973. *Pattern Classification and Scene Analysis*. Wiley, New York.

62. Tou, J. T., Gonzalez, R. C. 1974. *Pattern Recognition Principles*. Addison-Wesley Reading, MA.

63. Fu, K. S. 1982. *Syntactic Pattern Recognition and Applications*. Prentice-Hall, Englewood Cliffs, NJ.

64. Rosenblatt, F. 1958. The perceptron: A probabilistic model for information storage and organization in the brain. *Psycho Rev*, **65,** 386-408.

65. Widrow, B., Lehr, M. A. 1990. 30 years of adaptive neural networks: Perceptron, madaline and backpropagation. *Proc IEEE*, **78,** 1415-1442.

66. Hush, D. R., Horne, B. G. 1993. Progress in supervised neural networks: What's new since Lippmann in *IEEE Sig Process Mag.* pp. 8-39.

67. Demuth, H., Beale, M. 2005. *Neural Network Toolbox*. The MathWorks Inc., Natick, MA.

68. De Luca, C. J. 2002. *Surface Electromyography: Detection and Recording*. DelSys Inc. Retrieved from the World Wide Web on 11 January 2005: http://www.delsys.com/library/tutorials.htm.